1987

Frequency Analysis Of The Rapidly Oscillating Ap Star Hd 60435

Jaymie Mark Matthews

CANADIAN THESES

THÈSES CANADIENNES

NOTICE

The quality of this microfiche is heavily dependent upon the quality of the original thesis submitted for microfilming. Every effort has been made to ensure the highest quality of reproduction possible

If pages are missing, contact the university which granted the degree.

Some pages may have indistinct print especially if the original pages were typed with a poor typewriter ribbon or if the university sent us an inferior photocopy.

Previously copyrighted materials (journal articles, published tests, etc.) are not filmed

Reproduction in full or in part of this film is governed by the Canadian Copyright Act, R.S.C 1970, c C-30

AVIS

La qualité de cette microfiche dépend grandement de la qualité de la thèse soumise au microfilmage Nous avons tout fait pour assurer une qualité supérieure de reproduction

S'il manque des pages, veuillez communiquer avec l'université qui a conféré le grade.

La qualité d'impression de certaines pages peut laisser à désirer, surtout si les pages originales ont été dactylographiées à l'aide d'un ruban usé ou si l'université nous a fait parvenir une photocopie de qualité inférieure

Les documents qui font déjà l'objet d'un droit d'auteur (articles de revue, examens publiés, etc) ne sont pas microfilmés.

La reproduction, même partielle, de ce microfilm est soumise à la Loi canadienne sur le droit d'auteur, SRC 1970, c. C-30.

THIS DISSERTATION HAS BEEN MICROFILMED EXACTLY AS RECEIVED

LA THÈSE A ÉTÉ MICROFILMÉE TELLE QUE NOUS L'AVONS REÇUE

LIST OF FIGURES

ISBN 0-315-36608-7

ABSTRACT

The rapidly oscillating Ap (roAp) star HD 60435 has been monitored in a programme of rapid Johnson B photometry during which approximately 355 hours of observations were collected from the Las Campanas Observatory, Cerro Tololo Inter-American Observatory, and South African Astronomical Observatory in two coordinated campaigns from January 1984 to March 1985.

Fourier analysis of these data indicate that the star undergoes oscillations in a spectrum of nearly equally spaced frequencies, corresponding to a range of periods from about 12 to 20 minutes. Typical amplitudes are only a few millimagnitudes. The dominant oscillations occur near a frequency of 1.4 mHz (P ~ 12 min). Fourier peaks at frequencies near 2.8 and 3.6 mHz have also been detected sporadically; these may be 2:1 and 3:1 resonances with the first oscillation, or harmonics produced by the nonsinusoidal shape of the light curve.

Comparison of the overall frequency pattern to the asymptotic theory of nonradial acoustic pulsation has led to identification of the oscillations as a series of high-overtone ($13 \leq n \leq 28$) p-modes of degree 1 and 2. The fundamental frequency spacing $\nu_0 \sim 52$ μHz is consistent with a slightly evolved late A star whose radius is 2.2 ± 0.3 $R_\odot$. The location of HD 60435 in Stromgren multi-colour diagrams, and classification spectra of the star obtained at Las Campanas, are in general agreement with that result.

The amplitudes of the dominant oscillations are modulated over a long timescale near eight days, and also show rapid modulation in only a few hours. The latter is primarily due to beating among the many

frequencies present in HD 60435, but there is evidence that actual growth and decay of modes occur in the star in less than a day, as postulated by Dolez and Gough (1984) for rapid pulsations in magnetic A stars.

The rotation period of HD 60435, based on the star's long-term light curve, is 7.6662 ± 0.0001 days. (HD 60435 also appears to be a mild spectroscopic variable with a similar timescale) Kurtz' (1982) oblique pulsator model for the *roAp* stars predicts that the oscillation amplitude of the star should be modulated with the same period, as is in fact observed. Application of a dynamical version of this model (Dziembowski and Goode 1985) to the fine splitting observed in the Fourier spectrum of the oscillations places constraints on the inclination of the star and obliquity of its (as yet unconfirmed) magnetic field, predicts that any observed field variations will exhibit polarity reversal, and suggests that HD 60435 may have a relatively weak internal field compared to some of the other *roAp* stars.

These latter predictions are consistent with the upper limits set by the only direct magnetic measurements of this star available to date, as well as the oblique rotator interpretation of the long-term light variations.

ACKNOWLEDGEMENTS

On the subject of acknowledgements, a certain *Style Manual for Students* I have on my bookshelf states that "a student may without compunction refrain from expressing thanks, however heartfelt, to his thesis supervisor for routine work. Acknowledgements should be phrased concisely and circumspectly." Well, I have rarely been accused of circumspection... and even less often of conciseness. And as for the efforts of my advisor, I would hardly describe them as routine. Dr. Bill Wehlau has been both an unfailing wellspring of good advice and a vast reservoir of patience during the years of my doctoral research. This thesis and its author have benefited enormously from his expertise.

Although only one name appears on the jacket of this volume, there are several individuals whose direct contributions deserve both my gratitude and the reader's recognition.

First and foremost of these is Dr. Don Kurtz (University of Cape Town), who played a key role in the development of this thesis. He originally suggested HD 60435 as a promising "centrepiece" for a Ph.D. dissertation, and provided the second-site observations of the star which made this study feasible. His early encouragement and insightful comments in our correspondence and conversations are sincerely appreciated.

Important observations were also supplied by a few others. Dr. John Landstreet and his graduate students David Bohlender and Brian Ventrudo graciously sacrified precious observing time at Las Campanas to attempt a few magnetic measurements of HD 60435. Bob Slawson, then of the University of Toronto Southern Observatory (UTSO), agreed to

collect spectra of the star while I was engaged in rapid photometry at another location. My own observations would not have been possible were it not for generous allocations of time by Dr. Bob Garrison, Director of UTSO, and Dr. Bob Williams, Director of the Cerro Tololo Inter-American Observatory, and the excellent support provided by the staffs of those facilities.

Technical support for this thesis in the post-observation phase was also plentiful. Much of the computing was performed on the Department's then-fledgling PDP 1123 mini-computer. What could have been a frustrating experience was made fruitful by the expert tutelage and good humour of Henry Leparskas. Ron Lyons (University of Toronto) and David Bohlender helped with the PDS digitization of the photographic spectra of HD 60435. Many of the figures in this thesis were originally prepared for publication in scientific journals; some of these were the result of the keen eye and skilled hand of Mira Rasche.

Under the category of moral support, I'd like to acknowledge the minds, hearts and elbows of my fellow members of The Tycho Brahe Society. Their unabated interest in my progress over the years (e.g., "Aren't you finished *yet?*", "Do we have to listen to *another* talk on rapidly oscillating Ap stars?", "Can I have your office space when you leave?") and useful scientific discussions (ahem) at The Graduate Centre helped make my tenure here one I will always recall with fondness.

Finally... (remember my opening comments on conciseness?), I extend my thanks to the Department of Astronomy and The Faculty of Graduate Studies of UWO for their continued financial support.

TABLE OF CONTENTS

LIST OF TABLES

LIST OF FIGURES

TABLE 1.1
THE RAPIDLY OSCILLATING Ap STARS

HD HR	Name	V	b-y	T_{eff} (K)	Periods (min)	ΔB_{max} (mmag)	H_{eff} (gauss)	Refs	Spectral type	Refs
6532		8.45	0.084	8000-8800	6.9	2.5			Ap SrCrEu	11
24712 1217		5.99	0.183		6.14	14.5	+300 → +1200	1	A5p	12
60435		9.00	0.132		20 - 12 6, 4	15.7	< 1300	This thesis	Ap SrCr	13
83368 3831		6.17	0.146		11.7, 5.8	10.2	-700 → +700	2	Ap SrCrEu	13
101065	Przybylski's Star	8.00	0.448	7400?	12.14	14.6	-2200	3	?	14
128898 5463	α Cir	3.20	0.152		6.825	4.8	-300	4,5,6	Ap SrCrEu	15
134214		7.48	0.211		5.65	11.8			F0p SrEu	16
137949	33 Lib	6.67	0.188	7960-8800	8.27	2.8	-1400 → +1800	7	Fp SrCrEu	13
166473		7.5	0.223		8.9				Ap SrCrEu	11
201601 8097	γ Equ	4.68	0.147	7500-8100	12.45	2.8	+500 → -800	8,9,10	F0p	12
203932		8.82	0.169		5.94	2.4			Ap SrEu	13
217522		7.52	0.289		13.72	4.2			Fp SrEu	13

I. INTRODUCTION

The rapidly oscillating Ap stars

The rapidly oscillating Ap (*roAp*) stars are cool peculiar A-F stars[+] which exhibit rapid variations in broadband light. The oscillations of these stars are characterized by (1) their short periods (approximately 4 - 20 minutes), (2) low amplitudes ($\Delta B < 0^m015$; typically only a few millimagnitudes), and (3) amplitude modulation which occurs over timescales from days to weeks. (For stars whose magnetic variations have been determined, the modulation period equals the magnetic period of the star. Maximum oscillation amplitude is observed during the phase of maximum magnetic field strength.) The oscillations sometimes also show (4) splitting in the Fourier spectrum of the dominant frequency into components spaced by the modulation cycle frequency, and (in the case of at least one *roAp* star, HR 3831) (5) 180° phase shifts in the dominant oscillation occurring twice per modulation cycle.

The first *roAp* star, HD 101065 (Przybylski's Star), was discovered in 1978 by Kurtz (1978). Since then, membership in the class has grown to 12, thanks mostly to the efforts of Kurtz and a few of his collaborators (e.g. Kurtz 1983*a*,*b*; Kreidl 1985*a*). All of the known variables are south of 10° in declination, which is probably only a selection

[+] The Ap stars are main sequence stars roughly between B8 and F0 ($15000 > T_{eff} > 8000$ K) whose spectra feature anomalous line strengths which are interpreted as atmospheric over- and underabundances. The coolest members are most overabundant in rare earths ("SrEuCr"); the hottest, in silicon ("Si"). All are helium-deficient. Strong ordered magnetic fields (up to 20 kG) are common - possibly ubiquitous - among these stars. The brightness, spectrum, and magnetic field are observed to vary with periods greater than one day. The properties of the Ap class have been reviewed by Wolff (1983).

effect of the search observations being so far conducted primarily at Southern Hemisphere observatories. Recent reviews of the *roAp* class have been written by Kurtz (1986), Weiss (1986), and Shibahashi (1987).

All but three of the known *roAp* stars have persistent oscillations with periods near 6 and/or 12 minutes. Several are observed to be multiperiodic; 2:1 frequency ratios have been found in three instances.

The characteristics of the oscillations [(1) - (5)] summarized above are illustrated by Figures 1.1 - 1.3. Two typical light curves (obtained six days apart) of a well-studied *roAp* star, HD 24712, are presented in Figure 1.1. Note the small amplitude which never exceeds $0^{m}.01$. The dominant period is 6.14 minutes, but this is only one of six identified by Kurtz and Seeman (1983). The beating of those closely spaced frequencies is responsible for the obvious amplitude modulation of the net oscillation on each night. Neglecting this short-term modulation, the difference in the mean amplitudes of the oscillations on the two nights is quite apparent from the figure. The two sets of observations, showing the oscillations at maximum and minimum amplitude, are separated by about half of the magnetic period of this star (12.54 days; Preston (1972)). Figure 1.2 plots the nightly B amplitude of the net oscillation together with the magnetic curve for HD 24712, demonstrating the phase relationship between the oscillations and field strength.

Figure 1.3 shows the phase shifts detected in the primary oscillation of HR 3831; the sharp changes occur during zero crossover of the magnetic field. These phase shifts and the long-term modulation typified by Figure 1.2 can be explained by the *oblique pulsator model* (Kurtz 1982), which is described later in this chapter.

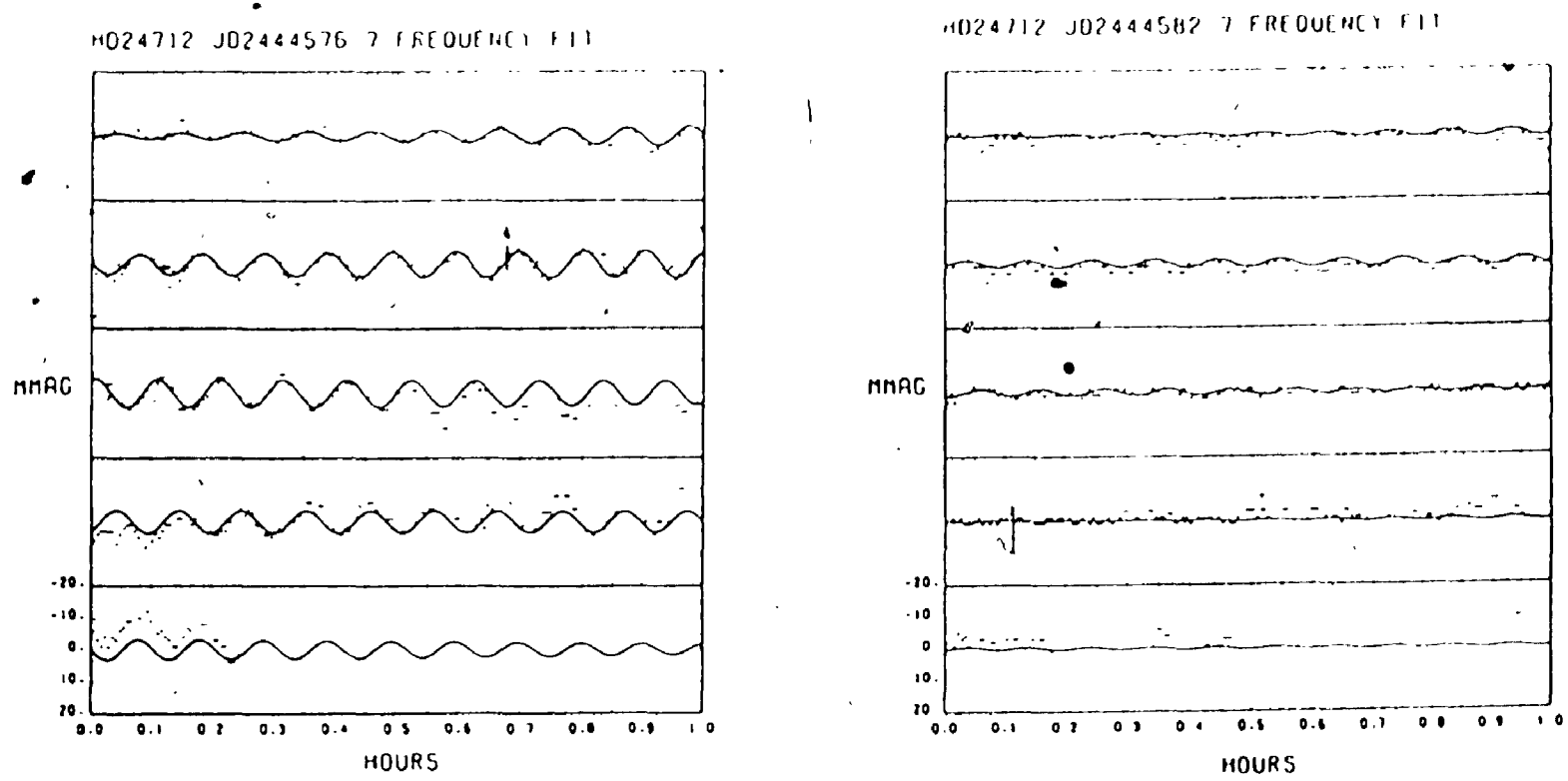

FIGURE 1.1 Light curves showing rapid oscillations in B light of the *roAp* star HR 1217 (HD 24712) on two dates separated by roughly half of the rotation (magnetic) period of the star. Each point represents a 20-sec integration. The solid lines are the curves which result from the superposition of seven sinusoids with the frequencies originally identified by Kurtz. [*Taken from Kurtz (1982)*]

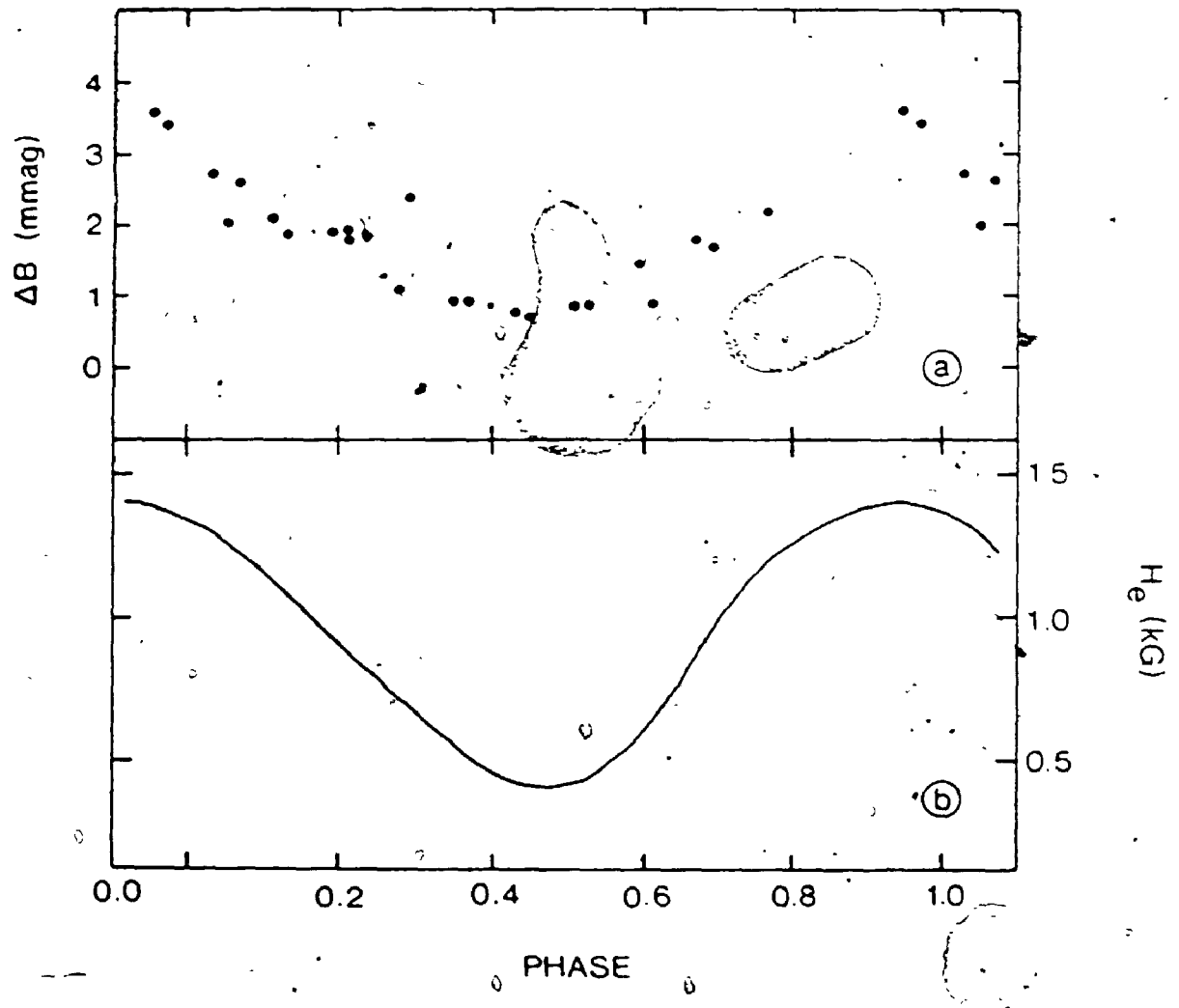

FIGURE 1.2 (*a*) The amplitude modulation of the oscillations of HR 1217 (Kurtz 1982) plotted at the same phases as (*b*) the magnetic variations of the star (Preston 1972).

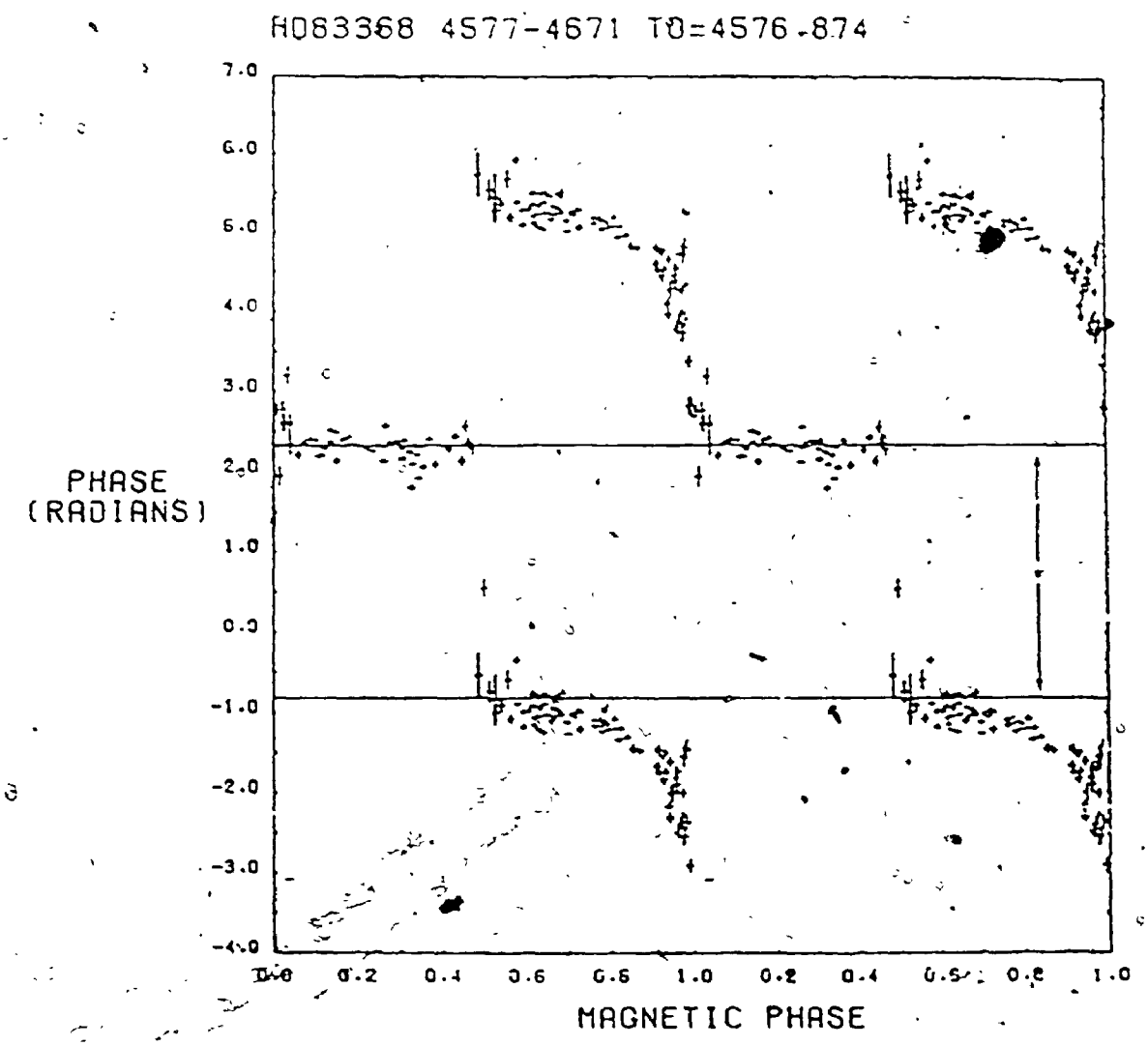

FIGURE 1.3 Phase shifts of the oscillations of the *roAp* star HR 3831 (HD 83368) (Kurtz, private communication) relative to the magnetic phase of the star (Thompson 1983).

The oscillations themselves are thought to be nonradial pulsations; specifically, acoustic (p-) modes of low degree and high overtone. (See Appendix A for a brief introduction to the nomenclature of nonradial pulsation.) The visibility of the oscillations in integrated light requires pulsation patterns of low degree ($\ell \leq 3$); their short periods imply high radial overtones, since fundamental pulsation periods of a few hours are expected for A and F V stars. The most compelling evidence for identifying the oscillations as p-mode waves comes from two *roAp* stars which oscillate in patterns of frequencies with roughly equal spacing. This type of pattern is predicted by asymptotic theory (Tassoul 1980) and has been observed in the Sun's five-minute oscillations, which are now recognized to be the product of acoustic waves. The *roAp* stars which exhibit this behaviour are HD 24712 (Kurtz and Seeman 1983) and *HD 60435*. The discovery of such a pattern in HD 60435, and the information about the star inferred from it, are major results of this thesis.

Empirical parameters

Some of the basic observed properties of the known *roAp* stars are summarized in Table 1.1. A complete set of observed Stromgren indices is provided in Table 1.2. Several reddening-independent Stromgren indices ([u-b], $[m_1]$, and $[c_1]$) were calculated from the photometric values in that table and are listed in Table 1.3.

The *roAp* stars appear to be confined to the low temperature end of the Ap range; none have a (b-y) colour less than about 0.08. As such, they may be restricted to the δ Scuti instability strip, whose blue border falls near (b-y) = 0.06 on the main sequence (Breger 1979). The

TABLE 1.1
THE RAPIDLY OSCILLATING Ap STARS

HD HR	Name	V	b-y	T_{eff} (K)	Periods (min)	ΔB_{max} (mmag)	H_{eff} (gauss)	Refs	Spectral type	Refs
6532		8.45	0.084	8000-8800	6.9	2.5			Ap SrCrEu	11
24712 1217		5.99	0.183		6.14	14.5	+300 → +1200	1	A5p	12
60435		9.00	0.132		20 - 12 6, 4	15.7	< 1300	This thesis	Ap SrCr	13
83368 3831		6.17	0.146		11.7, 5.8	10.2	-700 → +700	2	Ap SrCrEu	13
101065	Przybylski's Star	8.00	0.448	7400?	12.14	14.6	-2200	3	?	14
128898 5463	α Cir	3.20	0.152		6.825	4.8	-300	4,5,6	Ap SrCrEu	15
134214		7.48	0.211		5.65	11.8			F0p SrEu	16
137949	33 Lib	6.67	0.188	7960-8800	8.27	2.8	-1400 → +1800	7	Fp SrCrEu	13
166473		7.5	0.223		8.9				Ap SrCrEu	11
201601 8097	γ Equ	4.68	0.147	7500-8100	12.45	2.8	+500 → -800	8,9,10	F0p	12
203932		8.82	0.169		5.94	2.4			Ap SrEu	13
217522		7.52	0.289		13.72	4.2			Fp SrEu	13

1. Preston (1972)
2. Thompson (1981)
3. Wolff and Hagen (1976)
4. Wood and Campusano (1975)
5. Borra and Landstreet (1975)
6. Borra and Landstreet (1980)
7. Wolff (1975)
8. Babcock (1958)
9. Bonsack and Pilachoski (1974)
10. Scholz (1979)
11. Houk (1982)
12. Hoffleit (1982)
13. Bidelman and MacConnell (1973)
14. Kurtz and Wegner (1979)
15. Houk and Cowley (1975)
16. Henry Draper Catalogue

TABLE 1.2
OBSERVED STROMGREN INDICES OF THE *roAp* STARS+

HD	b-y	m_1	c_1	β	δc_1	Refs
6532	0.084	0.237	0.846	...	-0.142	1,2
24712	0.183	0.212	0.634	2.744	-0.034	1,2
60435	**0.132**	**0.234**	**0.843**	**2.79***	**+0.035**	**3**
83368	0.146	0.203	0.796	2.827	-0.035	1,3
101065	0.448	0.368	-0.014	2.641	-0.368	4
128898	0.152	0.195	0.760	2.831	-0.077	1,3
134214	0.211	0.288	0.597	2.766	-0.115	6,7
137949	0.188	0.321	0.584	2.833	-0.256	1,3
166473	0.223	0.311	0.517	...	-0.092	8
201601	0.147	0.238	0.760	2.819	-0.058	1,2
203932	0.169	0.196	0.736	2.814	-0.072	3,5
217522	0.289	0.215	0.487	2.701	-0.046	3,5

1. Hauck & Mermilliod (1980)
2. Blanco *et al.* (1970)
3. Vogt & Faundez (1979)
4. Kurtz & Wegner (1979)
5. Weiss (private communication)
6. Olsen & Perry (1984)
7. Olsen (1983)
8. Kurtz (1986)

+ Adapted from Table 1 of Kurtz (1986)
* Estimated from equivalent width of Hβ by author (Chapter V)

TABLE 1.3
REDDENING-FREE STROMGREN INDICES OF THE *roAp* STARS

HD	$[m_1]$	$[c_1]$	[u-b]	$\Delta[m_1]$	"Golay" spectral class
6532	0.252	0.829	1.333	...	
24712	0.245	0.597	1.087	+0.062	F0
60435	**0.258**	**0.817**	**1.333**	**+0.044**	**A8**
83368	0.229	0.767	1.225	+0.022	A7
101065	0.449	-0.104	0.794	...	
128898	0.222	0.730	1.174	+0.015	A6 - A7
134214	0.326	0.555	1.207	+0.236	A8 - A9
137949	0.355	0.546	1.256	+0.147	A7
166473	0.351	0.472	1.174	...	
201601	0.264	0.731	1.259	+0.058	A7
203932	0.226	0.702	1.154	+0.020	A8?
217522	0.267	0.429	0.963	-0.1	> F0

$$[m_1] = m_1 + 0.18(b-y)$$
$$[c_1] = c_1 - 0.20(b-y)$$
$$[u-b] = [c_1] + 2[m_1]$$

question of whether *all* of the *roAp* stars occupy the lower instability strip cannot be answered definitely at the moment, given the uncertainties of the derived T_{eff} and M_v values for the peculiar stars. Furthermore, the observed colour boundaries of the δ Scuti strip may not be entirely appropriate for comparison with the location of the *roAp* stars in the HR diagram. Stepién and Muthsam (1980) have pointed out systematic differences between the temperatures of peculiar and normal A model atmospheres having the same (B-V) colour. The cooler Ap stars appear to have systematically higher effective temperatures than one would derive for a normal star of the same colour. A similar effect is probably valid for (b-y).

In fact, the lower (b-y) boundary for the *roAp* phenomenon is not itself well determined. Most of the surveys for new *roAp* stars have concentrated on the cooler A-Fp stars, introducing a bias to the sample of variables. Even so, a number of apparently hotter stars with smaller (b-y) have been carefully monitored with rapid photometry and no oscillations were detected; e.g., the A0p(Si) star HD 92664 (Kurtz, private communication) and the A2p (SrCrEu) star 53 Cam (Matthews and Wehlau 1985; Kreidl 1985*b*).

The [u-b],β values of the *roAp* stars (Tables 1.2 and 1.3) fall within or close to the main sequence band defined by Golay (1974*a*) between ~A7 and F0. A notable exception is Przybylski's Star (HD 101065). The spectral classes appropriate for "normal" stars with the same values of [u-b],β in the Golay scheme are given in the last column of Table 1.3. All of the *roAp* stars have $[m_1]$ values which exceed those of normal stars on Golay's main sequence and in Crawford's (1979) m_1 vs. β relation for A-type stars. (This is true of most, if not all,

peculiar A stars, since [m_1] is a metallicity indicator.) All but one of the stars (HD 60435) have c_1 indices which also fall below Crawford's standard c_1 vs. β relation (as shown by δc_1 in Table 1.2). Since c_1 is usually taken to be a luminosity indicator for A-F stars, this might seem to suggest that these stars have sub-dwarf luminosities. However, the unusual flux distributions of the peculiar A stars are likely responsible for the abnormally low c_1 values.

The reason can be found in the definition of the c_1 index:

$$c_1 = (u-v) - (v-b) \qquad (1.1)$$

where the u bandpass mainly samples wavelengths just shortward of the Balmer discontinuity of λ3647; the v filter, several hundred Å longward ($\lambda_{eff} \approx 4100$ Å); and the b filter, still further towards the red ($\lambda_{eff} \approx 4700$ Å). Although the coolest Ap stars do have many absorption lines in the near ultraviolet, they also have relatively little continuum in that region of the spectrum. Therefore, flux redistribution from the UV is not as important for these stars as it is for the hotter Si Ap stars. However, Baschek and Oke (1965) and Wolff (1967) found that line blanketing in the visible becomes significant for the coolest (or most peculiar) of the Ap stars. The richness of the absorption spectrum at wavelengths near 4100 Å should result in an increase in (v-b) due to blanketing. The increase in v magnitude should also more than cancel the increase in (u-v) due to UV flux redistribution, causing a net drop in that colour. The end result is a decrease in c_1 compared to a "normal" star.

If abundance effects were not important, a plot of c_1 vs. (b-y) would essentially be a luminosity - T_{eff} diagram. Just such a plot of

the c_1 and (b-y) indices from Table 1.2 is presented in Figure 1.4. Also plotted are lines corresponding to models of main sequence stars with solar composition and surface gravities of log g = 4.0 and 4.5 (Hauck and Mermilliod 1975). Observe that the *roAp* stars fall roughly along a line of similar slope to the models, except for (again) HD 101065. It would appear that any abundance differences among the stars are small enough so as not to destroy the general main sequence behaviour; rather, the abundance peculiarity manifests itself as an apparent shift of the curve to higher surface gravity. Therefore, c_1 (or δc_1) may prove to be useful as an indicator of *relative* luminosity among the sample of rapid oscillators. (We will return to this point in relation to HD 60435 in Chapter IV.)

The rapid oscillators all seem to belong to the cooler SrCrEu classes of Ap stars, with the possible exception of HD 101065.[+] They are all expected to have the strong ordered magnetic fields normally associated with peculiar stars. Seven of the 12 stars have been searched for magnetic fields, resulting in positive detections for six (see Table 1.1). The single null detection was obtained for HD 60435, but this is based on only three measurements of relatively low precision (~ ±600 gauss). (The magnetic measurements of HD 60435 and their significance will be discussed in Chapter VI.)

Not all magnetic peculiar stars in the range of colours spanned by the *roAp* variables are found to be rapid oscillators. Promising candidates which yielded no detectable oscillations after repeated observations include β CrB (Weiss and Kurtz, 1987) and HR 4330

[+] This star *does* exhibit enhanced rare earths, but the strongest of these are holmium and dysprosium. The iron peak elements are very weak in the spectrum, or perhaps missing altogether.

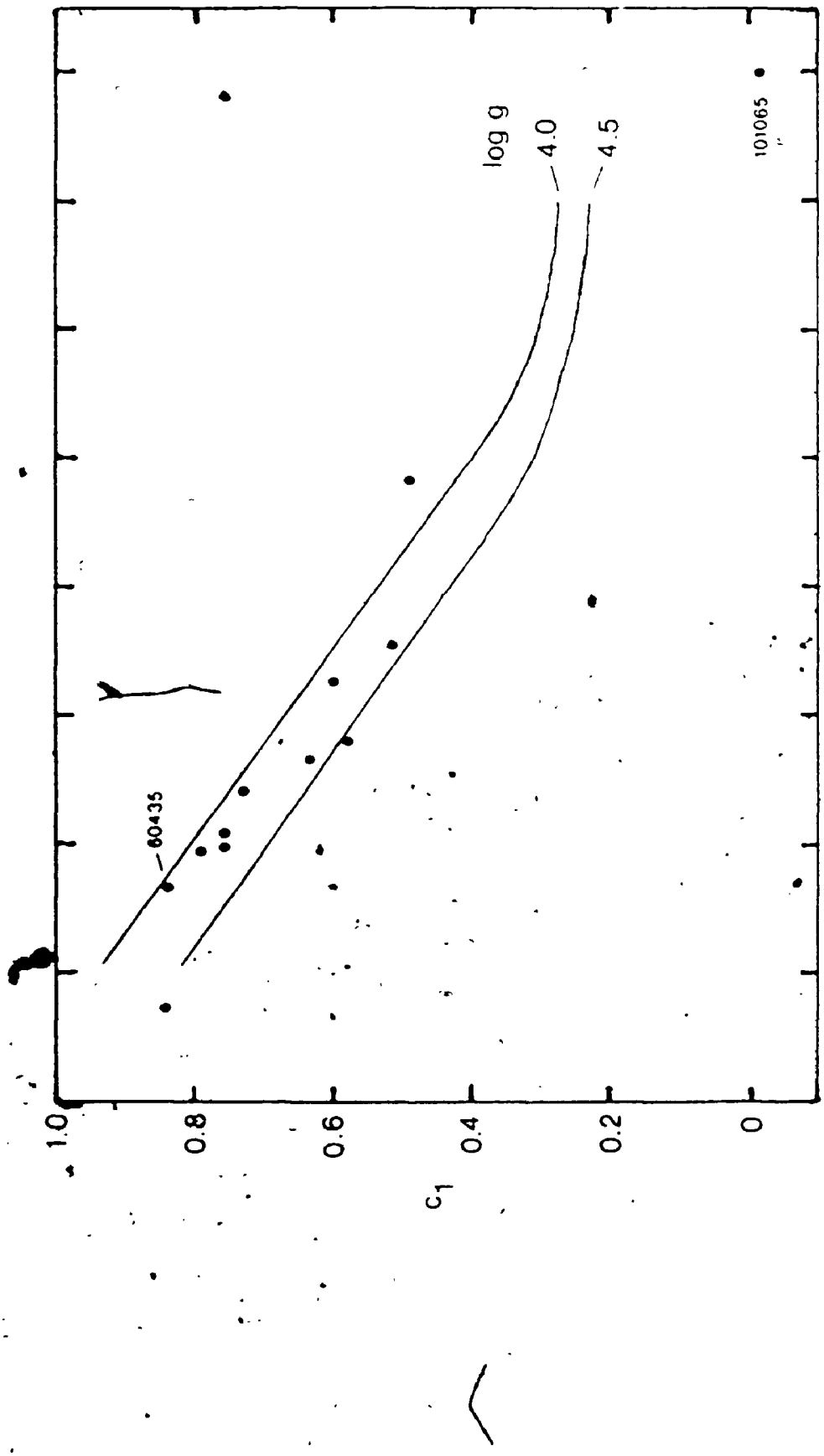

FIGURE 1.4 A plot of c_1 vs. (b-y) for the known roAp stars. The solid lines are model curves for main sequence stars of log g = 4.0 and 4.5 (Hauck and Mermilliod 1975).

(Matthews and Wehlau 1985) There is clearly some missing parameter(s) which distinguishes an roAp star from other apparently similar - but constant - cool Ap stars.

The classical Oblique Pulsator Model (Kurtz 1982)

The most successful model in explaining the long-term variations observed in Ap stars has been the "oblique rotator", in which the axis of the stellar magnetic field (assumed to be dipole or near-dipole) is inclined to the rotation axis. As the star rotates, different aspects of the field are presented to the observer, along with abundance and surface brightness anomalies associated with the field geometry. This accounts for the equality of the magnetic, spectroscopic, and (long-term) photometric periods of an Ap star, plus features such as polarity reversal of the magnetic field, often observed in these stars.

Kurtz's oblique pulsator model (OPM) extends this picture to the rapid oscillations by supposing that nonradial pulsations in an Ap star may not be aligned with the rotation axis - as is normally assumed - but rather with the magnetic axis. Hence, different aspects of the pulsation are observed as the star rotates. This readily explains the observed modulation of the oscillation amplitude with the magnetic (= rotation) period of the star. And the observed phasing (maximum oscillation amplitude with magnetic extremum) arises naturally if the pulsation pattern is zonal (i.e. $m = 0$). The phase shifts come about if the magnetic field undergoes polarity reversal; when the star passes through quadrature, different zones of the pulsation pattern (varying in anti-phase) alternately dominate the visible disc, and 180° jumps in phase are observed. These effects are illustrated schematically in

Figure 1.5, which represents the rotation of an $\ell = 1$, $m = 0$ oblique pulsator with moderate inclination and obliquity (such that polarity reversal of the field takes place).

The OPM can also be treated somewhat more quantitatively. Consider the nonradial pulsation pattern as a simple spherical harmonic. The luminosity variations at the sub-solar point on the stellar disc may be represented by a Legendre polynomial $P_{\ell,0}$, such that

$$\frac{\Delta L}{L} = P_\ell(\cos\alpha)\cos[\omega(t-t_o) + \Phi] \qquad (1.2)$$

where α is the angle between the axis of symmetry of the pulsation and the line of sight, ω is the pulsation frequency, and t_o and Φ are an arbitrary epoch and phase. The angle α is related to the star's inclination i and the obliquity β of its pulsation axis by spherical trigonometry:

$$\cos\alpha = \cos i\cos\beta + \sin i\sin\beta\cos A. \qquad (1.3)$$

Here, A is the longitude of the pulsation pole on the stellar surface, measured such that the longitude of the sub-solar point is 0°. For an oblique pulsator, $A = \Omega t$, where Ω is the angular rotation frequency of the star, so $\cos\alpha$ is a periodic function of time. The angle β in equation (1.3) is now the obliquity of the magnetic field, and the epoch t_o in equation (1.2) is chosen to coincide with maximum effective magnetic field.

If we assume $\ell = 1$, $P_\ell(\cos\alpha) = \cos\alpha$. Equation (1.2) can then be decomposed (using trivial trigonometric identities and the time-dependent version of equation (1.3)) into

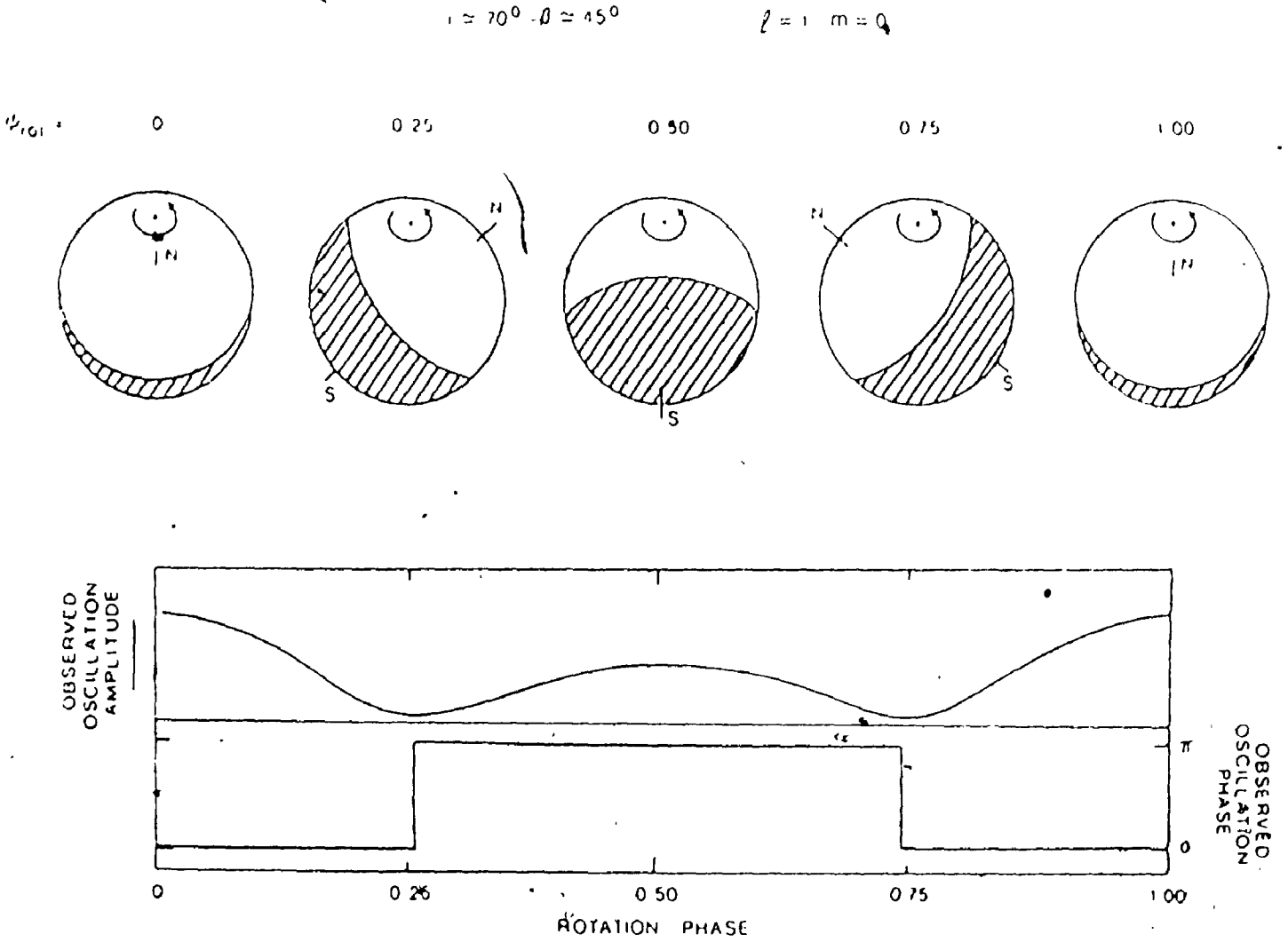

FIGURE 1.5 The oblique pulsator model for an *roAp* star. The rotation and magnetic poles of the star are indicated. The shaded portion is a hemisphere whose motions and luminosity changes are opposite in phase to the other half of the star.

$$\frac{\Delta L}{L} = A_0 \cos[\omega t' + \Phi] + A_1\Big[\cos[(\omega-\Omega)t' + \Phi] + \cos[(\omega+\Omega)t' + \Phi] \Big] \quad (1.4)$$

where $t' = t - t_o$, $A_0 = \cos i \cos\beta$, and $A_1 = \frac{1}{2}\sin i \sin\beta$. In other words, the oscillation is split into a frequency triplet whose central component is at the oscillation frequency in the star's rest frame and whose sidelobes are spaced by the star's rotation frequency. (Note that when $\cos\alpha$ changes sign, then $-P_1\cos(\omega t' + \Phi) = P_1\cos(\omega t' + \Phi \pm \pi)$, which reproduces the observed phase shifts at magnetic quadrature.)

A similar expansion for $\ell = 2$ shows that a frequency quintet is produced with the same spacing. In general, the OPM predicts that a mode of degree ℓ will be split into $(2\ell + 1)$ components, centred about the oscillation frequency in the star's rest frame and spaced by its rotation frequency. This type of frequency splitting has been observed in the Fourier spectra of several *roAp* stars (Kurtz 1982).

Kurtz's OPM is a purely phenomenological model; it does not attempt to explain the underlying mechanism by which the magnetic field controls the pulsation geometry.

One difficulty with Kurtz's simple model is that Coriolis forces on the obliquely rotating pulsation pattern should tend to make the pulsation axis precess with respect to the magnetic axis (i.e., advection). Therefore, the peaks in oscillation amplitude should not remain in phase with the magnetic maxima. However, several years of observation of *roAp* stars such as HR 1217 (Kurtz *et al.* 1985) have shown that the phase equality holds to high precision.

To avoid this apparent paradox, Dolez and Gough (1982) proposed that the magnetic field might selectively excite modes which are aligned with it. They estimated the lifetimes of the excited modes to

be short (hours) compared to a typical rotation period (days). Thus, as the field is carried around by rotation, the modes which are no longer favourably oriented with that field die out quickly, while new modes are in turn generated. This picture is not without its problems as well. It is difficult to understand how individual pulsations can maintain phase coherence over long intervals of time (as is observed) if modes are being continually re-excited. Also, the rotation period of one of the *roAp* stars, HR 3831 = HD 83368, is under two days (Kurtz and Marang 1987); modes must have *very* short lifetimes in this star for the selective excitation process to be effective.

The "dynamical" Oblique Pulsator Model (Dziembowski and Goode 1985)

The complexity of the Dolez and Gough scenario, and its incomplete success in accounting for the observations, led Dziembowski and Goode (1985) to return to Kurtz's "classical" OPM and show how the amplitude modulation is consistent with the perturbing effects of both a magnetic field *and* rotation.

Consider first a nonrotating, nonmagnetic pulsating star. The eigenfunctions of its pulsation modes (ℓ,m) may be expressed in terms of the spherical harmonics $\xi_{\ell m} \propto Y^m_\ell(\theta,\phi)$, where the reference frame for θ and ϕ is completely arbitrary. If a dipole magnetic field H is then introduced, the Lorentz forces due to the field lines can modify the equilibrium configuration of the star, causing an asymmetry such that the normal modes now satisfy $\xi_{\ell m} \propto Y^m_\ell(\theta_H,\phi_H)$, where the magnetic axis is defined as $\theta_H = 0$.

The field also perturbs the eigenfrequencies of the oscillations:

$$\omega_{\ell,m} = \omega^{(0)} + \omega_{\ell,|m|}^{mag} \qquad (1.5)$$

where $\omega^{(0)}$ is the frequency in the absence of a magnetic field, and $\omega_{\ell,|m|}^{mag}$ is the perturbation due to the field acting on a mode (ℓ,m). Therefore, the eigenfunction becomes

$$\xi_{\ell m} = Y^m_\ell(\theta_H,\phi_H)\ \exp\left[i(\omega^{(0)} + \omega_{\ell,|m|}^{mag})t\right] + O(H^2t) \qquad (1.6)$$

where $m = -\ell, \cdots, \ell$; and the last term represents the effect of the field on the equilibrium state of the star (of order H^2).

Adding the effects of rotation about an axis inclined by an angle β to the magnetic axis, and neglecting the equilibrium term of order H^2:

$$\xi_{\ell m} = \left[Y^m_\ell(\theta_H,\phi_H) + \sum_{\substack{n=-\ell \\ (n\neq m)}}^{\ell} \alpha_{nm}^{(\ell)}\ Y^n_\ell(\theta_H,\phi_H)\right]\ \exp\left[i(\omega^{(0)} + \omega_{|m|}^{mag} + mC\Omega\cos\beta)t\right] \qquad (1.7)$$

where the term $mC\Omega\cos\beta$ is the rotational splitting derived by Aizenman *et al.* (1984); C is the Ledoux constant (see Appendix A), and

$$\alpha_{nm}^{(\ell)} = \frac{\sum_{k=-\ell}^{\ell} k\ d^{(\ell)}_{nk}(\beta)\ d^{(\ell)}_{mk}(\beta)\ C\Omega}{\omega_{\ell,|m|}^{mag} - \omega_{\ell,|n|}^{mag}} \qquad (1.8)$$

This latter term contains the transformation from the reference frame of the magnetic field to that of the rotation axis, by applying the well-known Clebsch-Gordon coefficients $d^{(\ell)}_{nk}(\beta)$ to the spherical harmonics according to the following expansion,

$$Y^m_\ell(\theta_H,\phi_H) = \sum_{n=-\ell}^{\ell} d^{(\ell)}_{mn}(\beta)\ Y^n_\ell(\theta_R,\phi_R) \qquad (1.9)$$

where (θ_R,ϕ_R) are measured relative to the rotation axis.

For the case of a mode with $(\ell,m) = (1,0)$, then the appropriate matrix of Clebsch-Gordon coefficients can be written as (Kurtz and Shibahashi 1986),

$$d(\beta) = \begin{bmatrix} \frac{1}{2}(1 + \cos\beta) & \frac{\sqrt{2}}{2}\sin\beta & \frac{1}{2}(1 - \cos\beta) \\ -\frac{\sqrt{2}}{2}\sin\beta & \cos\beta & \frac{\sqrt{2}}{2}\sin\beta \\ \frac{1}{2}(1 - \cos\beta) & -\frac{\sqrt{2}}{2}\sin\beta & \frac{1}{2}(1 + \cos\beta) \end{bmatrix} \qquad (1.10)$$

and equation (1.7) can be solved for the relative variation in luminosity using the approach of Dziembowski (1977), giving...

$$\frac{\Delta L}{L} = A_0 \cos[(\omega^{(o)} + \omega_0{}^{mag})t + \Phi] + A_{+1}\left[\cos[(\omega^{(0)} + \omega_0{}^{mag} + \Omega)t + \Phi]\right] + A_{-1}\left[\cos[(\omega^{(0)} + \omega_0{}^{mag} - \Omega)t + \Phi]\right]$$

where $A_0 = \text{cosicos}\beta$, and

$$A_{\pm 1} = \tfrac{1}{4}\text{sinisin}\beta\left[1 \pm \frac{C\Omega}{\omega_1{}^{mag} - \omega_0{}^{mag}}\right]. \qquad (1.11)$$

Note that this result is very similar to that of the classical OPM (equation 1.4), in that the dynamical model also predicts that an $(\ell,m) = (1,0)$ mode should be split into three components spaced by exactly the rotation frequency of the star. However, the amplitudes of the sidelobe components are now governed by the relative perturbations from the rotation ($-C\Omega$) and the magnetic field ($\omega_1{}^{mag} - \omega_0{}^{mag}$). The use of this in the interpretation of HD 60435 will be discussed in Chapter VI.

The Spotted Pulsator Model (Mathys 1985)

Whereas Dziembowski and Goode have argued that a global magnetic field can force the pulsation pattern to corotate with the field axis, Mathys (1985) has proposed an alternative model to explain the amplitude modulation which does not require the pulsation mode to be symmetric about the magnetic axis. His *spotted pulsator model* can reproduce the observed modulation by invoking inhomogeneous distributions of surface brightness $F(\theta,\Phi)$, as well as the amplitude ratio $f(\theta,\Phi)$ and phase

lag $\psi(\theta,\Phi)$ of the flux and radius oscillations.

Unfortunately, a given amplitude modulation curve for an *roAp* star does not correspond to a unique combination of F, f and ψ, so the model is very difficult to test against observation.

Cause of the variations

The mechanism which produces the oscillations in these variables has not yet been established. The two leading contenders are considered to be: an envelope ionization (or "kappa") mechanism, like that which governs the pulsating δ Scuti stars (Appendix A), and "overstable magnetic convection".

The former is attractive because the position of the *roAp* stars on the HR diagram appears to overlap a known region of pulsational instability, that of the δ Scuti variables. However, there are several unanswered questions associated with this interpretation. First, the periods of the *roAp* stars (minutes) are much shorter than those of the δ Scuti stars (typically about two hours); the rapid oscillators are apparently pulsating in much higher overtones. Why? Does the magnetic field play a role in damping all but the higher overtones? Second, if diffusion is occurring in the atmospheres of Ap stars, then one would expect that most - if not all - of the helium will have settled below the HeII ionization zone (the main source of the driving in δ Scuti stars). Surveys (e.g. Kreidl 1987) appear to indicate that Ap stars and δ Scuti-timescale variability are mutually exclusive. Perhaps the reason for this exclusion is not the complete removal of He from the ionization zone in Ap stars, but again the possible selective excitation/damping of certain overtones by the magnetic field.

An alternative mechanism for the excitation of rapid oscillations in Ap stars has been proposed by Shibahashi (1983): overstable magnetic convection. (See also a more qualitative treatment by Cox (1984a).) This overstability arises from the resistance of the tension of the magnetic field lines to the convective motions in the atmosphere. If the convective motions occur in a superadiabatic region, that region would be convectively unstable if no field (or abundance gradient) is present. If a field is present, then the "restoring" force applied to a rising element of plasma will increase, and the result will be oscillations of increasing amplitude. Cox (1984), using reasonable values for the magnetic field and atmospheric parameters, derives oscillation periods of several hundred seconds, in the same range as the observed values.

Currently, there is no definitive observational test to choose one of these mechanisms over the other. However, the discovery of a magnetic *roAp* star far outside the instability strip would constitute strong evidence in favour of overstable magnetic convection.

HD 60435

This star is one of the more recent additions to the class of *roAp* variables. It is the faintest (V = 9.00) of the known oscillators and the second most southerly (1950 coordinates: $\alpha = 07^h\ 30^m\ 01\overset{s}{.}8$; $\delta = -57°\ 53'\ 03\overset{''}{.}9$). Kurtz (1984) first detected periods near 12 and 6 minutes in this star in 1983. His 16-night observing run also revealed dramatic amplitude modulation of both oscillations. The "6-minute" oscillation appeared to be transient, appearing only when the "12-minute" oscillation was present at its largest amplitude. Unfortunately, the

data were insufficient for a thorough study of the frequency spectrum and any characteristic amplitude modulation.

HD 60435 had not garnered much attention prior to the discovery of its rapid oscillations. Kurtz included it in his *roAp* search programme at the South African Astronomical Observatory (SAAO) because of its classification by Bidelman and MacConnell (1973) and Houk and Cowley (1975) as Ap SrEu, and its relatively large (b-y) index of 0.132.

This study of HD 60435 was undertaken with the initial aims of

i) identifying the frequencies present in the star;

ii) determining a modulation period/timescale and a long-term photometric period/timescale as a test of the OPM;

iii) obtaining amplitude spectra with sufficiently high resolution and suppressed cycle/day aliasing, to investigate the fine-splitting of frequencies in the context of the OPM; and

iv) using these data to infer some of the physical properties of the star.

Although the initial lack of supporting data on the star (e.g. rotation period, strength and variability of magnetic field (if any)) could be considered a handicap to such a study, it also made HD 60435 an excellent proving ground for the role of oscillation observations and the oblique pulsator model in studying Ap stars.

II. OBSERVATIONS

Rapid photometry

Studying the short-term light variations of a star like HD 60435 presents several problems to the observer, the most serious of which are the high time resolution required and the spectral aliases inherent in the frequency analysis of astronomical time series.

Reliable detection of stellar oscillations with periods of only a few minutes demands monitoring of the star with a sampling interval of less than one minute[+]. One is left with two options: i) differential measurements using a "multi-star" photometer (or potentially, a calibrated imaging device such as a CCD detector), or ii) *non*-differential photometry with a conventional single-channel instrument.

In principle, the first alternative is ideal; the necessary time resolution is achieved with continuous compensation for extinction changes through simultaneous readings of one or more nearby comparison stars. In practice, however, the fact that no major southern hemisphere observatory (from which HD 60435 could be observed) is presently equipped with a multi-star photometer and the difficulties associated with bringing a visitor instrument to such an observatory, make this option less viable.

Fortunately, non-differential photometry can be used to detect oscillations with periods as long as 12 minutes from an observing site of suitable quality, as was previously demonstrated by Kurtz (e.g.

[+] It has been demonstrated theoretically (Beutler 1966) that a period P can be extracted via Fourier techniques from data containing a periodic signal, even if the average sampling interval is as long as P/2. However, in practice, one rarely has a sufficiently large sample and the high signal-to-noise ratio necessary to make this possible.

1982). The success of these observations hinges on the temporal incoherence and small amplitude of sky variations at short timescales on a good night.

Given a stable photometer system, the major sources of noise are these sky transparency (and background) fluctuations, and scintillation. Clarke (1980) has found that, even under the best conditions, the former can have amplitudes of order $0^m.001$ in a period range from minutes to tens of minutes. Scintillation noise, on the other hand, is primarily a function of telescope aperture. However, experiments by Kurtz (1985) using a 0.5- and 1.9-m telescope indicate that, for periods near five minutes and longer, scintillation is not the dominant contributor to the limiting noise in rapid photometry. Therefore, the only constraint on telescope aperture in this type of observing is that it be large enough to make the photon noise in a single integration (where the integration time must be less than half of the shortest period of interest) smaller than the scintillation noise. For relatively bright stars such as HD 60435, this can be attained with a telescope in the 0.5- to 1-m class.

The other major difficulty is one common to any search for periodicities in data with large gaps: spectral aliasing. (This will be discussed in greater detail in the next chapter.) The topic is introduced here because aliasing is a product of the time sampling of the observations, and it is most effectively dealt with at the observing stage, if permitted by scheduling constraints. The most severe aliases are those with spacings of 1 cycle/day, which arise from the natural diurnal pattern of nighttime astronomical observations. The problem is exacerbated in the case of the rapidly oscillating Ap stars by the pre-

sence of many closely spaced and/or rotationally-split frequencies in several of these variables. Identification of each true frequency from its aliases (and those of other neighbouring frequencies) is not always a simple matter, particularly if the intrinsic frequency spacing is close to an integer multiple of 1 cycle/day.

By reducing or eliminating the large gaps between sets of observations, one can in turn reduce or eliminate the corresponding aliases in the frequency spectrum. Strategies for continuous monitoring of a star from a single site involve the use of a near-polar station or a satellite in a suitable orbit. Suitable facilities for rapid stellar photometry do not currently exist to realize either of these options. A more practical approach is to make contiguous sets of observations from *several* ground-based sites spaced widely in longitude. (The value of an observing programme like this was aptly demonstrated by the history of the frequency analysis of the rapid oscillator HR 1217. Kurtz (1982), on the basis of his SAAO observations alone, identified only two frequencies in this star, each finely-split into a triplet. Contemporaneous observations made later from both South Africa and Chile (Kurtz and Seeman 1983) showed that aliasing in the earlier data set had masked the true pattern of six equally spaced frequencies.) In principle, given clear weather and an appropriately-placed star, a minimum of only three observatories located at 8-hour intervals in longitude could offer complete daily coverage of the star and the elimination of the cycle/day aliases in the frequency analysis of the data. (Feasibility and site-testing studies carried out for proposed global monitoring of the Sun (e.g. Global Oscillation Network Group 1985) recommend a minimum of six stations to achieve a ~92% duty cycle.)

For this investigation of HD 60435, rapid photometry was carried out in two campaigns from three locations+ (observers are indicated in boldface):

a) the Las Campanas Observatory (LCO), Chile, using the University of Toronto 0.6-m telescope and 1P21 (S-4) photometer (the author);

b) the Cerro Tololo Inter-American Observatory (CTIO), also in Chile, using its 0.9-m telescope and photometer, with an FW-130 (S-20) phototube (the author); and

c) the Sutherland station of SAAO, using its 0.5-m telescope (and on three nights, the 0.75-m telescope) and The People's Photometer, with an S-20 tube (Dr. Donald Kurtz and his assistant, Fred Marang).

The observing campaigns, conducted primarily in the early months of 1984 and 1985, resulted in a total of 64 nights of data of which 11 were contiguous or overlapping between SAAO and one of the Chilean sites. Since only two longitudes were available, daily gaps in the resultant data were unavoidable; the longest "continuous" run lasted about 14 hours. However, the mere shortening of some of the daily gaps in the record serves to reduce the amplitudes of the cycle/day side-lobes in the Fourier spectra and thus to clarify the identification of the true frequencies.

The observing routines at all three observatories were essentially the same. Measurements consisted of continuous 20-second integrations of HD 60435 through a Johnson B filter. (A broad bandpass was necessary to ensure sufficiently high photon count rates. White light measurements would guarantee good rates, but would have made extinction

+ An observer had been recruited to monitor the star from a fourth observatory in New Zealand during the 1985 campaign, but no results were obtained from there.

corrections and comparisons to the results of other observers more difficult. The Johnson system had already been employed by previous observers in the field; the B filter was chosen since earlier multicolour observations of roAp stars (e.g. Kurtz 1980) indicated that oscillation amplitudes are much smaller in V.) A large (~30-40 arcsec) diaphragm was used to minimize edge effects and guiding errors. Star observations were occasionally interrupted for sky background measurements and telescope guiding. (At CTIO, however, an offset guider was employed.) Sky readings were made as often as once an hour when the moon was above the horizon, but spaced aperiodically to avoid introducing additional aliases to the data.

Typical stellar counting rates at the LCO telescope were ~12000 counts s^{-1}; at CTIO, ~23000 counts s^{-1}. The sky background varied between about 15% (during full moon and at large zenith distances) down to 0.2% (during "dark time") of the stellar photon flux.

Numbers of counts and starting times of integration were automatically recorded by computer on various media, depending on the observatory and year (e.g. LCO 1984 - thermal printer tape; LCO 1985 - floppy disk; CTIO - magnetic tape). The times were obtained from the computers' internal clocks, synchronized at the beginning of each night with WWV standard time signals to within 0.5 second or better. (The drift of each of the clocks was less than 1 second in 24 hours.)

A complete log of observations is provided in Table 2.1, listing calendar and Julian date, observatory and observer, length (in hours) and number of integrations per night, and the standard deviation, σ (in mmag), of one 20-sec integration relative to the nightly mean. (The term σ contains contributions from the Poisson noise of the measure-

TABLE 1
LOG OF PHOTOMETRIC OBSERVATIONS

Date	HJD (2440000+)	observatory/ observer	t (hr)[1]		N	σ (mmag)	A_{999} (mmag)
			First campaign				
1984 Jan 19/20	5719	LCO/JMM	7 33		1186	8 1	1 7
20/21	5720	LCO/JMM	6 89		1110	8 4	1.8
21/22	5721	LCO/JMM	7 15		1128	11 7	2 5
22/23	5722	LCO/JMM	7.46		1273	8 8	1 8
23/24	5723	LCO/JMM	7.54		1280	5 6	1 1
25/26	5725	SAAO/DWK	6 48		1105	3 8	0 8
		LCO/JMM	7.47	(13.43)	1281	6 1	1.2
26/27	5726	SAAO/DWK	4.64		789	3 6	0.9
		LCO/JMM	7.38	(12.02)	1260	12 1	2.4
28/29	5728	SAAO/DWK	6.63		1110	4 1	0.9
		LCO/JMM	6.74	(13.53)	1149	7.5	1.6
29/30	5729	SAAO/DWK	4.70		829	3.5	0.9
		LCO/JMM	7.46	(14.58)	1279	17 0	3.4
30/31	5730	SAAO/DWK	6.20		1099	3.2	0.7
		LCO/JMM	7.65	(13.59)	1316	11 5	2.2
Jan 31/Feb 1	5731	SAAO/DWK	5.71		1007	3 [illegible]	0.7
		LCO/JMM	7.62	(13.61)	1318	9.6	1.9
Feb 1/2	5732	SAAO/DWK	5.76		1024	4.0	0.9
2/3	5733	SAAO/DWK	5.61		993	2.9	0.6
3/4	5734	SAAO/DWK	5.66		1004	3.2	0.7
4/5	5735	SAAO/DWK	5.42		962	3.8	0.9
5/6	5736	SAAO/DWK	5.96		1057	3.4	0.7
6/7	5737	SAAO/DWK	1.89		328	2 8	1.1
			Second campaign				
1984 Nov 13/14	6019	SAAO/DWK	1.32		217	4.5	2.0
15/16	6021	SAAO/DWK	1.20		204	4.9	2.2
16/17	6022	SAAO/DWK	2.82		477	4.7	1.4
17/18	6023	SAAO/DWK	2.65		452	4.8	1.5
18/19	6024	SAAO/DWK	2.76		485	8.3	2.5

(continued)

TABLE 2 1 cont'd

Date	HJD (2440000+)	Observatory/ observer	t (hr)[1]	N	σ (mmag)	Adopt (mmag)	
1985 Jan 8/9	6074	SAAO/FM	2 25	371	4 3	1 5	*
9/10	6075	SAAO/FM	0.48	77	5 5	3 8	*
		LCO/JMM	6.49 (10 40)	1029	4 4	1 0	*
10/11	6076	SAAO/FM	2.02	315	4 8	1 8	*
11/12	6077	LCO/JMM	7.22	1169	4 8	1 8	
12/13	6078	LCO/JMM	7.20	1181	5 6	1 0	
13/14	6079	LCO/JMM	7.20	1144	5 3	1 1	*
16/17	6082	SAAO/FM	2.00	326	6 9	1 9	*
17/18	6083	SAAO/FM	0.47	80	4 7	3 2	
21/22	6087	SAAO/FM	1 74	280	5 0	1 9	*
26/27	6092	SAAO/DWK	2.93	466	8 7	2 7	
27/28	6093	SAAO/DWK	1.99	340	12 2	4 4	
28/29	6094	SAAO/DWK	1.95	336	7 1	2 5	
		LCO/JMM	6.59 (12.82)	1027	13 9	3.0	
29/30	6095	SAAO/DWK	5.63	947	9 7	2.2	
		LCO/JMM	4.85 (10.81)	775	5 9	1.5	
30/31	6096	SAAO/DWK	1.19	182	4 7	2 2	
		LCO/JMM	4.56 (7.54)	722	11 1	2.8	
Jan 31/Feb 1	6097	SAAO/DWK	0.91	148	5 4	2.8	
		LCO/JMM	4.88 (6.51)	757	8 3	2 1	
Feb 1/2	6098	LCO/JMM	4.89	828	7.2	1.7	
2/3	6099	SAAO/DWK	1.76	289	7.2	2.8	
3/4	6100	SAAO/DWK	5.38	909	8.8	2.0	
4/5	6101	SAAO/DWK	5.67	950	8.6	1.9	
		CTIO/JMM	6.40 (12.77)	1051	4 9	0.9	
5/6	6102	CTIO/JMM	7.41	1235	5.0	1.0	
6/7	6103	SAAO/DWK	1.61	231	6.6	2.8	
		CTIO/JMM	7.51 (13.36)	1253	6.0	1.2	
7/8	6104	CTIO/JMM	7.47	1265	3.6	0.7	
8/9	6105	CTIO/JMM	7.22	1211	4.4	0.7	
9/10	6106	CTIO/JMM	6.70	1139	3.7	0.8	
10/11	6107	SAAO/DWK	5.52	921	6.5	1.5	
		CTIO/JMM	6.48 (12.79)	1103	4.1	0.9	
11/12	6108	SAAO/DWK	4.33	648	5.2	1.4	
		CTIO/JMM	6.31 (12.54)	1084	3.2	0.7	
12/13	6109	CTIO/JMM	6.61	1144	3.1	0.6	
13/14	6110	CTIO/JMM	5.22	894	2.5	0.6	*
14/15	6111	CTIO/JMM	6.43	1091	3.3	0.6	
15/16	6112	CTIO/JMM	6.61	1144	5.2	1.1	
Mar 19/20	6144	SAAO/DWK	1.29	222	5.2	2.2	*

[1] The numbers in parentheses represent the total coverage (in hours) from two sites when contiguous sets of observations were obtained.

JMM - Jaymie Matthews; DWK - Donald Kurtz; FM - Fred Marang

ments, sky transparency variations during the night, and any intrinsic variability of the star itself).

The final column of Table 2.1 offers an estimate of the minimum amplitude, $A_{99\%}$ (again in mmag), of an oscillation which should be detectable with 99% confidence in a Fourier periodogram of each night of data. This parameter is based on Scargle's (1982) "false alarm probability" for properly normalized spectra of unequally-spaced time series. (This is also discussed in greater detail in the next chapter.)

Data reduction

The raw LCO and CTIO photometric measurements were reduced by the author at UWO. (The SAAO observations were provided by Dr. Kurtz in the form of instrumental magnitudes already normalized to a mean of zero.) The reduction procedure involved:

i) Linearly interpolated sky subtraction.

ii) Coincident pulse (or "dead time") correction, by a simple commonly-used formula (e.g. Harris *et al.* 1981) valid for counting rates less than 0.5 MHz (Fernie 1976)

$$N = n[1 + \tau n] \qquad (2.1)$$

where N = actual photon arrival rate at the detector, n = number of pulses generated, and τ = the "dead time" of the tube/preamplifier combination (i.e. the shortest time between two photon arrivals in which two distinguishable pulses will be produced). The quoted values of τ for the systems used all fall near 10^{-9} seconds. In any event, for the maximum counting rates encountered in this programme, the coincidence correction is not very important.

iii) Correction for atmospheric extinction. For the initial reductions, a mean first-order extinction coefficient, k_B, for each site was employed. (The coefficient k_B represents the amount of light (in magnitudes) absorbed by one air mass (i.e. the thickness of atmosphere in the direction of the zenith) as measured through the B bandpass. It is usually estimated by measuring the brightness of a star known to be intrinsically constant at several zenith angles and plotting those magnitudes vs. air mass. On a stable night, and if the zenith angles are less than about 60-70°, the points should fall along a straight line whose slope is k_B.)

When the rapid and long-term photometric behaviour of HD 60435 was better understood, k_B was calculated using the programme star itself. The star's *mean* intrinsic variability is considerably less than -0^m01 in B over a 7-8 hour interval. Once this was recognized, observations of HD 60435 were averaged in bins of 20-minute duration to remove the effects of the rapid oscillations. These averages were then used to construct a plot of instrumental magnitude vs. air mass. A least squares straight-line fit to the points yielded an estimate of k_B. The extinction coefficients so derived are recorded in Table 2.2.

iv) Conversion of recorded times to heliocentric Julian dates, centred on the actual intervals of integration.

An example of a light curve of HD 60435, in which the "12-minute" oscillations first found by Kurtz (1984) are easily seen above the noise, is presented in Figure 2.1.

Mean photometry

A rapidly oscillating Ap star also may be expected to exhibit the

TABLE 2.2
EXTINCTION COEFFICIENTS AT LCO AND CTIO

Date	k_B	Date	k_B	Date	k_B
LCO 1984		*LCO 1985*		*CTIO 1985*	
Jan 19/20	0.33	Jan 9/10	0.35	Feb 4/5	0.26
20/21	0.29	11/12	0.32	5/6	0.20
21/22	0.33	12/13	0.34	6/7	0.19
22/23	0.34	13/14	0.32	7/8	0.21
23/24	0.38	28/29	0.28	8/9	0.18
24/25	0.26	29/30	0.31	9/10	0.21
25/26	0.26	30/31	....	10/11	0.20
26/27	....	Jan 31/Feb 1	0.22	11/12	0.19
28/29	....	Feb 1/2	0.40	12/13	0.19
29/30	0.22			13/14	0.18
30/31	0.25			14/15	0.15
Jan 31/Feb 1	....			15/16	0.19
	$\langle k_B \rangle = 0.30$		$\langle k_B \rangle = 0.32$		$\langle k_B \rangle = 0.20$

Note - "...." denotes a night during which a reasonable straight-line fit to the extinction plot could not be obtained. On these nights, the mean extinction for the site was used in the reduction.

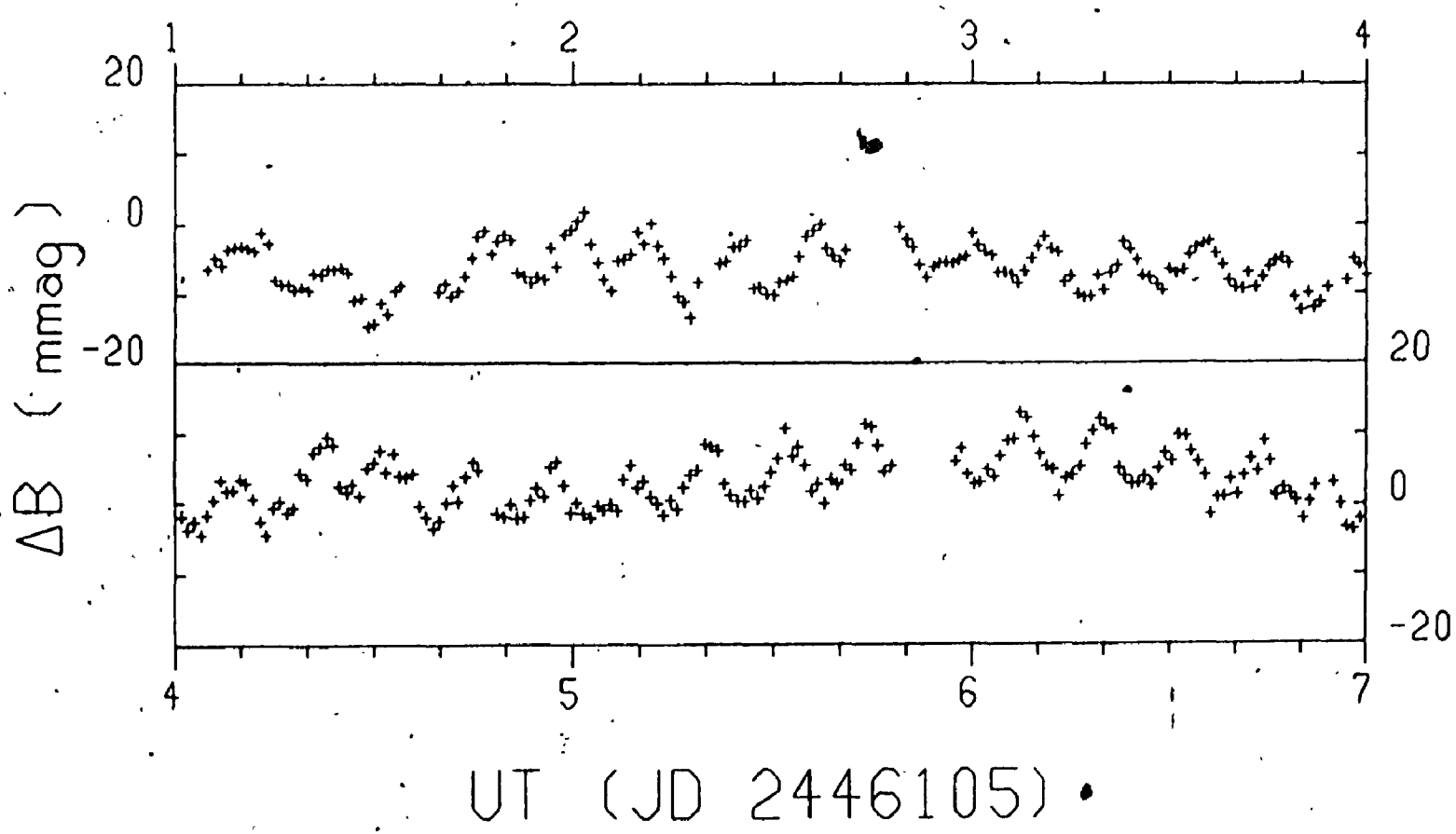

FIGURE 2.1 A light curve of the rapid oscillations of HD 60435. Each cross is an average of three 20-sec integrations through a Johnson B filter.

longer-term photometric variations, associated with rotation, found in many magnetic peculiar stars. Such variations typically have periods of a few days.

In order to determine if this type of variability exists in HD 60435, a comparison star was observed at the beginning and end of most nights. The measurements of the programme star (HD 60435) at the start and end of each run were later averaged over the longest period of oscillation detected. The difference between the respective programme and comparison values, corrected for mean extinction, provided instrumental magnitudes twice each night per site.

The comparison star used was HD 59994AB, which has a visual magnitude of 8.5 and spectral classifications by several authors of A2m, A5, and A7 (Houk and Cowley 1975). Its (1950) coordinates are: $\alpha = 7^h\ 28^m\ 26^s.2$, $\delta = -55°\ 12'\ 0''.2$, placing the star about 2° 40′ from HD 60435. It was selected by Kurtz (1984) for his first observations of HD 60435, as the closest star of comparable spectral type and suitable brightness which showed no evidence of variability.

In general, these comparison measurements were made on each night that rapid photometry took place. On some nights, though, measurements were missed for a variety of reasons (e.g. power failure near the end of the night). Those nights are indicated in Table 2.1 by an asterisk.

The actual differential measurements are presented in Table 2.3.

Spectroscopy

Many Ap stars show spectroscopic variability as well, with the same period as the mean photometric variations. Changes in the line strength of HD 60435 may be correlated with its rapid oscillations.

TABLE 3
MEAN PHOTOMETRY OF HD 60435

HJD (2440000+)	ΔB	Observatory	HJD (2440000+)	ΔB	Observatory
First campaign					
5385.299	0.528	SAAO	5724.559	0.527	LCO
5385.499	0.527	SAAO	5725.552	0.533	LCO
5386.286	0.523	SAAO	5725.567	0.526	SAAO
5387.285	0.535	SAAO	5725.860	0.523	LCO
5387.495	0.531	SAAO	5726.340	0.520	SAAO
5409.260	0.526	SAAO	5726.526	0.518	SAAO
5409.425	0.526	SAAO	5726.556	0.528	LCO
5410.260	0.535	SAAO	5728.305	0.532	SAAO
5410.460	0.537	SAAO	5728.553	0.535	LCO
5412.261	0.525	SAAO	5728.560	0.535	SAAO
5412.425	0.520	SAAO	5728.862	0.539	LCO
5413.260	0.534	SAAO	5729.302	0.549	SAAO
5413.450	0.535	SAAO	5729.553	0.547	LCO
5415.258	0.540	SAAO	5729.902	0.538	LCO
5415.426	0.536	SAAO	5730.303	0.534	SAAO
5423.251	0.525	SAAO	5730.505	0.536	LCO
5426.249	0.518	SAAO	5730.554	0.529	SAAO
5427.249	0.525	SAAO	5731.303	0.518	SAAO
5427.326	0.523	SAAO	5731.533	0.519	SAAO
5428.247	0.530	SAAO	5731.550	0.521	LCO
5429.372	0.531	SAAO	5731.865	0.506	LCO
5719.545	0.521	LCO	5732.303	0.520	SAAO
5719.847	0.513	LCO	5732.535	0.526	SAAO
5720.568	0.528	LCO	5733.301	0.530	SAAO
5720.852	0.543	LCO	5733.527	0.528	SAAO
5721.567	0.539	LCO	5734.301	0.520	SAAO
5721.861	0.538	LCO	5734.529	0.517	SAAO
5722.550	0.535	LCO	5735.300	0.527	SAAO
5722.857	0.522	LCO	5735.518	0.521	SAAO
5723.532	0.514	LCO	5736.298	0.542	SAAO
5723.863	0.514	LCO	5736.539	0.535	SAAO
			5737.300	0.544	SAAO

Note - ΔB = B(HD 60435) - B(HD 59994);
LCO magnitudes normalized to SAAO values;
<ΔB(SAAO)> = <ΔB(LCO)> + 0.019.

(continued)

TABLE 2.3 (cont'd)

HJD (2440000+)	ΔB	Observatory	HJD (2440000+)	ΔB	Observatory
		Second campaign			
6019.479	0.514	SAAO	6097.554	0.540	LCO
6021.541	0.538	SAAO	6097.757	0.540	LCO
6022.468	0.525	SAAO	6098.552	0.527	LCO
6022.578	0.525	SAAO	6099.440	0.522	SAAO
6023.476	0.517	SAAO	6100.298	0.516	SAAO
6023.579	0.520	SAAO	6101.295	0.522	SAAO
6024.468	0.525	SAAO	6101.551	0.512	CTIO
6024.576	0.528	SAAO	6102.542	0.511	CTIO
6077.545	0.505	LCO	6103.301	0.512	SAAO
6078.554	0.518	LCO	6103.540	0.510	CTIO
6092.342	0.513	SAAO (0.75)	6104.538	0.531	CTIO
6093.303	0.529	SAAO (0.75)	6105.544	0.544	CTIO
6094.300	0.524	SAAO (0.75)	6106.535	0.536	CTIO
6094.552	0.520	LCO	6107.286	0.519	SAAO
6095.305	0.516	SAAO	6107.507	0.524	SAAO
6095.548	0.521	LCO	6107.544	0.515	CTIO
6095.753	0.523	LCO	6108.290	0.523	SAAO
6096.432	0.520	SAAO	6108.541	0.509	CTIO
6096.553	0.519	LCO	6109.539	0.526	CTIO
6097.489	0.539	SAAO	6111.546	0.518	CTIO
			6112.538	0.537	CTIO

Note - Magnitudes obtained at SAAO 0.75-m telescope normalized with respect to other measurements;
<ΔB(LCO,CTIO,SAAO 0.5m)> = <ΔB(SAAO 0.75m)> - 0.006.

During the second observing campaign (January/February 1985), a dozen photographic spectra of HD 60435 were obtained by the author and Robert Slawson, using the Garrison spectrograph of the U of T telescope at LCO. (Rapid photometric observations were also collected on the same nights, either simultaneously or contiguously.) The spectra were recorded on IIa-O plates (both baked and unbaked) at a dispersion of 67 A/mm. Wavelength coverage was ~3800 - 4900 Å, with S/N ratios of ~30 - 40. Exposure times were generally under two hours for the baked plates. A spectrum of a neon-argon comparison lamp was exposed for about 40-60 seconds before and after each stellar exposure and adjacent to it on the plate. Table 2.4 is a log of the spectral exposures.

The photographic spectra were later digitized using the PDS microdensitometer of the David Dunlap Observatory for quantitative analysis of any line strength variations. Continuum flattening, wavelength calibration (using the Ne-Ar comparison spectra), and normalization of the scans were performed at the same time.

TABLE 2.4
LOG OF SPECTROSCOPIC OBSERVATIONS

Date (1985)	HJD (2440000+)	UT (Start)	Length of exposure (min)	Observer	LCO/CTIO photometry on same night?
Jan 30/31	6096	06:39	129	JMM	✓
Jan 31/Feb 1	6097	06:33	130	JMM	✓
Feb 1/2	6098	06:32	127	JMM	✓
2/3	6099	05:04	110	RWS	
3/4	6100	01:00	101	RWS	
4/5	6101	06:02	110	RWS	✓
5/6	6102	06:19	118	RWS	✓
6/7	6103	00:47	109	RWS	✓
7/8	6104	02:38	114	RWS	✓
8/9	6105	07:11	120	RWS	✓
9/10	6106	02:53	113	RWS	✓
10/11	6107	04:00	112	RWS	✓

JMM - Jaymie Matthews; RWS - Robert Slawson

III. FREQUENCY ANALYSIS

Many techniques exist for the detection of periodicities in data. Those applied to the analysis of astronomical photometry include:

▽ Methods which seek to minimize some period-dependent quantity, such as the 'string length' of a set of phase-ordered points (Lafler and Kinman 1965), or the magnitude dispersion in pre-selected phase bins (Stellingwerf 1978), for a set of trial periods.

▽ Maximum Entropy Spectra Analysis (MESA), which attempts to "optimize" the information about the original time series contained in its power spectrum (e.g. Burg 1975).

▽ Least squares fitting to a small number of sinusoids whose periods, amplitudes, and phases are treated as free parameters (e.g. Bevington 1969).

▽ Fourier periodogram analysis (e.g. Wehlau and Leung 1964).

The first two types of analysis, and their kin, make no assumptions about the form of the periodicity in the data; the remainder[+] attempt to represent the light curve by one or more sine waves. If the actual periodicity is markedly nonsinusoidal, then these techniques introduce harmonic terms (at integer multiples of the true frequency) into the solution.

Still, of these approaches, the Fourier periodogram has several advantages. It does not suffer from aliasing in gapped data quite as severely as the first two methods. (Fahlman and Ulrych (1982) have tried to "fill the gaps" in trial data sets by applying a predictive

[+] Scargle (1982) showed that Fourier periodogram analysis and least-squares fitting of sine waves are essentially equivalent.

filter to the observed data segments, to counter this drawback in MESA analysis. However, such techniques have so far only been used for short gaps and their reliability for extended ones is questionable.) The structure of the Fourier "window function" (which determines the sizes and spacing of alias peaks in the periodogram) can be well specified. Also, the statistical nature of the Fourier periodogram is arguably the best understood of the various types of frequency spectra, particularly in the wake of work by Deeming (1975) and Scargle (1982).

The Fourier transform and periodogram

There are many comprehensive reviews of Fourier analysis available to the interested reader (e.g. the texts by Blackman and Tukey (1958), Jenkins and Watts (1968), and Papoulis (1977)). A very brief introduction to the subject is provided below.

For a continuous function of a single variable, f(t), the Fourier transform is given by

$$F(\nu) = \int_{t=-\infty}^{\infty} f(t)\ e^{(i2\pi\nu t)}\ dt \qquad (3.1)$$

where t usually represents time and ν, frequency. When dealing with real data, sampled at a finite number of times t_i ($i = 1,\ldots,N$), one can define a *discrete Fourier transform*,

$$F_N(\nu) = \sum_{n=1}^{N} f(t_i)\ e^{(i2\pi\nu t_i)}. \qquad (3.2)$$

(A particular case of the discrete transform, where $\Delta t = t_i - t_{i-1}$ = constant, can be calculated using an algorithm known as the Fast Fourier Transform or FFT. It is so named because it makes very

efficient use of machine time. Unfortunately, the large gaps between nights of data make use of an FFT impractical for analysis of more than a single night's worth of HD 60435 data at a time. Since the computing time needed for one night of data using the general form of the transform is quite small, no significant advantage is gained by switching to the FFT method for this analysis.)

For equal data spacing, the transform need be evaluated only up to an upper limiting frequency known as the Nyquist frequency,

$$\nu_{Nyq} = 1/(2\Delta t). \qquad (3.3)$$

Above this limit, the spectrum is a reflected image of the power present at $\nu < \nu_{Nyq}$. No additional information about the Fourier composition of the time series is available in this regime. When the data is not equally spaced, the Nyquist frequency is not rigourously defined. Scargle (1982) suggests the use of a "generalized" Nyquist frequency, using the *mean* data spacing as Δt in equation (3.3).

For the purposes of numerical evaluation, equation (3.2) can be expanded into its real and imaginary parts,

$$F_N(\nu) = \sum_{i=1}^{N} f(t_i) \left[\cos(2\pi\nu t_i) + i\cdot\sin(2\pi\nu t_i)\right] \qquad (3.2a)$$

and the periodogram -- an estimate of Fourier amplitude as a function of frequency - becomes

$$P_N(\nu) = \frac{2}{N}\left\{\left[\sum_{i=1}^{N} f(t_i)\cos(2\pi\nu t_i)\right]^2 + \left[\sum_{i=1}^{N} f(t_i)\sin(2\pi\nu t_i)\right]^2\right\}. \qquad (3.4)$$

Deeming (1975) has described the 'pathology' of periodogram analysis of unequally-spaced time series. His algorithm has found

widespread use in the astronomical applications of Fourier analysis. Scargle (1982) later modified that classical periodogram to recover the simple statistical behaviour of the equally-spaced case. He developed an expression for the "false alarm probability". Since power at a given frequency is exponentially distributed about that frequency, the probability η that a peak of height z (in power) occurs in a periodogram of a sample of pure white noise is

$$\eta = 1 - (1 - e^{-z})^N \qquad (3.5)$$

where N is the number of *independent* frequencies which are searched and the power z has been normalized with respect to the standard deviation of the sample. (Horne and Baliunas (1986) provide an empirical formula for the number of independent frequencies which are available from a given number of data, based for the most part on samples of even spacing.) One can then set some limiting probability, say $\eta = 0.01$, to calculate a minimum peak height above which there is only a 1% probability of observing a peak arising solely due to noise.

To apply the Scargle criterion to an *amplitude* rather than a power spectrum, z (actually a power "signal-to-noise" ratio) is expressed as

$$z = N_o \left[\frac{X}{2\sigma} \right]^2 \qquad (3.6)$$

where N_o = the number of points in the time series, X = the amplitude of the peak, and σ = the standard deviation of the data.

Values of the amplitudes corresponding to $\eta = 0.01$ (i.e. 99% confidence) and $N \leq 2000$ for the nightly data samples of HD 60435 were included in Table 2.1. These limiting amplitudes represent fairly conservative estimates for the 99% confidence level. The Scargle criterion is strictly valid for a data set which contains only a single

frequency and white noise. The results contained in this work demonstrate that HD 60435 can undergo multiple oscillations at one time. The presence of two or more oscillations simultaneously will raise the calculated value of σ, which in turn results in an overestimate of $A_{99\%}$. Also, the noise spectrum for non-differential photometry is *not* white; there is a significant frequency dependence in that the sky noise is greater at low frequencies (see Figure 4.1). Since only a single value of σ is calculated for each night of data, σ (and again, $A_{99\%}$) is likely overestimated for the frequency range of interest.

Aliasing and the Fourier spectral window

The sampling rate of observations, $1/\Delta t$, during a nightly run is fairly easy to control. It is selected to ensure that the Nyquist frequency for the sample is greater than the highest frequency of interest. Therefore, Nyquist aliasing does not present a problem in the analysis of these data. However, with observations from only two longitudes, daily gaps in the data record - and the resultant 1 d^{-1} aliasing in the Fourier spectrum - cannot be entirely eliminated. Fortunately, the alias signature or *spectral window* can be determined for any given time series.

The observing record might be thought of as an infinite sequence of discrete equally-spaced data multiplied by a series of "box" functions of unit height, whose separations and widths reproduce the segments of time during which data were actually collected. Let us refer to this as the *observing window*, which has a unique transform in the Fourier regime.

Figure 3.1 outlines how a simplified version of a typical astro-

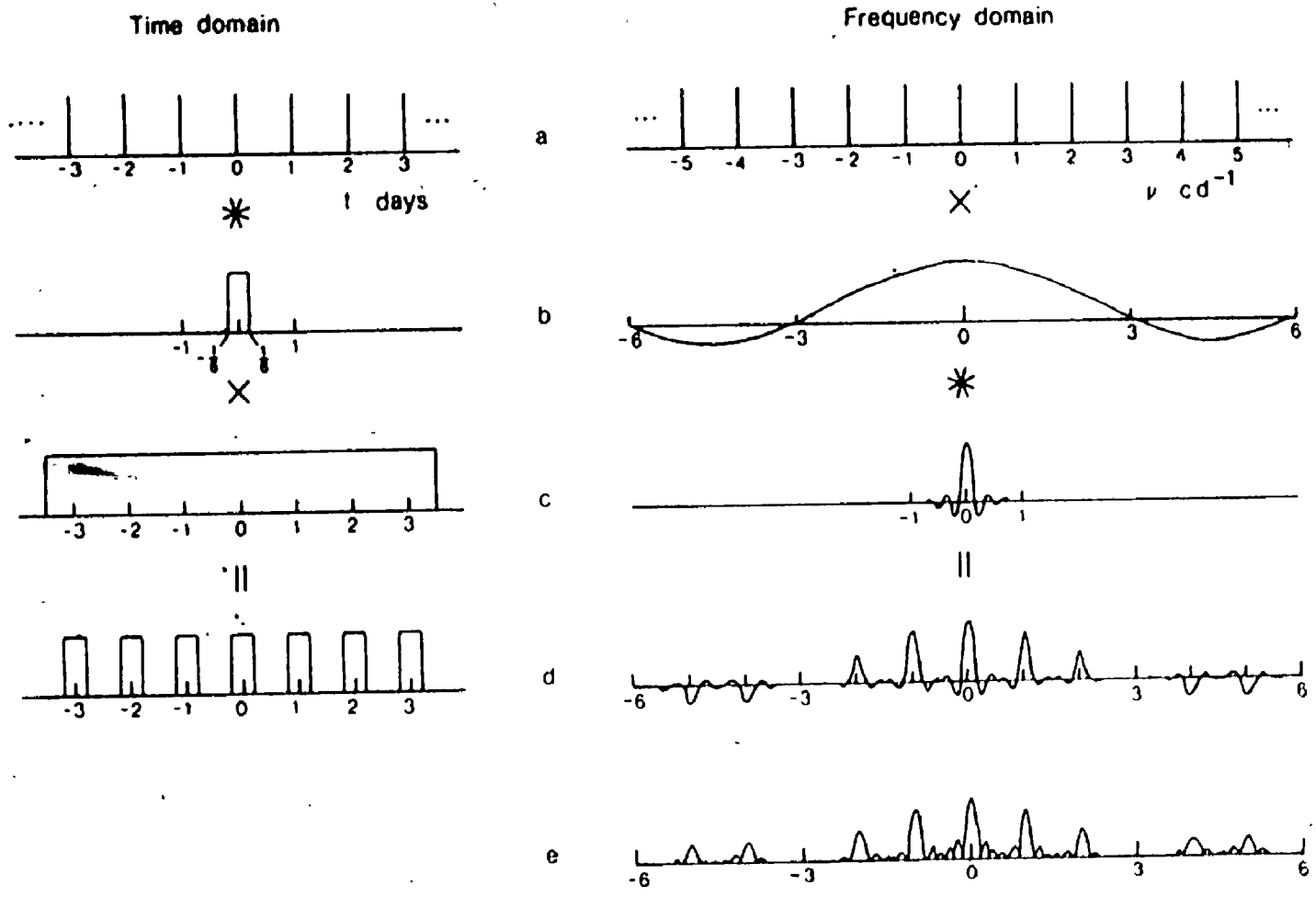

FIGURE 3.1 The "construction" of a simplified astronomical observing window in the time and frequency domains. (The "*" symbol denotes convolution.)

nomical observing window may be represented in both the time and frequency domains. (We assume that, while observations are being made, the sampling rate is high enough so that ν_{Nyq} is much greater than 6 c d^{-1} (the highest frequency represented in the transforms in Figure 3.1). On the left, a Shah comb of delta functions [*a*] spaced by 1 day (the nightly observing cycle) is convolved with a box [*b*] of width 8 hours = 1/3 day (the length of each night's run), and then multiplied by another box [*c*] of width 7 days (the span of the entire run) to produce the completed window [*d*].

The Fourier transform of each contributor to the observing window is shown on the right of Figure 3.1. Note that convolution (multiplication) in the time domain corresponds to multiplication (convolution) in the frequency domain. To the left in panel [*d*] is the tranform of the final window. The actual spectral window (in terms of absolute amplitude) for the sample is given in panel [*e*] of the figure. It shows how a single sinusoid sampled in this way spawns a number of 1 d^{-1} aliases of non-negligible amplitude.

For comparison, Figure 3.2*a* is the actual distribution of the HD 60435 observations during the first campaign, and Figure 3.2*b* is the amplitude window for that sample. The partial "filling-in" of some of the daily gaps has reduced the amplitudes of the alias sidelobes. Inequalities in the lengths and spacings of the nightly observing "boxes" account for the asymmetry of the spectral window.

The regular pattern of the spectral window helps to pick out true oscillations in a spectrum from random noise peaks. It can also be used to identify the frequencies present in the data by successively removing the power associated with candidate frequencies. Rather than

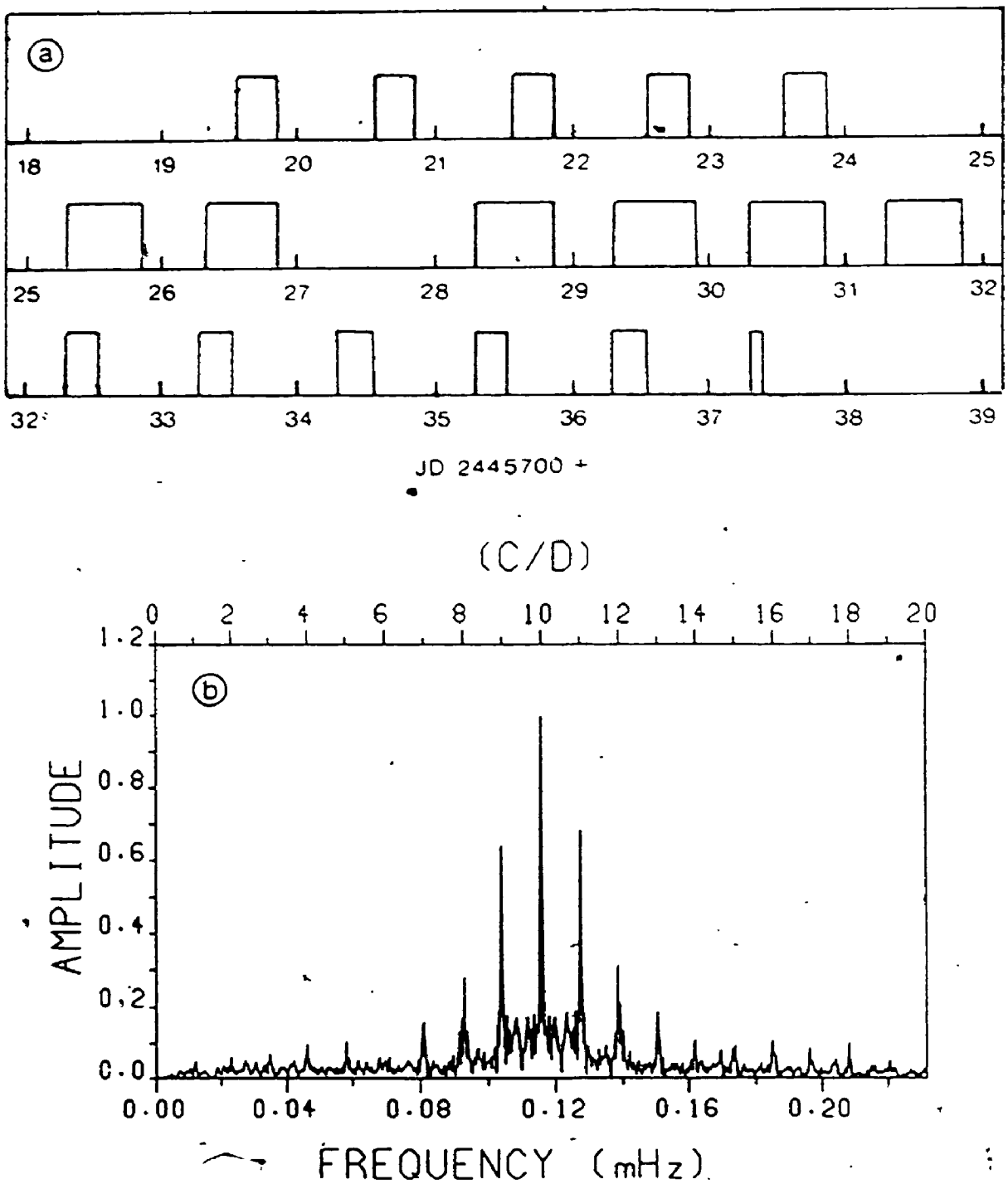

FIGURE 3.2 (*a*) The actual time-domain window for the 1984 observations of HD 60435. (*b*) The spectral (amplitude) window corresponding to (*a*).

doing this in the time domain by *prewhitening* the data (i.e. subtracting from the light curve a sinusoid of the selected frequency, amplitude, and phase), the removal can be carried out in the Fourier domain using the technique of Gray and Desikachary (1973). The spectral window pattern is centred on the chosen frequency in the periodogram, scaled to the amplitude of the peak there, and subtracted from it. The process is repeated until no further alias patterns can be recognized above the noise level of the spectrum.

Analysis of the HD 60435 observations

All of the rapid photometric data of HD 60435, *including* the SAAO observations provided by Kurtz, was analysed by the author at UWO. A routine similar to that of Deeming (1975) was employed. The FORTRAN programme was originally written by Dr. William Wehlau and later modified by the author. (See Appendix B for a complete listing.) There are two major differences between this programme and the Deeming approach:

i) Since the periodograms are always generated with a grid of constant frequency spacing, the number of explicit sine and cosine calculations required are reduced through the use of recursion relations which exploit the simple trigonometric identities

$$\sin(x + \Delta x) = \sin(x)\cos(\Delta x) + \cos(x)\sin(\Delta x) \qquad (3.7a)$$
$$\cos(x + \Delta x) = \cos(x)\cos(\Delta x) - \sin(x)\sin(\Delta x). \qquad (3.7b)$$

These are substituted into equation (3.4), where $x = 2\pi t_i \nu_j$, $\Delta x = 2\pi t_i \Delta\nu$, and $\Delta\nu = \nu_j - \nu_{j-1}$.

ii) Given a set of observations collected over many nights, there are advantages to treating the data in different segments. A periodo-

gram of the entire set will provide the best frequency resolution, while one based on a single night's data will be free of cycle/day aliases. If the data contain a modulated oscillation, then a subset of those data selected at times around maximum amplitude will enhance the signal and minimize the effects of strong beat frequencies.

Therefore, the Fourier periodogram programme is divided into two parts. In the first part, the sums of the sine and cosine terms enclosed in square brackets in equation (3.4) are calculated and stored as intermediate files. In the second, the sum files can be coadded with similar files from other nights of data and normalized to produce periodograms for various combinations of data without expensive recalculation. New data acquired later can also be introduced with relatively little effort.

Tests of this programme by the author using real and simulated data sets (and independent tests by Kurtz (private communication) with a similar periodogram routine) demonstrate that it yields the same results as the Scargle algorithm.

For every night of data, a periodogram was generated over a range of frequencies from zero to the Nyquist frequency (ν_{Nyq} = 25 mHz). At this stage, amplitudes and phases for 2500 frequencies in this range were calculated. The constant frequency spacing of 10 μHz represented a typical oversampling factor of about 3 - 4 x, simply to ensure adequate resolution of any spectral features.

Each amplitude spectrum was examined for significant peaks above the noise level. Significance criteria were twofold: i) The amplitude of the peak must exceed $A_{99\%}$, the minimum above which a peak has a false alarm probability less than 1%, and ii) the peak must occur at a

frequency uncontaminated by sky variations. In general, the latter requirement set a lower frequency limit of approximately 0.5 mHz (period ≈ ½ hour). In none of the spectra were significant peaks detected at frequencies above 4.5 mHz. Therefore, to more clearly display the frequency region of interest for HD 60435, the periodograms in this work are plotted only to a maximum of 4.5 mHz.

The data provided by Kurtz had already been filtered to remove much of the low-frequency power due to transparency/background variations. This was done by successively subtracting sine waves at frequencies corresponding to the low-frequency peaks.

Such filtering was avoided if possible in the author's data. In those cases where long-term variations might introduce harmonic power in the frequency range of interest for this study, the trends were removed by a cubic spline filter fit (see Appendix C) to averages of points separated by no less than 45 minutes. "Before" and "after" spectra were examined to ensure that the filter added no spurious power in the relevant frequency range. The Fourier spectrum of each spline filter, such as the example in Figure 3.3, was also checked for any undesired peaks.

After potential oscillation peaks were singled out, high-resolution ($\Delta\nu$ = 0.1 μHz) amplitude spectra were generated from many nights of data, in order to determine frequency values to greater precision and to study any fine structure present. These periodograms suffer from 1 d^{-1} aliases; in some cases, the spectral window filtering technique described above was used to distinguish individual frequencies where several aliasing patterns overlapped.

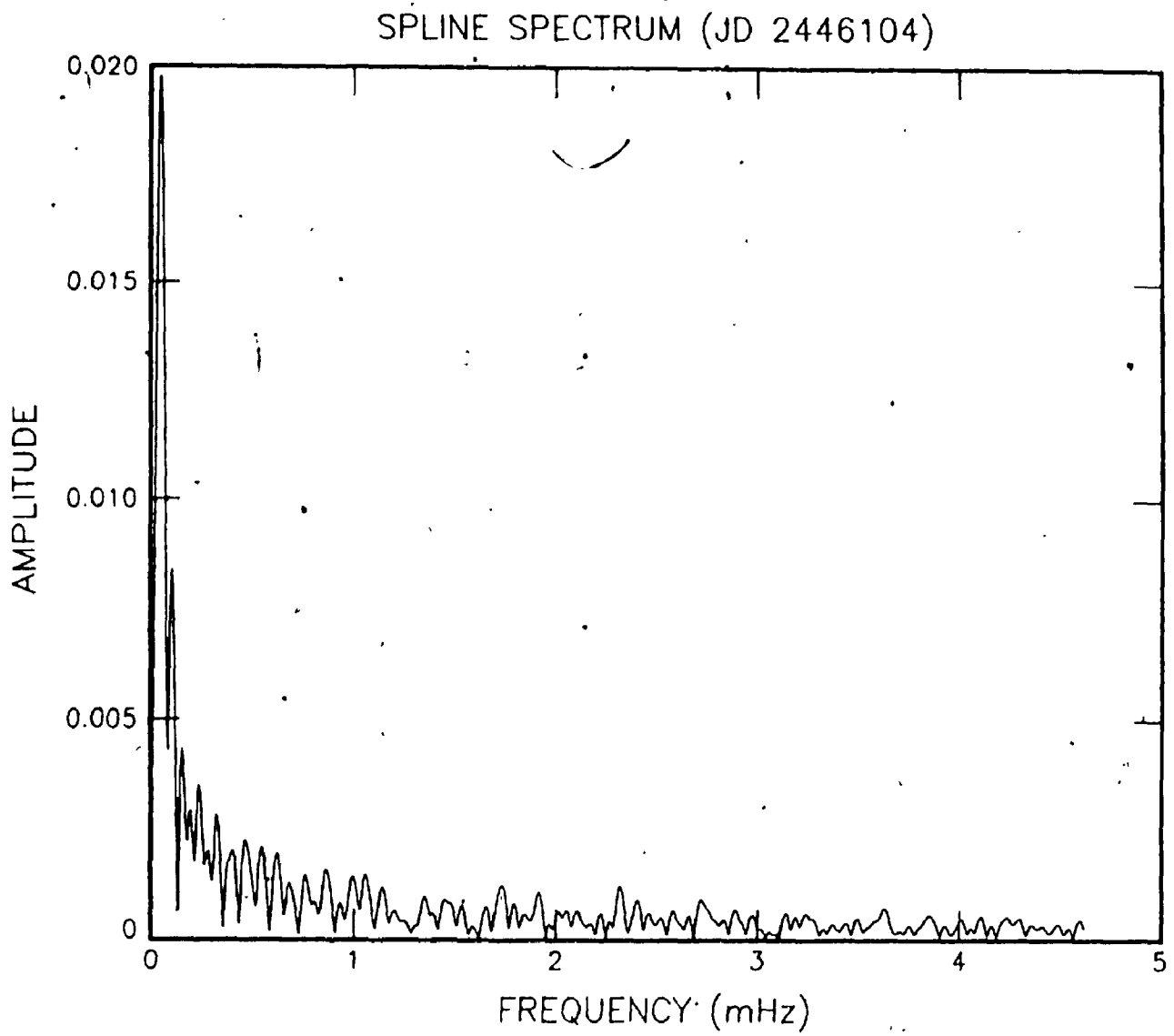

FIGURE 3.3 The Fourier periodogram of one of the spline filters used to remove gradual trends in the rapid photometry introduced by slow sky transparency variations. No significant power is present in this spectrum at $\nu \geq 0.5$ mHz.

IV. THE OSCILLATIONS OF HD 60435

The oscillation spectrum of this star is the most complicated yet studied among the *roAp* stars. Even after two extensive joint observing campaigns, the frequency behaviour of HD 60435 is not completely understood. The findings of the two campaigns are outlined separately below to establish for the reader how the frequency identifications were arrived upon.

Results of the first campaign

The amplitude spectrum of the data from the entire joint run (JD 2445719 - 737), covering frequencies from 0.5 to 4.5 mHz (i.e. periods from just over half an hour to less than four minutes), is shown in Figure 4.1. (At frequencies less than 0.5 mHz, the spectrum is dominated by residual sky variations. The upper limit of 4.5 mHz is close to the "generalized" Nyquist frequency for the complete sample.) Peaks are evident at frequencies near 1.1, 1.4, and 4.2 mHz (periods near 15, 12, and 4 minutes, respectively). Note the trend of higher noise with decreasing frequency. Also note that there is no evidence in the combined data of a 2.8 mHz ("6-minute") variation, as seen by Kurtz (1984) in his discovery observations.

a) Frequencies near 1.4 mHz (P ≈ 11.9 min)

Although the 1.1-mHz peak is the largest in Figure 4.1, the ones near 1.4 mHz - also detected by Kurtz in his earlier observations - appear more often in the spectra of individual nights. Two such spectra are shown in Figure 4.2. The presence of *multiple* oscillations here is revealed by the width and pronounced asymmetry of the peak in

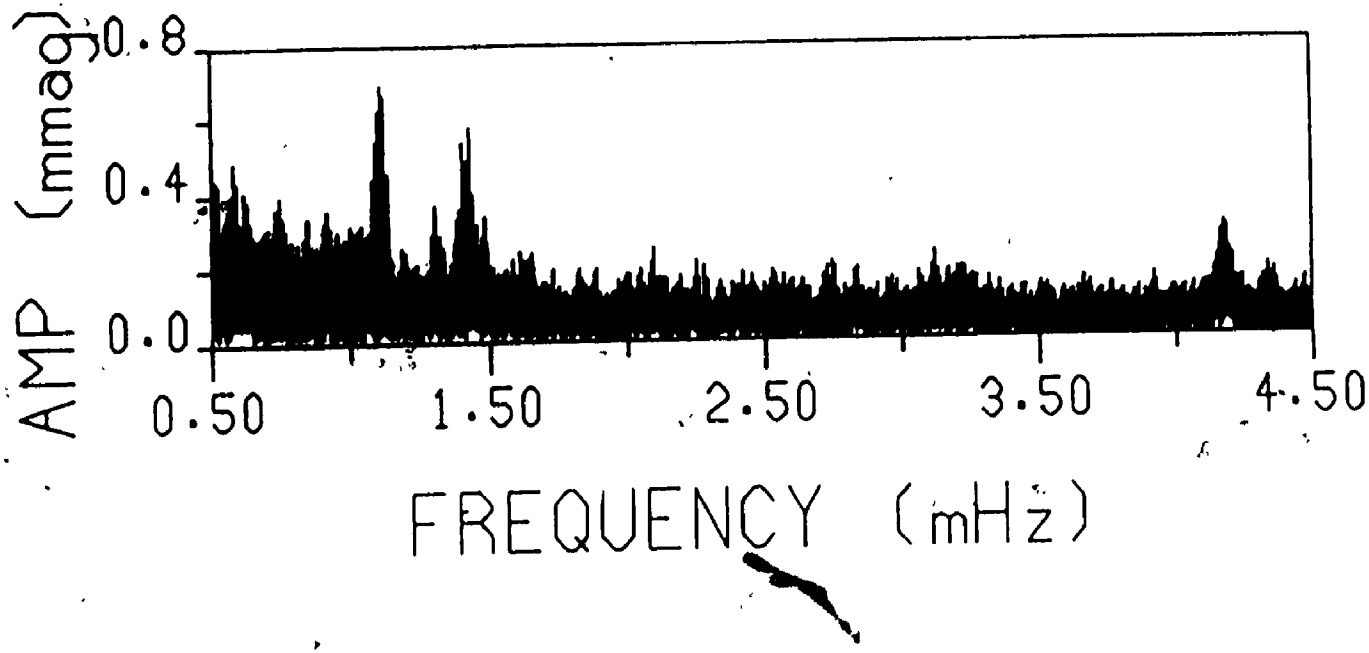

FIGURE 4.1 Amplitude spectrum of the entire set of HD 60435 rapid photometry from the 1984 campaign, spanning 19 nights. The obvious peaks occur at periods near 15, 12 and 4 minutes, respectively. (*Figures 4.1 - 4.9 taken from Matthews, Kurtz and Wehlau (1986).*)

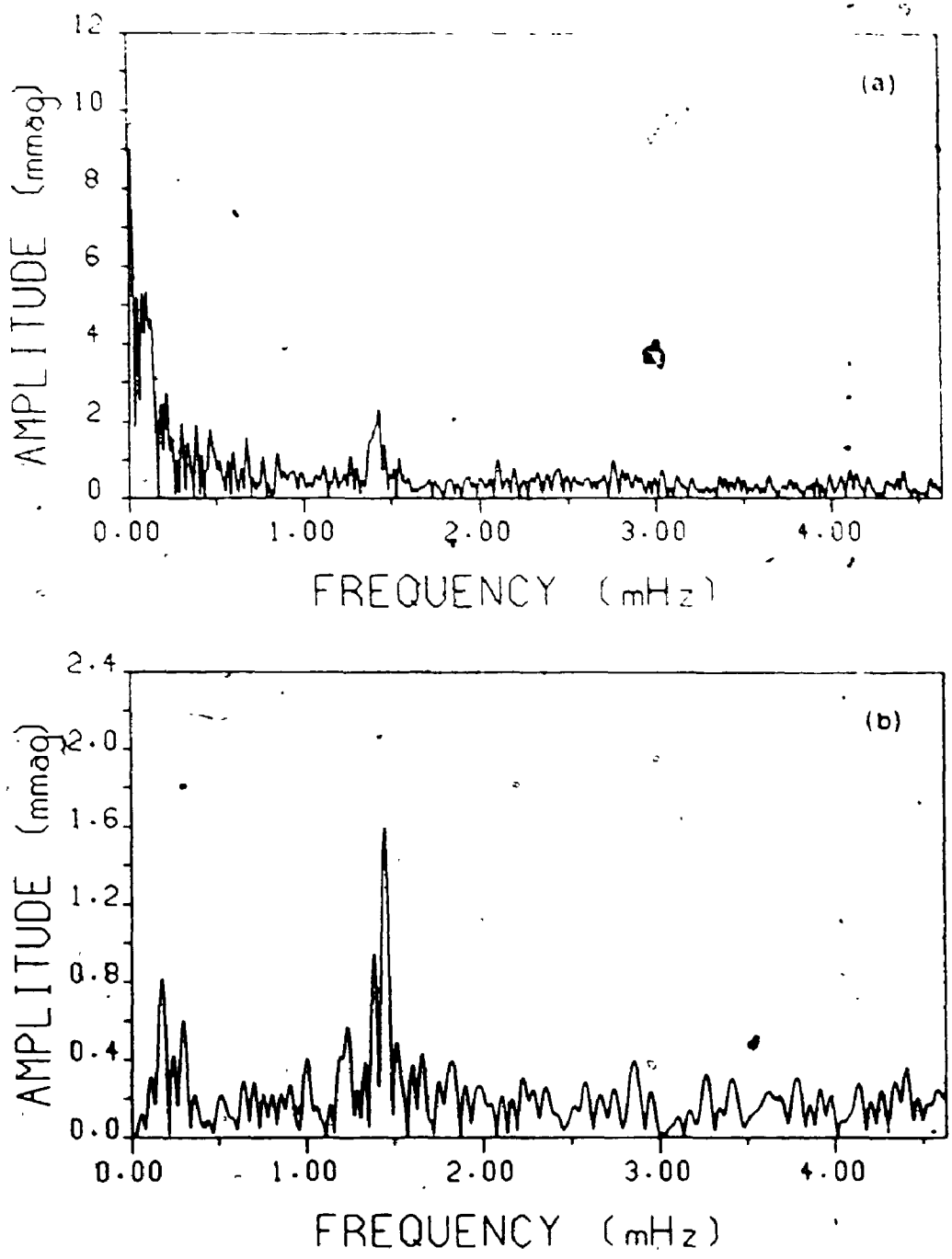

FIGURE 4.2 Amplitude spectra of the light curves of HD 60435 obtained (*a*) from LCO on JD 2445728, showing the peak near 1.4 mHz (P = 12 min), and (*b*) from SAAO on JD 2445736. (Note the different amplitude scales. The peaks at low frequencies in (*a*) are attributed to slow changes in sky transparency which have not been removed from the observations.).

Figure 4.2*a*, and by what appears to be another resolved peak just shortward of the largest one in Figure 4.2*b*.

Modulation of the amplitude of the "12-minute" oscillations over the 18 nights of the joint run is quite obvious in the variation of the 1.4-mHz peak in the nightly power spectra (Figure 4.3). Although no definitive period can be assigned to the modulation from these data alone, its timescale appears to be around eight days. On two nights (JD 2445728 and -729), the LCO and SAAO amplitudes seem discrepant. This may be an indication of more rapid modulation occurring over several hours.

Figure 4.4 is an amplitude spectrum of the entire joint run, this time sampling only frequencies between 1.24 and 1.54 mHz. This shows the fine structure suggested by Figure 4.2, but the situation is complicated by the aliasing. An amplitude spectrum of the contiguous light curve of SAAO and LCO data from JD 2445728, with higher resolution than the spectrum of Figure 4.2*a* but still *no* 1-d^{-1} aliases, is reproduced in Figure 4.5. At least three nearly equally spaced peaks are partially resolved; the spacing is approximately 26.3 μHz. (The resolution of this particular spectrum is $\Delta\nu = 1/13.53\ hr^{-1} = 20.5$ μHz. It is unlikely that the equal spacing of the three peaks is merely an artifact of the resolution limit for the data sample. The other smaller peaks in Figure 4.5 are separated from their neighbours by various unequal intervals ranging from about 21 - 36 μHz.)

The two highest sets of peaks in Figure 4.4, which covers roughly the same frequency range as Figure 4.5 but includes the entire data set, coincide with two of the prominent peaks described above. A third set of peaks matches the remaining frequency. The other peaks are pre-

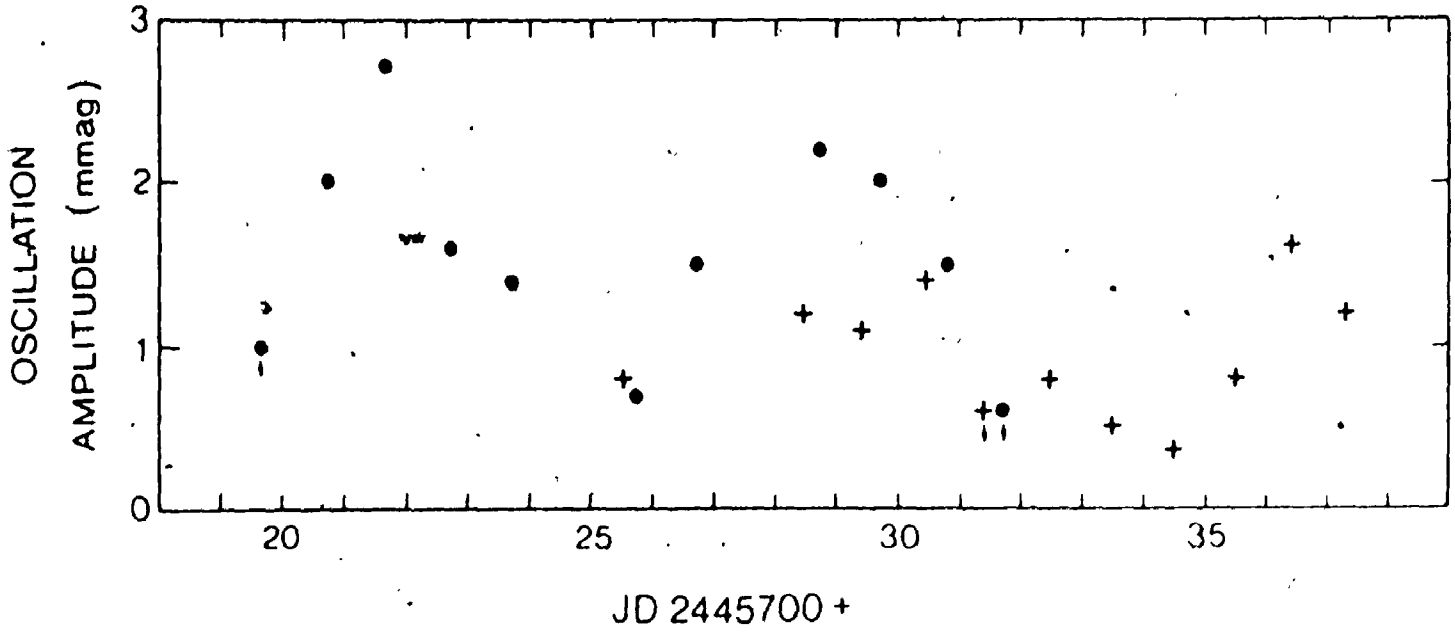

FIGURE 4.3 Amplitudes of the oscillation near 1.4 mHz vs. Julian Date. The amplitudes are estimated from the Fourier spectra of the LCO (dots) and SAAO (plus signs) data. Arrows indicate an upper limit determined by the noise level of the spectrum. The JD plotted is the mean for each nightly run.

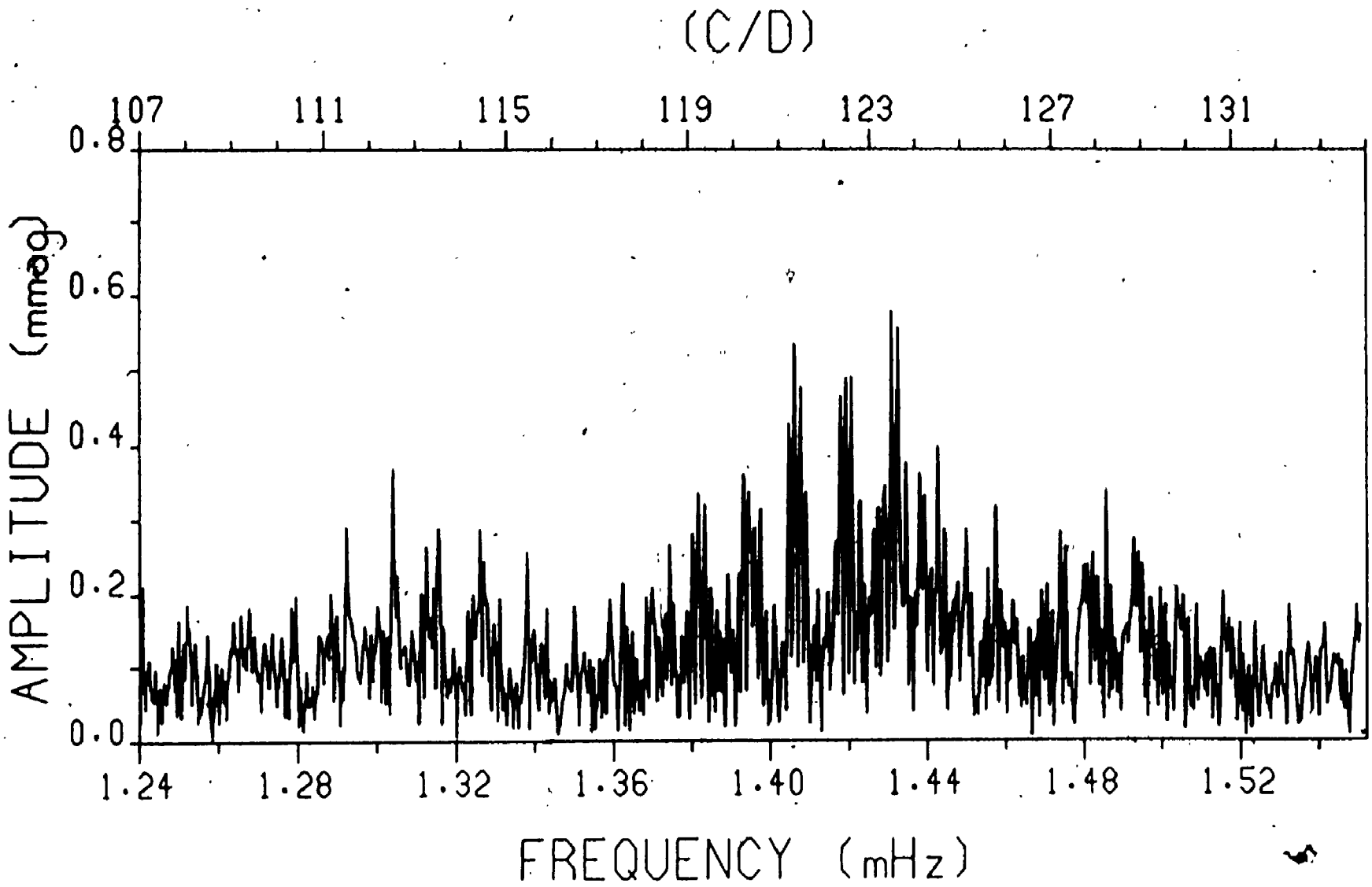

FIGURE 4.4 Amplitude spectrum of the entire 1984 data set showing only the oscillation peaks near 1.4 mHz.

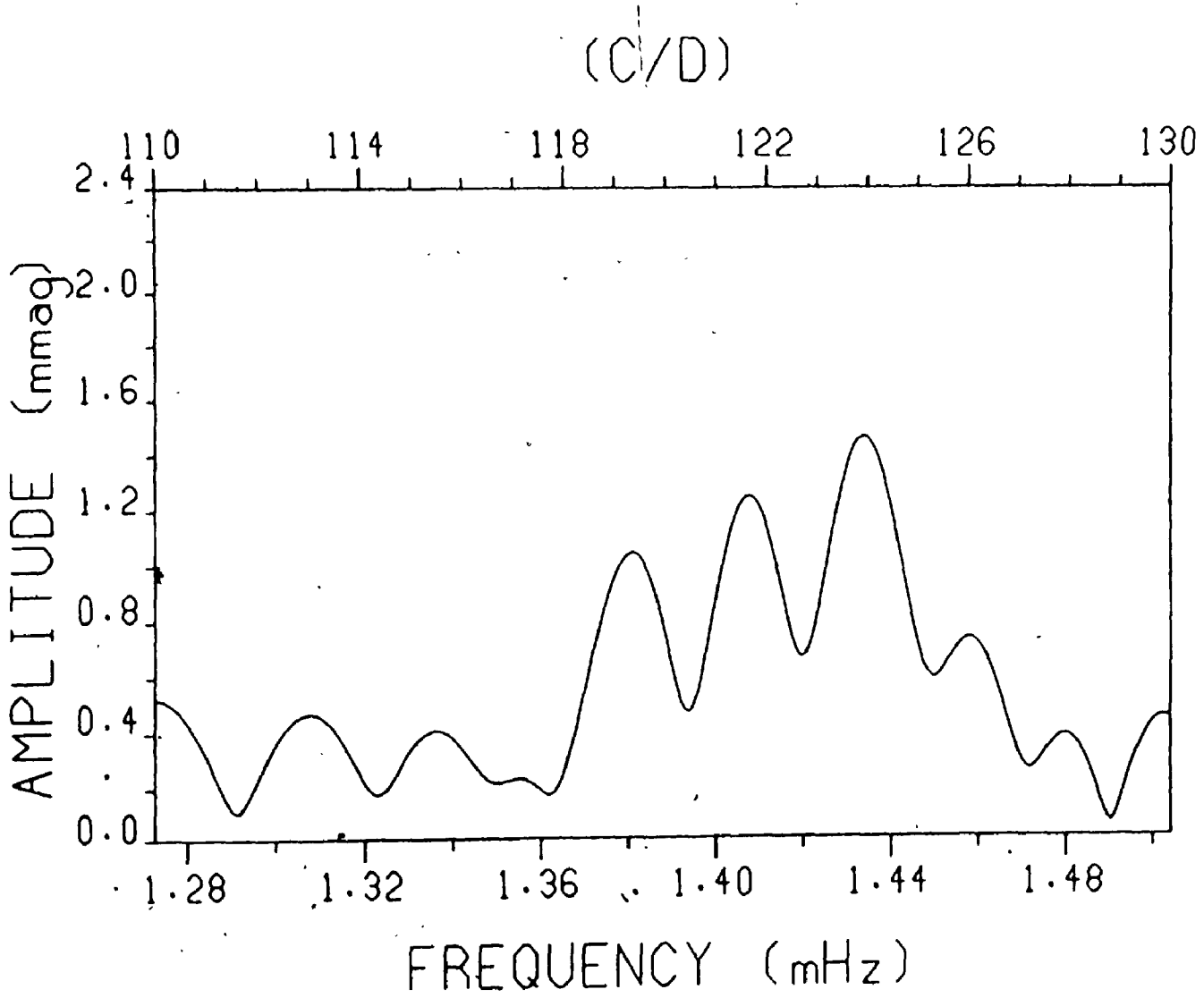

FIGURE 4.5 Amplitude spectrum of the light curve of HD 60435 obtained from LCO and SAAO on JD 2445728, covering the same frequency range as Figure 4.4. Although the resolution is considerably lower, there are no 1 c d^{-1} aliases in this spectrum.

sumed to be the results of individual and co-added aliases.

There is a single frequency at 1.30371 mHz in Figure 4.4 which roughly fits into the spacing pattern recognized in Figure 4.5. Furthermore, in another part of Kurtz's earlier photometry of HD 60435 (JD 2445383 - 387), one observes a frequency at 1.35210 mHz which also falls into this pattern. However, this latter frequency is notably absent from the data set of the first campaign

The entire set of frequencies detected near 1.4 mHz in the first campaign (and including the additional frequency from Kurtz's data) is shown schematically in Figure 4.6.

The fine structure evident in Figure 4.4 has a characteristic equal spacing of 1.4 ± 0.2 μHz. There appears to be at least one triplet present, although the most obvious candidate near 1.42 mHz is a byproduct of the aliases of the components of frequencies at 1.4075 and 1.4336 mHz.

b) Other frequencies

In the first six nights of LCO photometry, oscillations with periods near 15.2 and 4 minutes were observed. These oscillations declined in amplitude until, by the time monitoring had begun at SAAO they had disappeared into the noise. Both frequency peaks are visible in the periodogram shown in Figure 4.7.

Figure 4.8 is an amplitude spectrum of the entire data set, showing only frequencies between 0.98 and 1.22 mHz. The spectrum here has a somewhat unusual structure. One frequency is evidenced by the expected 1-d^{-1} alias sidelobes. However, two other frequencies seem to possess an anomalous aliasing pattern with a spacing of slightly greater than 1 d^{-1} (approximately 1.02 d^{-1} as determined from the

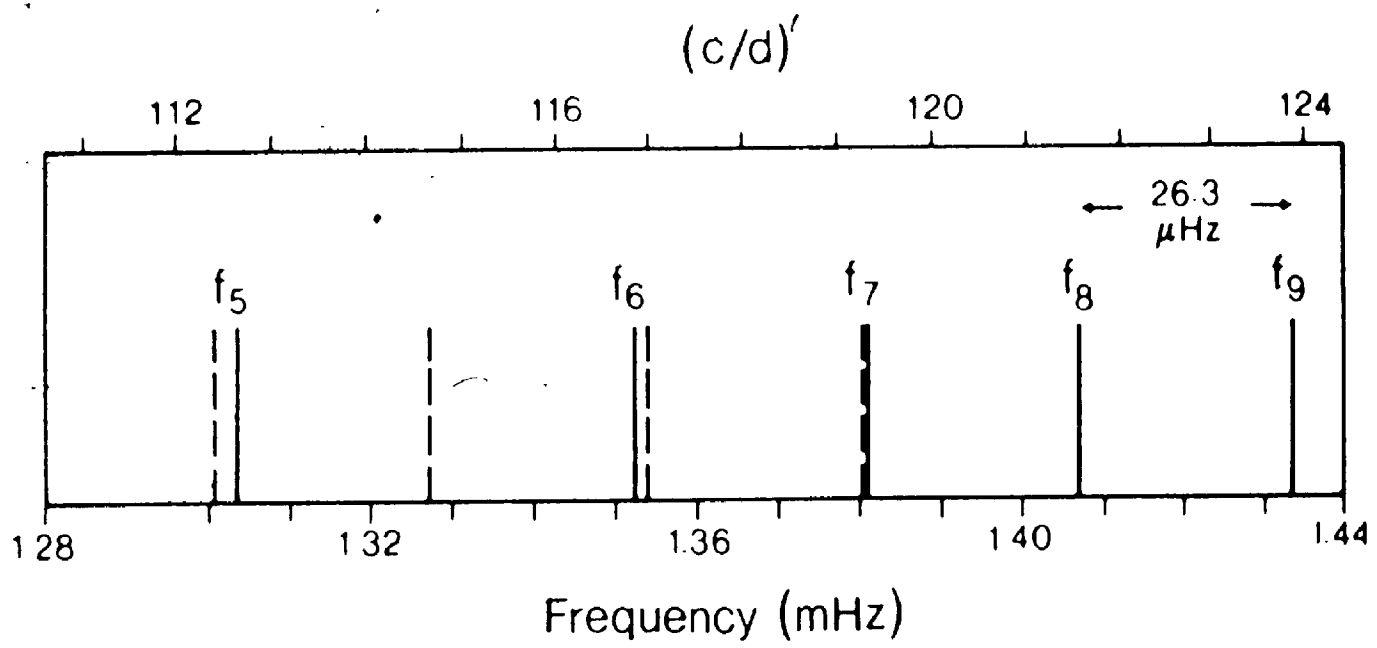

FIGURE 4.6 Schematic representation of the frequencies observed between 1.3 and 1.44 mHz in HD 60435 during the 1984 campaign. Dashed lines represent the expected positions of frequencies if the pattern spacing were a uniform 26.3 mHz.

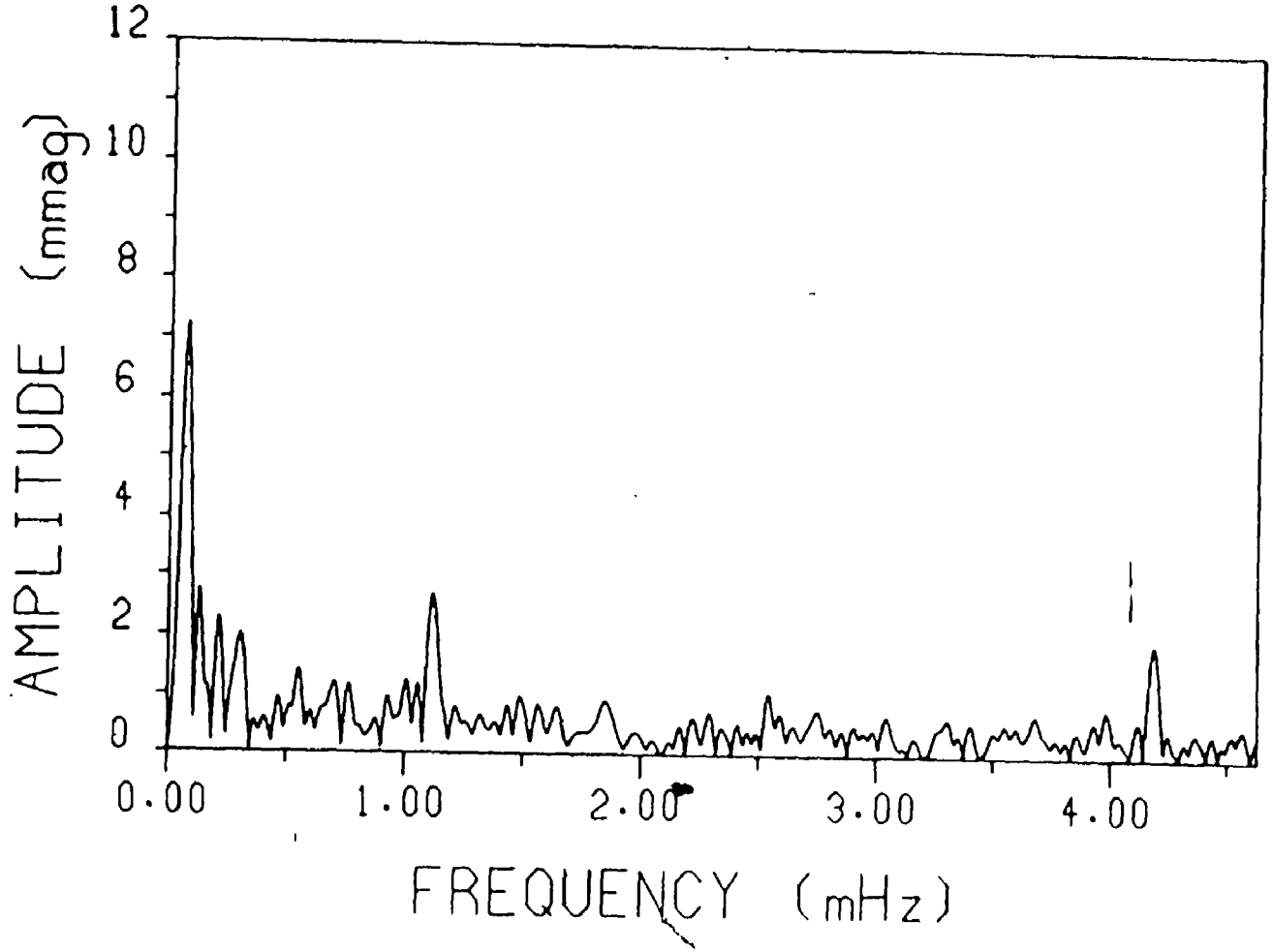

FIGURE 4.7 Amplitude spectrum of LCO observations of HD 60435 on JD 2445719 showing peaks with frequencies near 1.1 and 4.2 mHz (P ≈ 15 and 4 min).

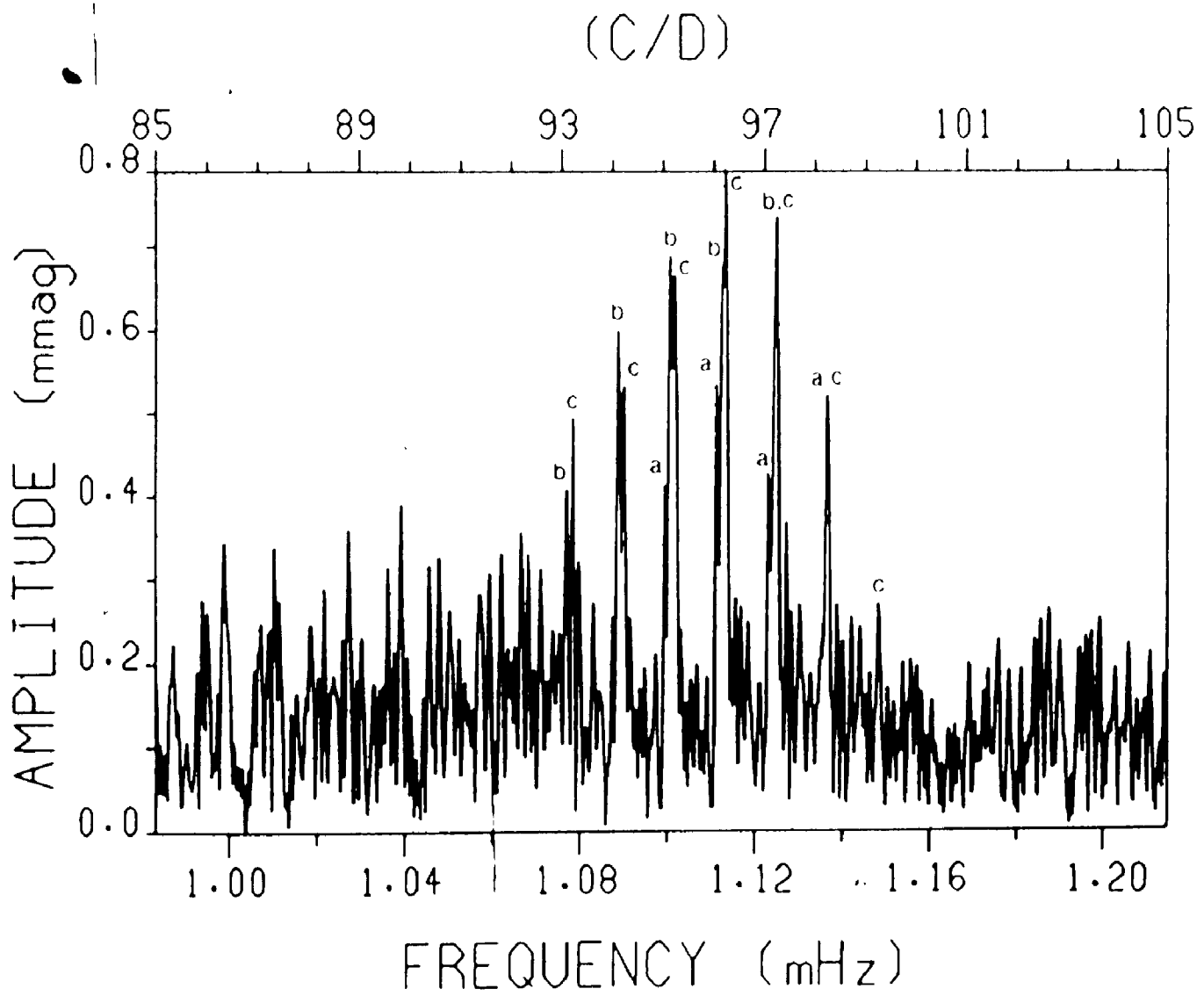

FIGURE 4.8 Amplitude spectrum of the entire 1984 data set showing only the oscillation peaks near 1.1 mHz. The letters refer to the discussion in the text of the unusual aliasing pattern.

maxima of the peaks). The two patterns can be seen to merge into the peaks of the first with increasing frequency. (The three aliasing patterns can be most easily distinguished using the composite peak near 1.10 mHz in Figure 4.8. The right-hand peak [c] belongs to the 1-d^{-1} aliasing pattern; the remaining two [*a*,*b*] are part of patterns with 1.02 d^{-1} spacings. In the peak near 1.125 mHz, for example, two of the peaks have merged completely.)

Such an effect can be produced by the addition of two unresolved aliasing patterns with central peaks of different amplitudes spaced by slightly more than 1 d^{-1}, but the frequency shift would be much smaller than that observed, given the resolution of this spectrum.

Frequency modulation of the oscillations (e.g. an increase in frequency by 0.02 d^{-2}) could reproduce such an anomalous pattern. However, it is difficult to understand how only two of the many frequencies present - all thought to arise from global variations in the star - would be independently modulated. Moreover, the only known mechanism for frequency modulation of pulsation is stellar evolution, certainly neither a rapid nor a selective process. (This argument assumes that the observed variations in HD 60435 are due to pulsation.) It seems most likely that the unusual aliasing pattern arises from the interference of more than three normal aliasing patterns superimposed upon one another.

Using the window filtering technique described in Chapter 3, it is possible to select a frequency triplet centred at 1.10077 mHz with a spacing of 1.39 ± 0.24 μHz (the same as the spacing observed in the spectrum of Figure 3.4, within the uncertainties) and a fourth single frequency at 1.11327 mHz to reproduce the observed spectrum. (The

fourth frequency is offset by 1.08 d^{-1} from the central frequency of the triplet; its proximity to a spacing of exactly 1 d^{-1} may account for the apparently "anomalous" aliasing pattern.) Even so, the reality of this identification is uncertain, since the data sample clearly does not span a single modulation period (if there is one) for these oscillations.

Note: A significant feature of the spectrum in Figure 4.8 is the resolution of any fine structure at all If the oscillations near 1.1 mHz were only present in the first six nights of these LCO data, then additional structure (beyond what is contained in a spectrum of the first six nights) should not be resolvable. But there is indeed more fine structure present. Clearly, some power must be present at these frequencies in subsequent data - albeit at very low amplitudes - to account for this.

The region of the spectrum near 4.2 mHz (P ≈ 4 min), shown in Figure 4.9, provides little information about fine structure, given the low amplitudes of the peaks relative to the noise. Whereas the noise "continua" in the amplitude spectra of Figures 4.4 and 4.8 are relatively flat, the noise level in Figure 4.9 appears raised between the peaks of the one definite aliasing pattern. There may be so many interwoven aliasing patterns that the "continuum" noise level of the spectrum is artificially raised by the co-addition of the bases of the peaks.

Only one frequency is readily identifiable: 4.17307 ± 0.00012 mHz. In light of the aliasing and low amplitudes, it is premature to attempt any other analysis based on this spectrum by itself.

There is little, if any, evidence for the presence of the "six-

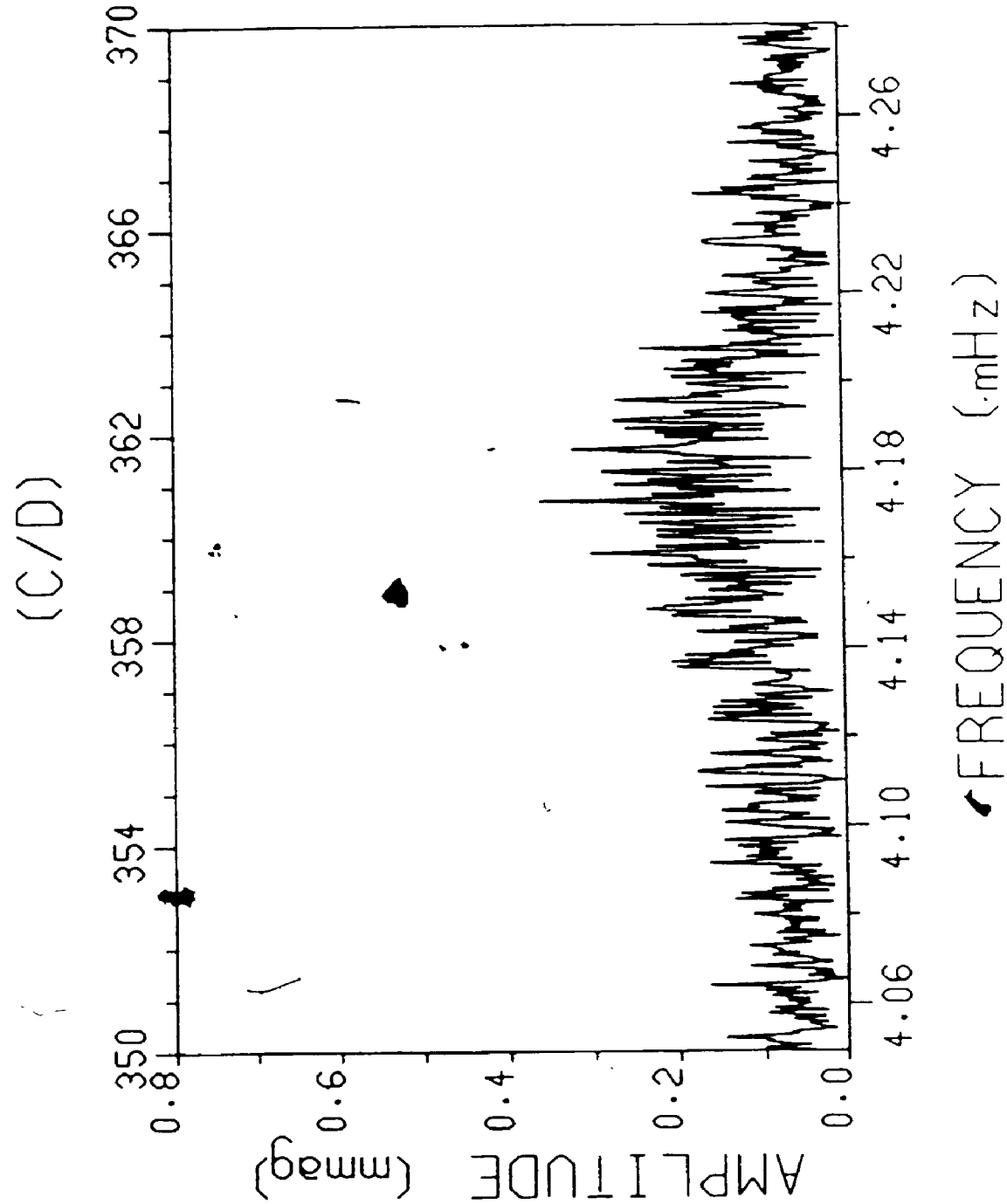

FIGURE 4.9 Amplitude spectrum of the entire 1984 data set showing only the oscillation peaks near 4.2 mHz.

minute" oscillation reported by Kurtz (1984) in any of the data from this initial campaign.

Results of the second campaign

Figure 4.10 is a sample of ten periodograms selected from the set of 35 nights in this campaign. Across each is a dashed line which represents the value of A_{998} for that night, as given in Table 2.1. The peaks evident at frequencies less than about 0.5 mHz reflect residual power which remains after the filtering process described in Chapter III. Peaks which rise above A_{998} are tagged with letters; these have been keyed to the list of frequencies in Table 4.1.

The differences in frequency resolution and noise level in the spectra come about primarily from the respective differences in nightly coverage and observing conditions for the corresponding data sets. The CTIO observations, for example, consist of runs of roughly equal length (6-7 hr) on nights of exceptional sky quality. Therefore the resolution and the values of A_{998} are comparable from spectrum to spectrum over these nights.

The periodograms of Figure 4.10 were chosen to illustrate a few of the noteworthy features of HD 60435's oscillations which came to light during the second campaign:

1. Frequencies near 1.4 mHz continue to dominate; these oscillations are the most persistent and reach the largest amplitudes.

2. The modulation timescale of 7-8 days for those oscillations is evident. JD 2446022, -082, -098, -105, and -112 are nights during which the "12-min" oscillations reached maximum - or near maximum - amplitude.

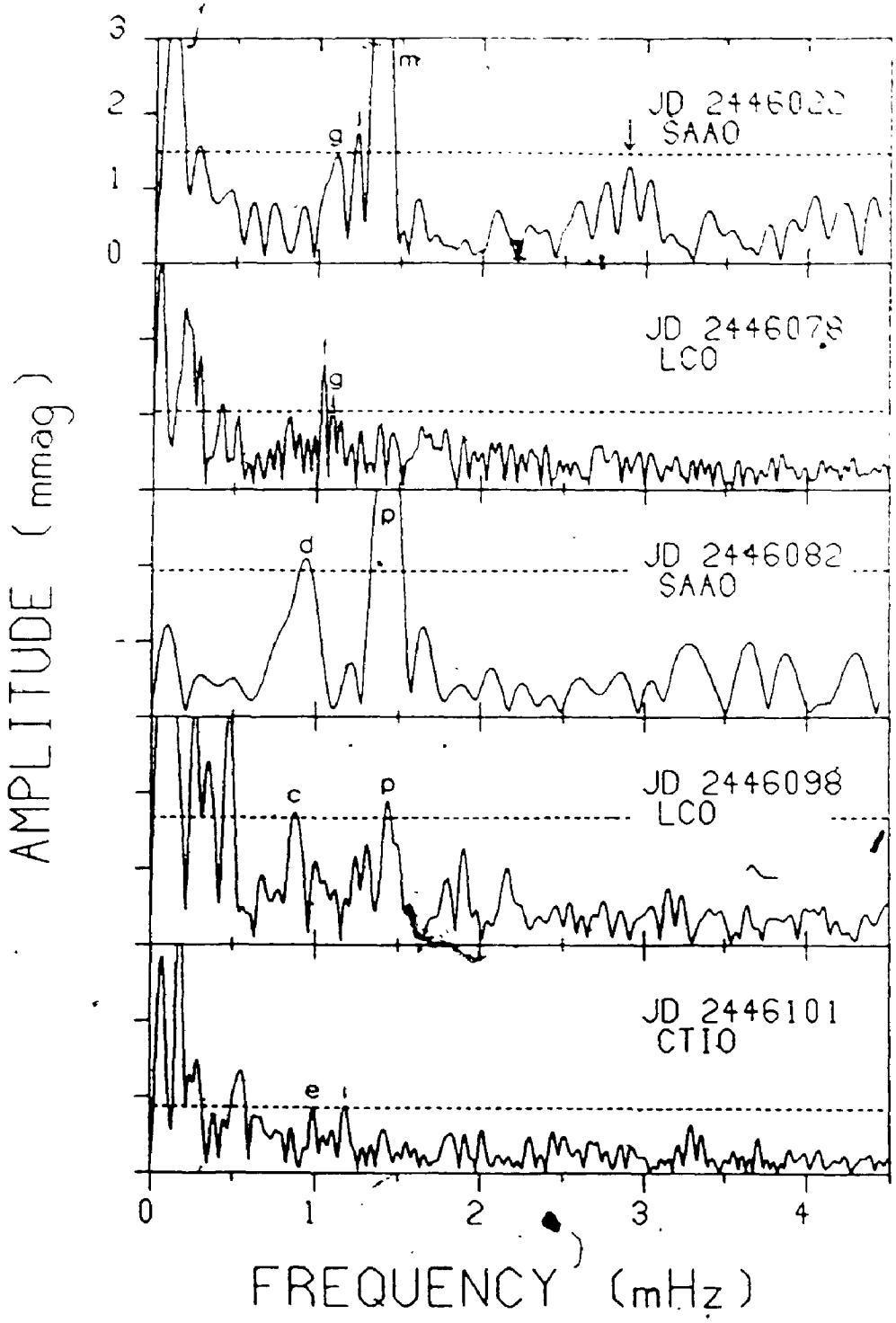

FIGURE 4.10 Amplitude spectra of ten representative nights of rapid photometry of HD 60435 from the 1985 campaign. Peaks at frequencies less than about 0.5 mHz are the residuals of sky transparency variations which have been filtered from the data. The dotted lines indicate amplitudes above

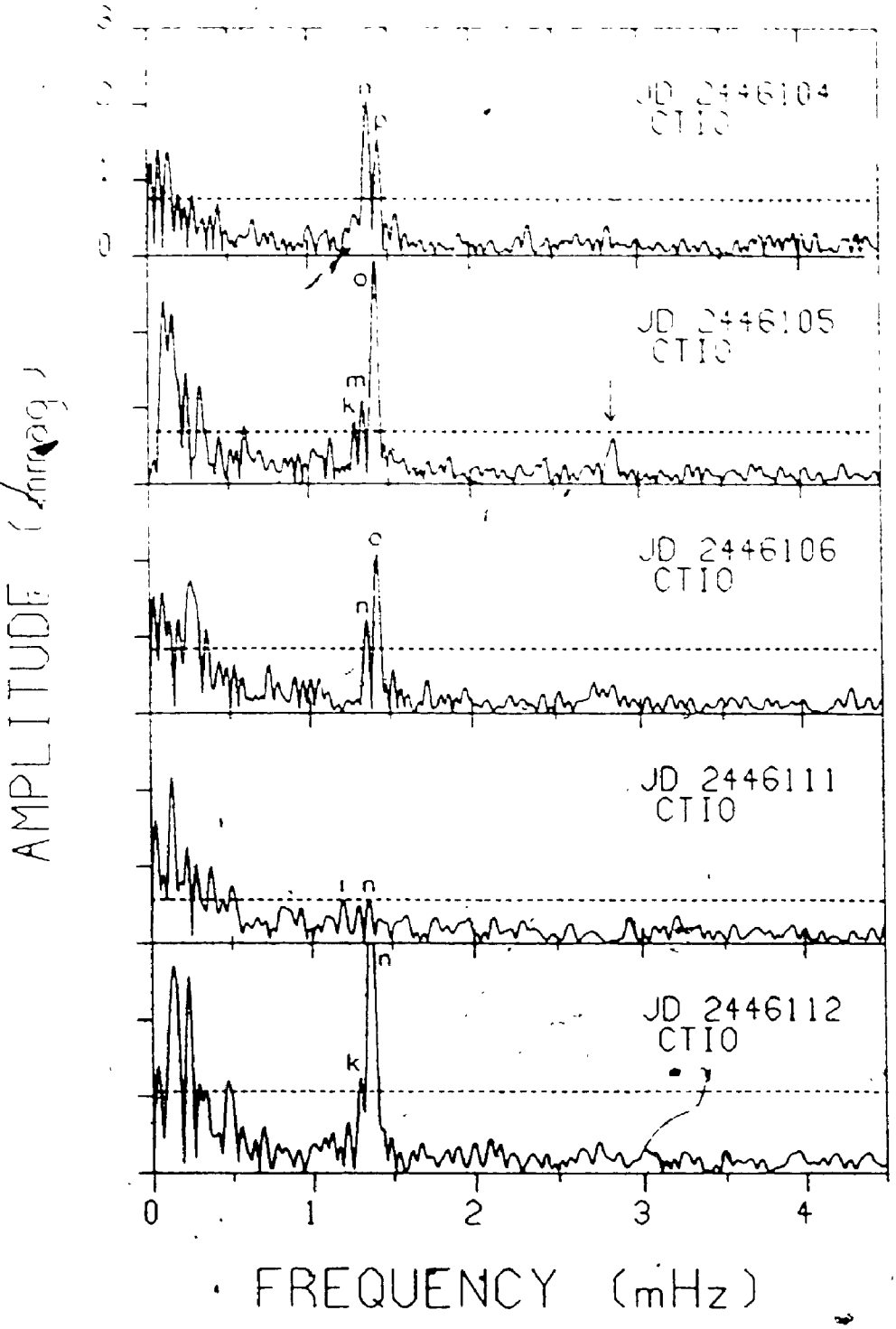

which peaks are considered statistically significant at the 99% level (see discussion in Chapter III). The letters above the peaks are keyed to the list of frequencies in Table 4.1. *(Figures 4.10 and 4.11 are taken from Matthews, Kurtz and Wehlau (1987).)*

TABLE 4.1
FREQUENCIES OBSERVED IN HD 60435

Frequencies in *italics* are values derived from the first campaign

	ν (mHz) + 0.0001	$\left(\frac{\nu - \nu_0}{25.8\ \mu Hz}\right)$	Possible mode[1] (w.r.t. ν_0)	Tentative Identification	Dates detected (JD 2445000 +)
a	0.7090	29.00 - 29	$\begin{bmatrix} n-15 \\ n-14 \end{bmatrix}$, $\ell \pm 1$	[n-14,1]	1077, 1097
b	0.7614	26.97 - 27	$\begin{bmatrix} n-14 \\ n-13 \end{bmatrix}$, $\ell \pm 1$	[n-13,1]	1097
c	0.8428	23.81 - 24	n-12, ℓ	[n-12,2] [n-11,0]	1098
d	0.9397	20.06 - 20	n-10, ℓ	[n-10,2]	1082
e	0.9906	18.09 - 18	n-9, ℓ	[n-9,2]	1101
f	1.0433	16.04 - 16	n-8, ℓ	[n-8,2]	1078
g	1.0990 *1.1008*	13.88 - 14	n-7, ℓ	[n-7,2]	1022, 1078
g'	*1.1133*				*719-723*
h	1.1482	11.98 - 12	n-6, ℓ	[n-6,2]	1077, 1079
i	1.1734	11.00 - 11	$\begin{bmatrix} n-6 \\ n-5 \end{bmatrix}$, $\ell \pm 1$	[n-5,1]	1101
j	1.2250	9.00 - 9	$\begin{bmatrix} n-5 \\ n-4 \end{bmatrix}$, $\ell \pm 1$	[n-4,1]	1022
k	1.2848	6.68[2]			1105, 1112
k'	*1.3037*	5.95 - 6	$\begin{bmatrix} n-4 \\ n-3 \end{bmatrix}$, ℓ	[n-3,2]	*1984 Combined*[3]
l	1.3281	5.00 - 5	$\begin{bmatrix} n-3 \\ n-2 \end{bmatrix}$, $\ell \pm 1$	[n-2,1]	1102, 1105
m	1.3525 *1.3521*[4]	4.06 - 4	n-2, ℓ	[n-2,2]	1019, 1021-23 1079, 1095-96 1105, 1107
n	1.3810 *1.3809*	2.95 - 3	$\begin{bmatrix} n-2 \\ n-1 \end{bmatrix}$, $\ell \pm 1$	[n-1,1]	1099, 1104 1106, 1111-12
o	1.4073 *1.4075*	1.93 - 2	n-1, ℓ	[n-1,2]	1074, 1105-06
p	1.4334 *1.4336*	0.92 - 1	$\begin{bmatrix} n-1 \\ n \end{bmatrix}$, $\ell \pm 1$	[n,1]	1075, 1082 1097-98, 1106
q	1.4572	0	n, ℓ	[n,2]	*1985 Combined*[3]

[1] According to equation (4 1), such that $(n-i), (\ell-j) \geq 0$

[2] $\nu_k = [(7 \times 25.8) - 8\ 2]\ \mu Hz$

[3] Detected in the amplitude spectra of several nights combined.

3. There exists a series of peaks across a range from about 0.7 to 1.5 mHz (i.e. periods from about 20 to 12 min). The low-frequency limit of this range is rather ill-defined, since real oscillations below 0.7 mHz are more likely to be masked by sky noise, or conversely, peaks due to sky noise at these lower frequencies can masquerade as stellar oscillations. In any event, the filter applied to the data invalidates an analysis at frequencies less than about 0.5 mHz.

4. On two of the nights listed in point 2 (JD 2446022 and -105), peaks - indicated by arrows in Figure 4.10 - occur near a frequency of 2.8 mHz (P ≈ 6 min). In these spectra, they have amplitudes just below the 99% confidence level; however, this level has been calculated for the detection of a peak at *any* frequency in the spectrum. The Scargle false-alarm probability of finding a random noise peak at a *particular* frequency (in this case, at a 2:1 ratio with one of the 1.4 mHz peaks) is different. The values of $A_{99\%}$ for a specific frequency in each of the two data sets are approximately 0.9 and 0.5 mmag, respectively. The peaks observed near 2.8 mHz are above these revised confidence limits.

5. Certain peaks can grow to (or decay from) observable amplitudes in less than a day; e.g. the development of peak 'n' in Figure 4.10 between JD 2446111 and -112.

On the basis of spectra like those in Figure 4.10, from both campaigns, a list of observed frequencies in HD 60435 was compiled in Table 4.1. The frequencies were determined to the quoted accuracy using higher resolution spectra of many nights of data (e.g. Figure 4.11b).

An examination of the frequencies of Table 4.1 revealed that

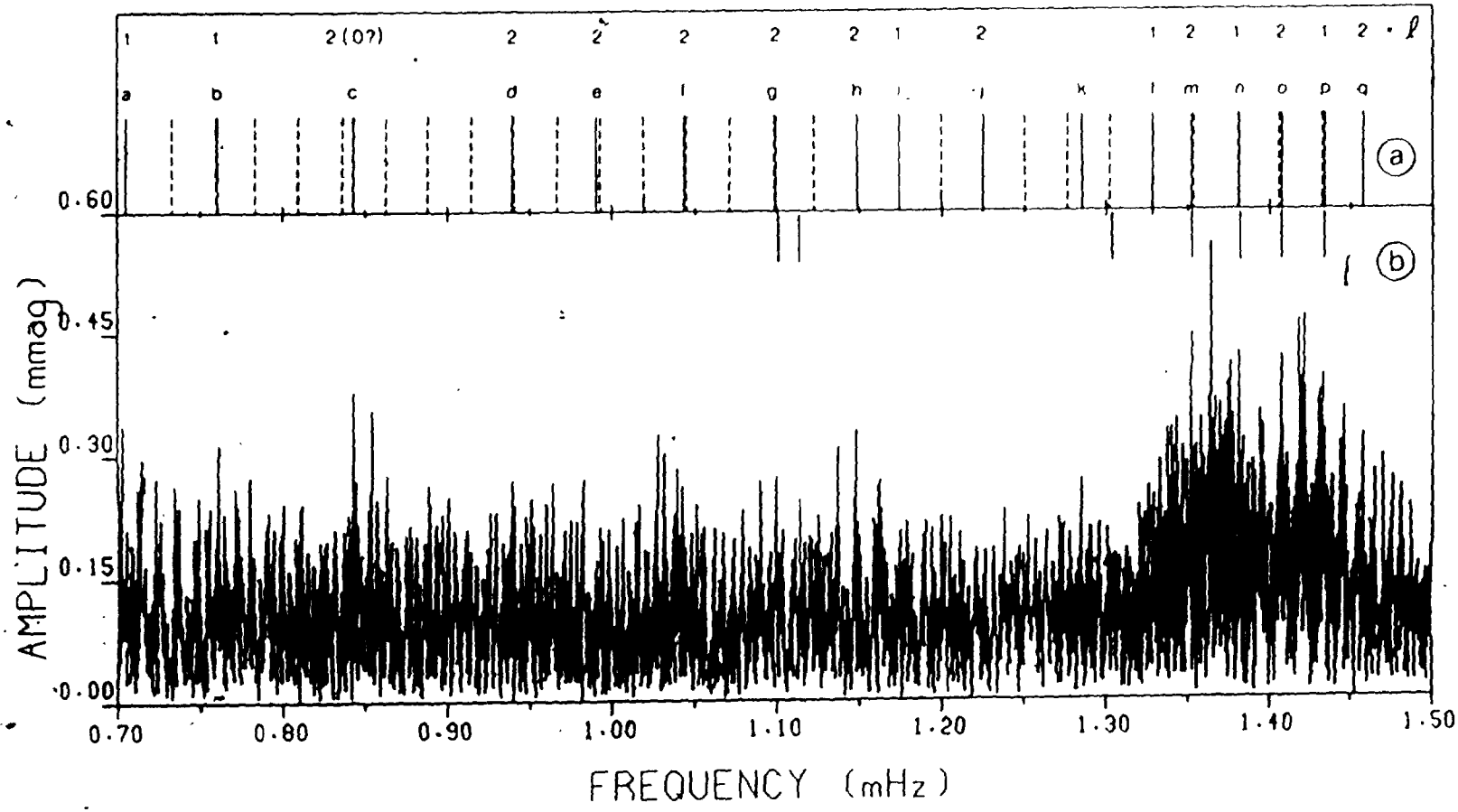

FIGURE 4.11 (*a*) A schematic depiction of the frequencies listed in Table 4.1. The frequencies which would be expected in a pattern with equal spacing $\Delta\nu$ = 25.8 μHz are shown as dashed lines. Arrows mark the frequencies found in the 1984 observations. (*b*) A high-resolution periodogram of the 1985 data set spanning JD 2446074 - 2446112, plotted to the same scale as (*a*). The noise level in this spectrum, outside of the frequency range where oscillations dominate, is roughly 0.15 mmag.

almost all of the values fell into a pattern of nearly-equal spacing which extended the comb of frequencies from the first campaign (shown in Figure 4.6). The entire pattern is depicted schematically in Figure 4.11a, where the dashed lines mark the expected positions of frequencies which have exactly constant spacing. This figure and the second column of Table 4.1 demonstrates that the best average value for the spacing is about 25.8 μHz.

The p-mode oscillation spectrum

The nearly equal spacing of frequencies observed in HD 60435 is reminiscent of the pattern seen in the solar oscillations, which are attributed to p-mode pulsations. Tassoul (1980) has shown that the frequencies of such pulsations, if the radial overtone n is much larger than the degree ℓ (where $\ell \approx 1$), are roughly given by

$$\nu_{n,\ell} \approx \nu_o \left[n + \frac{\ell}{2} + \epsilon \right] \qquad (4.1)$$

where ϵ is a small term which depends on the structure of the star and only weakly on ℓ and n, and

$$\nu_o = \left[2\int_0^R c(r)^{-1} dr \right]^{-1}. \qquad (4.2)$$

Here, c(r) is the sound speed of the gas at a distance r from the star's centre and R is the total radius of the star.

Note that, according to equation (4.1): if a star vibrates in consecutive overtones (n, n+1, n+2, ...) of a single mode of degree ℓ, then the observed frequency spacing will be ν_o; if the star vibrates in several modes of exclusively even or odd degree (ℓ, ℓ+2, ℓ+4, ...), the

spacing will again be ν_o; but if modes of both even and odd degree (l, l+1, l+2, ...) are present, then the frequency spacing will be only $\nu_o/2$. The observed spacing in HD 60435 is approximately 26 μHz; thus, for this star, ν_o should be either ~26 or 52 μHz.

Evolutionary status of HD 60435

Gabriel *et al* (1985) have calculated the eigenfrequency spectra of main sequence models between 1.5 and 2 $M_\odot$. Combining their results with observations of the solar oscillation spectrum, they conclude that for MS stars between 1 and 2 $M_\odot$,

$$\nu_o = (0.205 \pm 0.11) \left\{ \frac{GM}{R^3} \right\}^{\frac{1}{2}} \qquad (4.3)$$

where M is the star's mass and G is the gravitational constant. It is relatively easy to show that, based on the above equation, lines of constant ν_o are approximately straight lines in a log(luminosity) - log(effective temperature) diagram. Given that a star's luminosity L is related to its temperature T_{eff} and radius R by

$$L = \sigma T_{eff}^4 \times 4\pi R^2 \qquad (4.4a)$$

and to its mass by an empirical mass-luminosity relation for main sequence stars only a few times brighter than the Sun (Harris *et al.* 1963)

$$L \propto M^4, \qquad (4.4b)$$

then it follows that $\nu_o^2 \propto T_{eff}^6/L^{5/4}$, or

$$\log L = \frac{24}{5} \log T_{eff} - 2 \log \nu_o + \text{constant}. \qquad (4.5)$$

Shibahashi and Saio (1985) have calculated these ν_0 contours analytically based on the interior sound speeds of stellar models with masses near 2 $M_\odot$. A few such contours, along with some evolutionary tracks for several models in the same initial mass range, are plotted in Figure 4.12. The lower ends of the tracks mark the zero-age main sequence (ZAMS).

It can be seen from this figure that a value of $\nu_0 \approx 26$ μHz (contour D in Figure 4.12) would place HD 60435 well above the ZAMS (close to contour A), beyond the point at which core hydrogen exhaustion occurs in the model stars. It is unlikely that any observed Ap stars have evolved this far off of the main sequence. For example, peculiar stars are found in the young associations of Scorpio-Centaurus (Hill 1986) and Orion (Joncas and Borra 1981), whose ages are inconsistent with having members which are highly-evolved A stars. Therefore, a value of $\nu_0 \approx 52$ μHz (contour C) is more likely, suggesting that HD 60435 is somewhat evolved but still close to the ZAMS band. (The only other *roAp* star for which a similar pattern of near-equal frequency spacing has been discovered is HR 1217 (Kurtz and Seeman 1983). For this star, the observed spacing is ~38.5 μHz; by a similar argument to that used above, the inferred value of ν_0 is about 67 μHz. Therefore, examining the contours of Figure 4.12, HD 60435 appears slightly more evolved than HR 1217.)

Using equation (4.4a) and the $\nu_0 = 52$ μHz contour in Figure 4.12, and assuming that this *roAp* star falls somewhere within the δ Scuti instability strip, the radius of HD 60435 can be estimated:

$$R = 2.2 \pm 0.3\ R_\odot$$

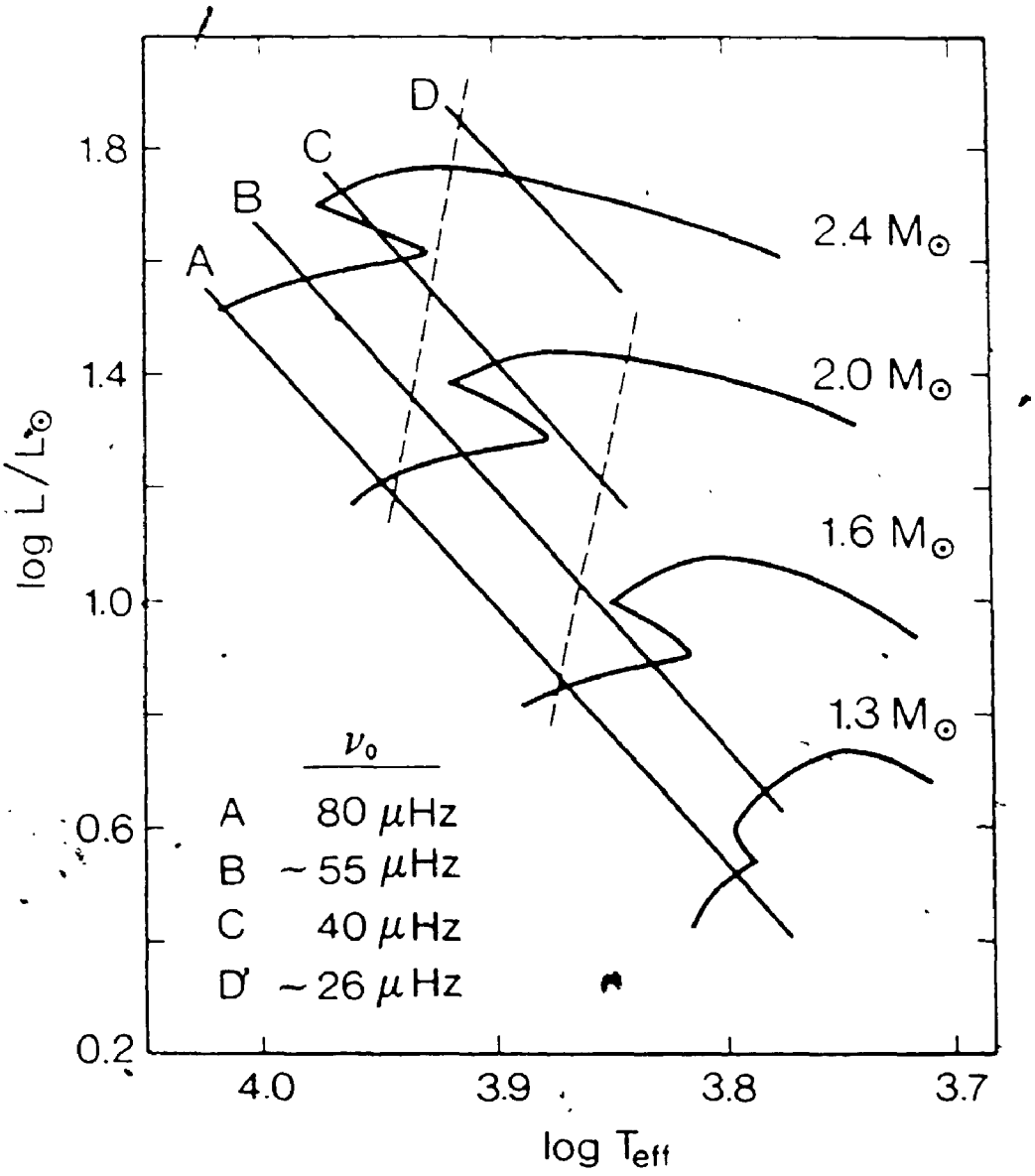

FIGURE 4.12 A theoretical H-R diagram of the evolutionary tracks of stars near 2 $M_\odot$ with chemical composition $(X_o, Z_o) = (0.70, 0.03)$ and a T-τ relation from Kurucz's (1979) standard model atmosphere (Shibahashi and Saio 1985). The solid straight lines labelled A-D are contours of constant ν_o. The dashed lines are the boundaries of the observed δ Scuti instability strip (Breger 1979) converted to log L vs. log T_{eff}.

which is roughly 1.4 × the radius of a main sequence star in the spectral range A5 - F0 which is most likely to encompass an *roAp* star.

The portrayal of HD 60435 as a star which has evolved further off of the main sequence than some of the other cool Ap stars is bolstered by the interpretation of its Stromgren indices (Chapter I). HD 60435 is the only one of the *roAp* stars which falls at the upper bound of Golay's (1974a) [u-b],β main-sequence zone. It also has the only positive value of δc_1, placing it above Crawford's (1979) c_1,(b-y) main sequence curve. Although some scatter in c_1 is to be expected due to differences in atmospheric abundance, this is still highly suggestive that HD 60435 is the most luminous of the *roAp* stars.

Mode identification

A value of $\nu_o \approx 52$ μHz in turn signifies that adjacent frequencies in the pattern depicted in Figure 4.11 represent overtones of alternating even and odd degree. The third column of Table 4.1 shows the combinations allowed by a limited number of degrees ℓ_1, where the frequency ν_q has been arbitrarily designated as (n,ℓ).

When examined in detail, the frequency spacing between adjacent modes is not expected to be precisely uniform, and the observed inequalities can further restrict the possibilities for specific mode identifications. Shibahashi and Saio's (1985) calculations of theoretical eigenfrequencies for their A star models indicate that these inequalities will be systematic, such that

$$\nu(n,1) - \nu(n,0) < \nu(n+1,0) - \nu(n,1) \qquad (4.6a)$$

$$\nu(n,1) - \nu(n-1,2) > \nu(n,2) - \nu(n,1) \qquad (4.6b)$$

in agreement with the findings of Shibahashi *et al.* (1983) for the solar case.

For HD 60435, frequencies $\nu_{k'}$ to ν_q represent a part of the overall pattern in which there are no gaps. These frequencies can be used to test the above relations by equating the observed values with a self-consistent set of (n,ℓ) and substituting them into equations (4.6) where appropriate. One finds that equation (4.6*a*) cannot be satisfied by the observed frequencies, and that equation (4.6*b*) is satisfied only if ν_q is a mode with $\ell = 2$, ν_p a mode with $\ell = 1$, and so on. This added constraint restricts the mode identifications to those provided in the fourth column of Table 4.1 and at the top of Figure 4.11a.

The frequency ν_k presents something of a problem in this scheme. It clearly does not fit the pattern of $\ell = 1$ and 2 modes that is proposed for the other frequencies. By combining Shibahashi and Saio's numerical results for $\ell = 0$, 1, and 2 modes, it can be shown that no mode with $\ell \leq 3$ should occur at frequencies between a given $\ell = 1$ mode and the next higher $\ell = 2$ mode. I offer no explanation for this frequency at present, although it does not seem to be spurious. (Note: One of the frequencies observed in the first campaign, $\nu_{g'}$, also does not fit the pattern of Figure 4.11*a*. However, it *is* compatible with either an $\ell = 0$ or 3 mode in the Shibahashi and Saio eigenfrequency set. In addition, that particular peak in the amplitude spectrum appears to have no sidelobes, which is expected of an $\ell = 0$ mode in an oblique pulsator.)

The overtones n_i of the modes in Table 4.1 cannot be determined with precision, but equation (4.1) can be used to estimate their range. The frequency ratio of consecutive overtones of like degree may

be approximated by reexpressing that equation as

$$\frac{\nu_{n+1,\ell}}{\nu_{n,\ell}} \approx \frac{n + (\ell/2) + 1}{n + (\ell/2)} \qquad (4.8)$$

Taking the frequencies and proposed ℓ values from Table 4.1, one finds that the overtones extend from -26 - 28 for the highest frequencies down to - 13 - 15 for the lowest.

The higher frequencies: Resonances or harmonics?

The peaks in the Fourier spectra at frequencies near 2.8 and 4.2 mHz have been detected only intermittently. These frequencies occur at -2:1 and 3:1 ratios with the dominant oscillations near 1.4 mHz. They might be the first two harmonics of the Fourier composition of the non-sinusoidal shape of the 1.4-mHz light curve on different nights.

The behaviour of the 2.8-mHz peak is consistent with the harmonic interpretation. One would expect the amplitudes of the harmonics to be modulated in tandem with that of the fundamental frequency, and this is indeed observed at 2.8 mHz. However, the 4.2-mHz peak was large at times when the 1.4-mHz oscillation was weak or undetected. It is possible that this may be an oscillation arising from a nonlinear resonant coupling. By inference, both the 2.8- and 4.2-mHz peaks may represent such resonant modes.

V. THE SPECTRUM OF HD 60435

The spectroscopic observations described in Chapter II were obtained in conjunction with simultaneous or contiguous rapid photometry to refine the spectral classification, and to determine:

i) if the star is indeed a spectrum variable, and if so, to what degree;

... and, in the event of sufficiently strong variations ..

ii) a rough estimate of the variation period (or timescale) for comparison with values derived from the oscillation data and the mean photometry; and

iii) any correlations between the line strength variations and the modulation of the oscillation amplitude (i.e phase of maximum/minimum line strength relative to the modulation cycle).

A tracing of the average of the twelve exposures, covering wavelengths from 3800 - 4600 Å, is shown in Figure 5.1. A few of the strongest lines have been labelled. Many lines which are apparent upon visual inspection of the photographic plates appear as "noise" in the continuum of the tracing.

Spectral classification

The strengths of the Sr and Cr lines are consistent with a late Ap or F0p (SrCr) classification for HD 60435. The equivalent width of the Hγ line, W(Hγ) ≈ 7.5 ± 0.5 Å, is normal for an F0 V or III star, based on the correlation between Sinnerstad's (1961, cf. Golay 1974*b*) measured widths and spectral type. The equivalent width of Hβ determined from these spectra is approximately 11 ± 0.5 Å, which matches a class of A7 III according to the Sinnerstad relation. (Crawford's (1958)

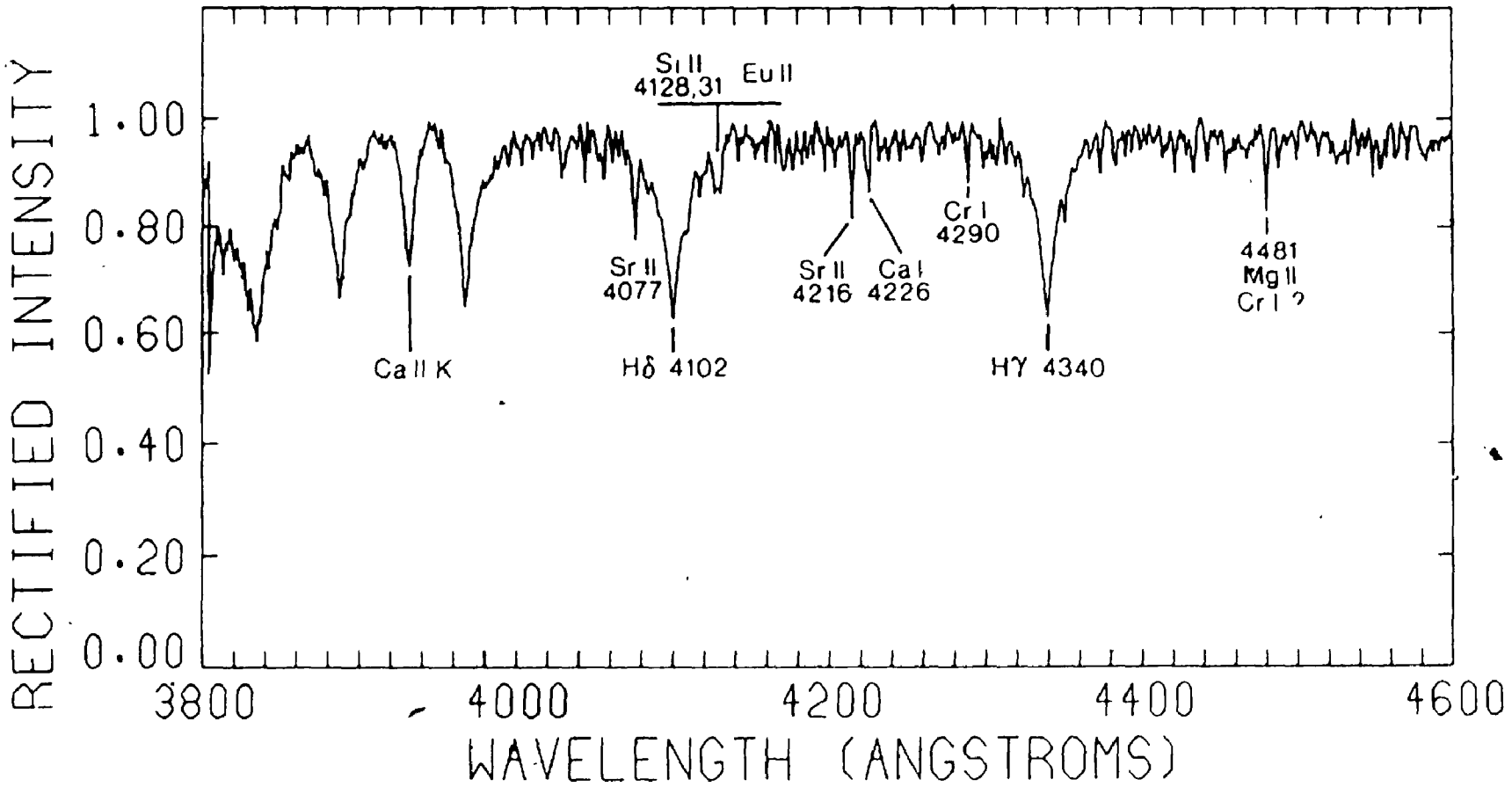

FIGURE 5.1 A scan of the average of the twelve digitized spectra of HD 60435. A few of the prominent lines are labelled. *(Figures 5.1 - 5.3 have been taken from Matthews, Slawson and Wehlau (1986).)*

calibration of W(Hβ) and the photometric index β leads to the value of β = 2.79 given in Table 1.2. The resultant position of HD 60435 in a [u-b],β diagram (see Chapter I) yields a rough spectral class of A8 V or III.)

The Ca II lines also seem to indicate a somewhat earlier spectral type. There are some concerns about the linearity of the plate at the short wavelength end, but they are not serious enough to disqualify the Ca II lines as classifying parameters. In an F0 V star, Ca K and [Ca H + Hε] should have roughly equal equivalent widths, but Ca K is clearly weaker in this spectrum. The Ca K equivalent width is roughly 5 ± 0.5 A, which matches A6-A8 (III-V) on Floquet's (1981) plot of W(Ca K) vs. spectral type for normal stars between B5 and F0. However, Adelman (1985) cautions that the Ca II K line may not be a reliable temperature indicator for the Ap stars, citing differences between the temperatures he derives from the UV energy distributions of peculiar stars and the results of Floquet. Also, Ca is variable in some Ap stars; for example, 53 Cam appears to have an inhomogeneous distribution of Ca on its surface (Landstreet, private communication).

Spectroscopic variability

To display variations in line strengths, each individual spectrum was divided by the averaged spectrum of Figure 5.1. In the divided (or "ratioed") spectra, lines weaker than average will appear as bumps in the continuum, while stronger lines are seen as depressions. Changes in line width will result in "double-humped" features. The divided spectra, showing only the range 4050 - 4550 A, are plotted in Figure 5.2. On at least one exposure (3 Feb), there are signs that the photometric properties of the plate are non-uniform, and hence, line infor-

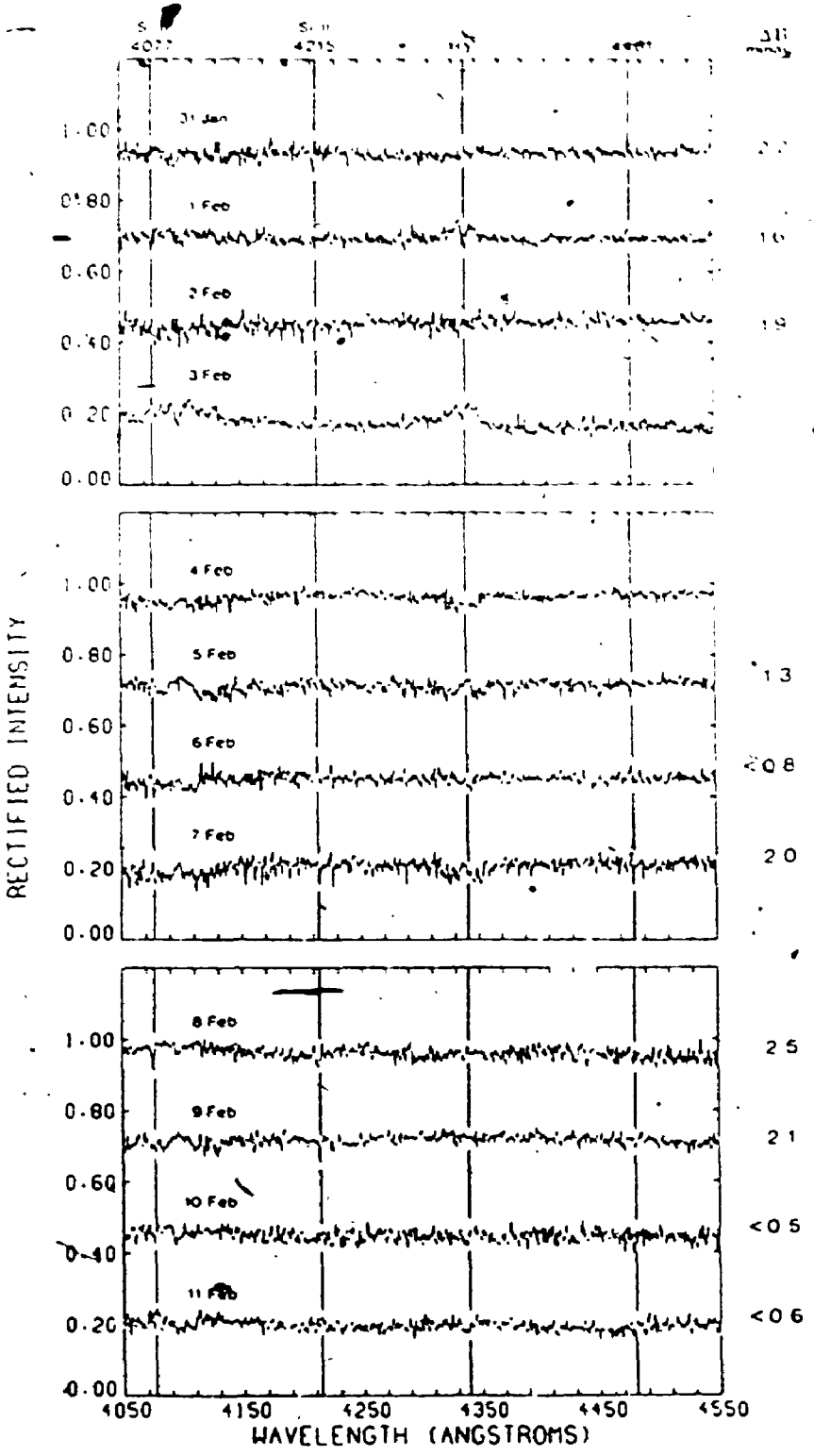

FIGURE 5.2 The twelve individual spectra of HD 60435, divided by the average spectrum of Figure 5.1. On the right are the corresponding B amplitudes of the 1.4-mHz oscillation measured on those nights.

during the 1985 campaign (also tabulated in Table 2.3). The light curves show clear evidence of a secondary minimum in brightness. Both sets of data have been plotted according to the ephemeris

$$JD(B_{min}) = 2445729.791 + (7.6662 \pm 0.0001)E. \qquad (6.3)$$

The period was determined by a "string length minimum" analysis of all of the data, similar to the technique of Lafler and Kinman (1965). (See Appendix B for a listing of the actual programme used and a brief description of the algorithm.) If the oblique rotator model applies to HD 60435, then 7.6662 d represents the rotation period of the star. The apparent double-wave shape of the light curve suggests that, if this star possesses a measureable dipole magnetic field, the observed effective field will undergo polarity reversal. This argument assumes that a dark photospheric patch is associated with each magnetic pole; hence, magnetic extrema would coincide with light minima.

A survey of magnetic and light curves of Ap stars available in the literature (Table 6.1) shows this to be a reasonable assumption. Of the sample of 19 stars, 17 reach minimum B magnitude during an extremum in magnetic field strength, and 13 of those at the *absolute* maximum in the magnetic curve. Furthermore, note that light minimum in HD 60435 coincides with oscillation amplitude maximum (Figures 6.1 and 6.2). Recall from Chapter V that the spectroscopic observations of this star suggest that peak Sr II line strength also occurs at the same phase. Another literature survey - this time of the magnetic and spectroscopic variations of 18 Ap stars - by Floquet (1979) indicates that the SrEuCr stars always have their rare earths, and elements such as Sr, concentrated at the longitudes of the magnetic poles. This tends to corrobo-

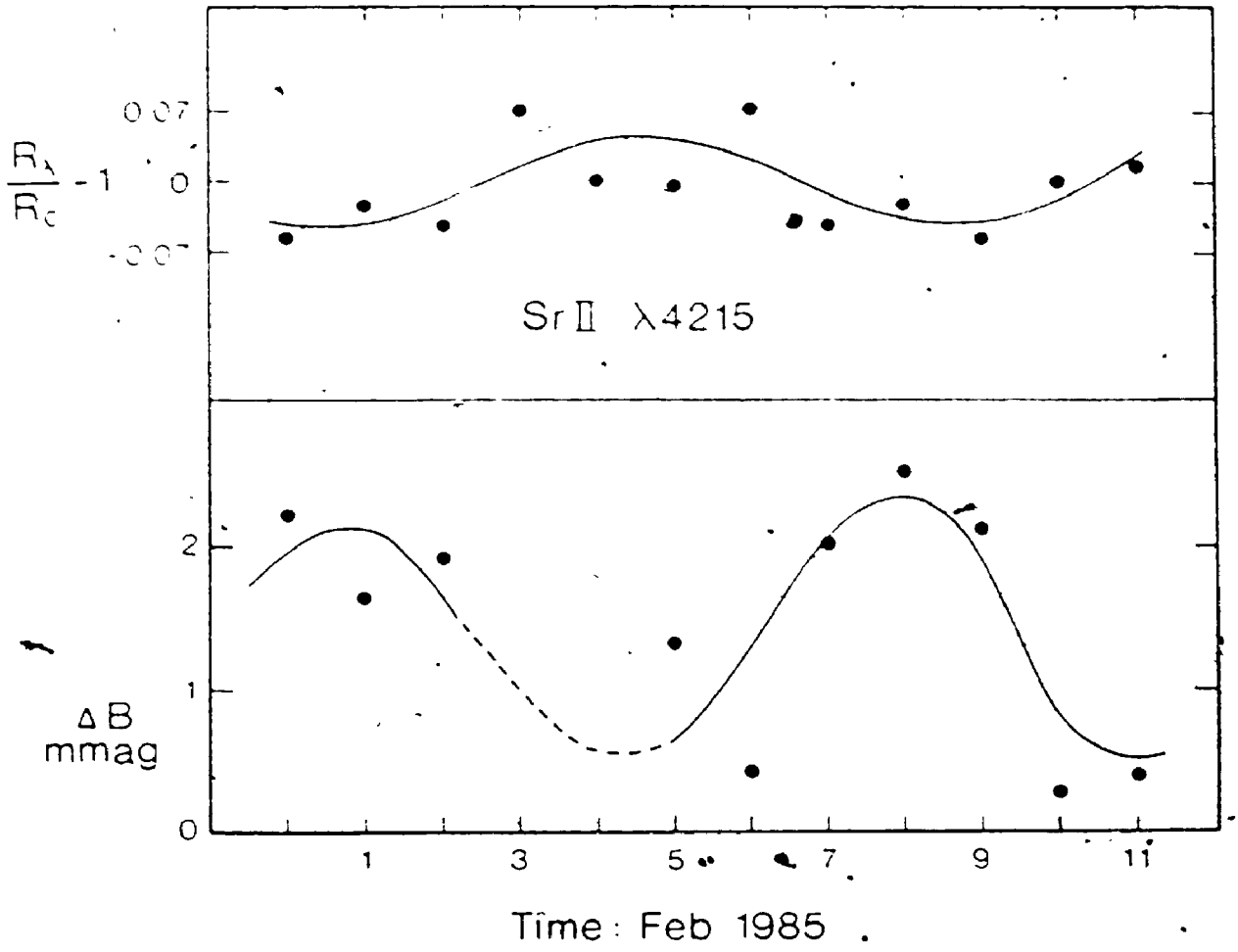

FIGURE 5.3 The variations of the Sr II λ4215 line strength and of ΔB (the amplitude of the light variability) plotted against time. The curves are fits by eye to both sets of data.

line shows no marked deviations from average on any other night.

iv) Variations of the λ4481 line reveal no obvious correlation with the photometric modulation, nor any indications of periodicity during the span of observation.

VI. HD 60435 AND THE OBLIQUE PULSATOR MODEL

The oblique pulsator model (OPM) makes several specific predictions about the observed behaviour of an *roAp* star:

i) Amplitude modulation of the oscillations implies the presence of a dipole or near-dipole magnetic field whose axis is inclined to the star's rotation axis. The overall field strength must be sufficiently intense to override - at least in part - the influence of rotation on the star's pulsations. (See also (v) below.)

ii) The period of that modulation is identical to the magnetic/rotation period.

iii) Maximum oscillation amplitude occurs at the phase of primary magnetic extremum.

iv) If the modulation curve shows a "double wave" (i.e. a primary and secondary maximum during each cycle), then the star must possess a *polarity reversing* magnetic field. In this case, the oscillations should also undergo 180° phase shifts twice per cycle, coinciding with phases of minimum amplitude of the oscillations and zero crossover in the magnetic field.

v) In the Fourier spectrum, a pulsation mode of degree ℓ will be split into $(2\ell + 1)$ components. For $\ell = 1$, the relative amplitudes of the central and sidelobe components supply constraints on the geometry and intensity of the star's magnetic field (based on the Dziembowski and Goode (1985) treatment; cf. Chapter I). From equation (1.11):

$$\frac{A_{+1} + A_{-1}}{A_0} = \tan i \tan\beta \qquad (6.1)$$

$$\frac{A_{+1} - A_{-1}}{A_{+1} + A_{-1}} = \frac{C\Omega}{\omega_1^{mag} - \omega_0^{mag}} \qquad (6.2)$$

where A_0 - the amplitude of the central peak in the frequency triplet,

A_{+1}, A_{-1} - the amplitudes of the respective components longward and shortward in frequency,

i - the inclination of the stellar rotation axis,

β - the obliquity of the magnetic field,

C - the Ledoux rotational splitting constant,

ω_0^{mag} - the magnetic perturbation of the frequency of an $(\ell,m) = (1,0)$ mode, and

ω_1^{mag} - the corresponding perturbation for $(\ell,m) = (1,\pm1)$.

(Note: If $A_{+1} = A_{-1}$, these equations reduce to Kurtz's "classical" oblique pulsator model, where the magnetic field *totally* dominates advection.)

Let us examine how well these predictions match the observations of HD 60435, and what in turn they may tell us about this star.

Existence of an oblique magnetic field (i)
Rotation period of HD 60435

All available evidence for the presence of an ordered magnetic field in HD 60435 is indirect. Its spectrum (see Chapter V) is fairly typical of a magnetic Ap(SrCrEu) star, and that spectrum shows line strength variations similar to those seen in other stars known to have strong dipole-like fields. The star also exhibits long-term photometric variability whose amplitude and period is consistent with that observed in almost all magnetic Ap stars. A phase diagram of the mean Johnson B measurements of (HD 60435 - HD 59994) from Table 2.3, spanning the 18 nights of the first campaign is presented in Figure 6.1a. Figure 6.2a is a phase diagram of comparable photometry collected

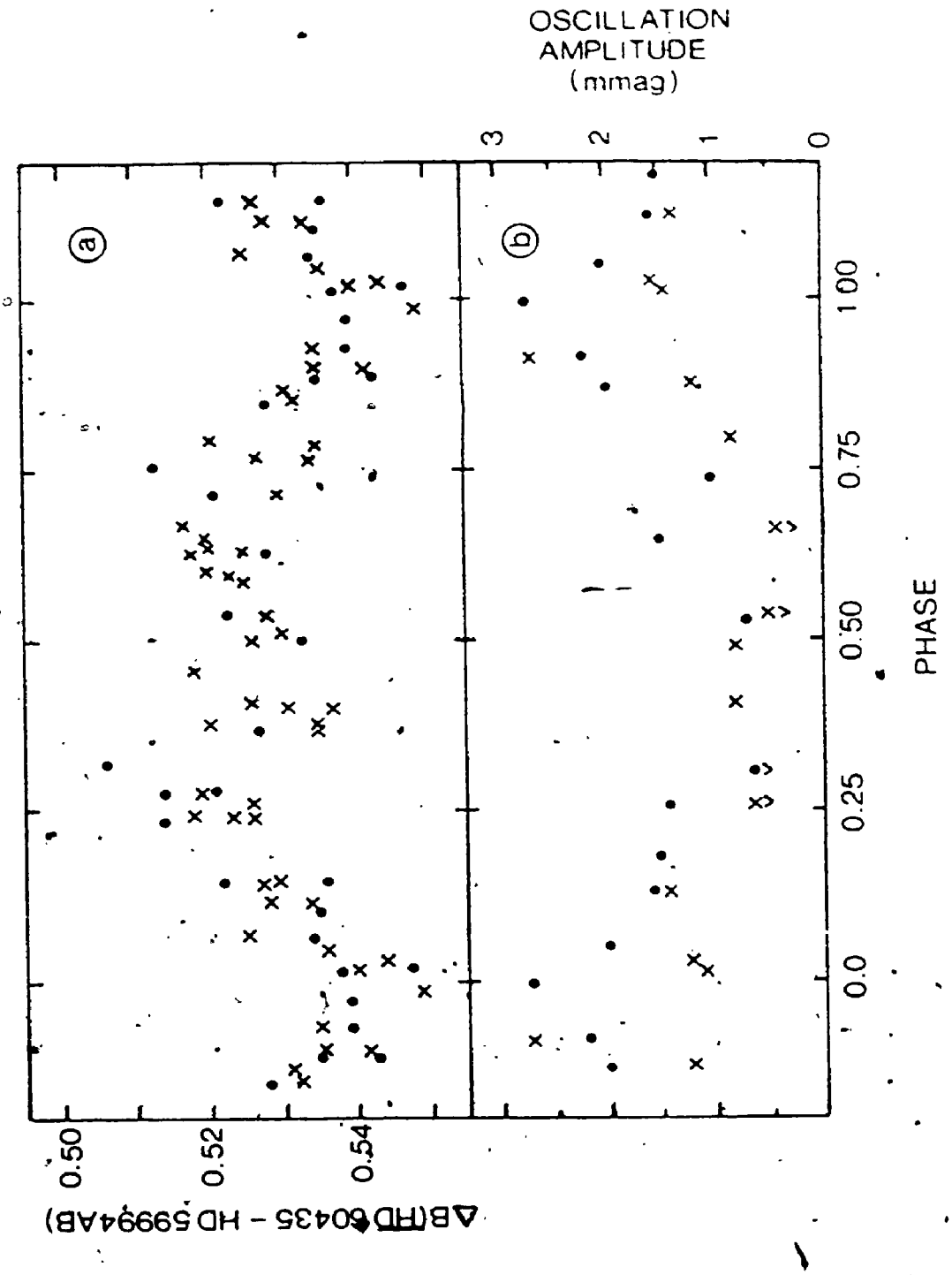

FIGURE 6.1 (a) A phase diagram of the mean photometry of HD 60435 from the 1984 campaign (Table 2.3), plotted according to the ephemeris $JD(B_{min}) = 2445729.791 + 7^d.66625E$. Dots are LCO measurements; crosses, SAAO. (b) Amplitudes of oscillations near 1.4 mHz (estimated from periodograms like those in Figure 4.2 and 4.7) plotted for the same ephemeris as (a). The "v" symbol means an upper limit.

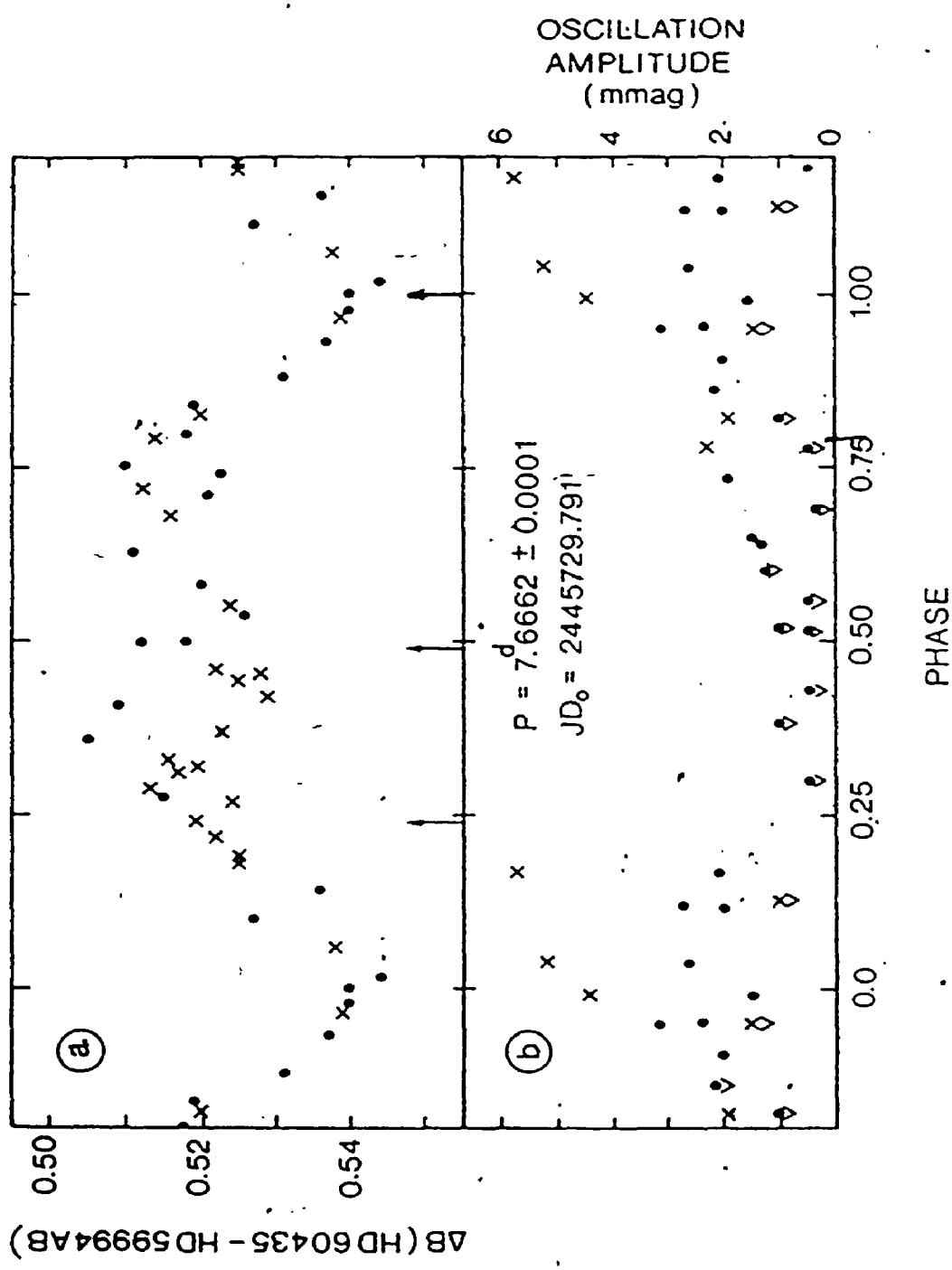

FIGURE 6.2 Same as Figure 6.1, for the mean photometry from the 1985 campaign. The dots in this figure represent measurements from LCO *and* CTIO. The phases of the three magnetic field readings of the star (see text) are shown by arrows. (*Taken from Matthews, Kurtz and Wehlau (1987).*)

during the 1985 campaign (also tabulated in Table 2.3). The light curves show clear evidence of a secondary minimum in brightness. Both sets of data have been plotted according to the ephemeris

$$JD(B_{min}) = 2445729.791 + (7.6662 \pm 0.0001)E. \qquad (6.3)$$

The period was determined by a "string length minimum" analysis of all of the data, similar to the technique of Lafler and Kinman (1965). (See Appendix B for a listing of the actual programme used and a brief description of the algorithm.) If the oblique rotator model applies to HD 60435, then 7.6662 d represents the rotation period of the star. The apparent double-wave shape of the light curve suggests that, if this star possesses a measureable dipole magnetic field, the observed effective field will undergo polarity reversal. This argument assumes that a dark photospheric patch is associated with each magnetic pole; hence, magnetic extrema would coincide with light minima.

A survey of magnetic and light curves of Ap stars available in the literature (Table 6.1) shows this to be a reasonable assumption. Of the sample of 19 stars, 17 reach minimum B magnitude during an extremum in magnetic field strength, and 13 of those at the *absolute* maximum in the magnetic curve. Furthermore, note that light minimum in HD 60435 coincides with oscillation amplitude maximum (Figures 6.1 and 6.2). Recall from Chapter V that the spectroscopic observations of this star suggest that peak Sr II line strength also occurs at the same phase. Another literature survey - this time of the magnetic and spectroscopic variations of 18 Ap stars - by Floquet (1979) indicates that the SrEuCr stars always have their rare earths, and elements such as Sr, concentrated at the longitudes of the magnetic poles. This tends to corrobo-

TABLE 6.1
PHASE RELATIONS BETWEEN MAGNETIC AND LIGHT CURVES OF Ap STARS

HD	Star ref.	Name	H_e extrema maximum	minimum
9996	12		(+1000)	(-1500)*/
10783	1,11		+2000 *	(- 500) /?
19832	3,4		(+ 300)	(- 300)
			B(min) at +ve crossover	
24712	2,6	HR 1217	+1200 */	(+ 400)
32633	17		+3000	-5000 *
			B(min) at -ve crossover?	
65339	10	53 Cam	+3500	-4800 */
71866	5,8,14		+2000 */	-1700
78316	13,15	κ Cnc	+ 200 */	- 200 *
83368	6,16	HR 3831	(+ 700)*/	(- 700)*
108662	1,13	17 Com A	+ 400	-1000 */
111133	22		- 300 /	-1400 *
112413	5	α CVn	+1500 */	-1300
118022	7,15	78 Vir	- 300 /	-1100 *
124224	3,18	CU Vir	+ 750 */	- 400
125248	3,19	CS Vir	+2800 */	-2500
133029	1,19		+4000 */	+2500
137909	20,21	β CrB	+ 750 *	- 500 /
153882	15		+2500 *	-2500 */
196502	18,19	73 Dra	+ 700 */	(- 550)

* = absolute maximum field
/ = minimum in B light

1. Babcock (1958)
2. Bonsack (1979)
3. Borra and Landstreet (1980)
4. Hardie and Schroeder (1963)
5. Jarzebowski (1960)
6. Kurtz (1982)
7. Preston (1969)
8. Preston and Pyper (1965)
9. Preston and Stepien (1968a)
10. Preston and Stepien (1968b)
11. Preston and Stepien (1968c)
12. Preston and Wolff (1970)
13. Preston *et al.* (1969)
14. Rakos (1962)
15. Stepien (1968)
16. Thompson (1983)
17. Trasco (1972)
18. Winzer (1974)
19. Wolff and Bonsack (1972)
20. Wolff and Wolff (1970)
21. Wolff and Wolff (1971)
22. Wolff and Wolff (1972)

rate the assertion that B light minimum and magnetic extremum in HD 60435 coincide.

If times of minimum brightness are also times of maximum effective field strength, then the secondary minimum in the HD 60435 light curve would correspond to a secondary magnetic extremum. Any magnetic variation detected should also match the 7.6662 d period.

Nevertheless, these are only circumstantial signs of a dipole field associated with the star. At the author's request, J.D. Landstreet and D.A. Bohlender (private communication) obtained two field measurements of HD 60435 in 1986 March using the UWO photoelectric Pockel's cell polarimeter, attached to the 2.5-m telescope of the Las Campanas Observatory. Their results were:

HJD 2446513.582 (1.8 hr) H_e = -250 ± 560 Gauss
15.522 (1.6 hr) - 70 ± 680

where the values in parentheses indicate the exposure times. The observations were made at phases relative to the ephemeris of equation (6.3) of 0.240 ± 0.001 and 0.493 ± 0.001, respectively. In 1987 February, Landstreet and B. Ventrudo (private communication) provided a third measurement using the same telescope and instrument:

HJD 2446833.669 (2.0 hr) H_e = -770 ± 570 Gauss

at a phase of 0.990 ± 0.001 on the above ephemeris. These three particular phases are marked in Figure 6.2*a* with arrows.

Given the estimated observational errors, the measurements are compatible with either a near-zero magnetic field, or with a field as intense as -1300 G. If one continues to assume that primary light minimum occurs during primary magnetic extremum, then the phases of the first two magnetic observations (spaced by almost exactly ½ cycle) fall very close to zero crossover and secondary extremum in a polarity

reversing field. The shallow secondary dip in the mean light curve suggests only a weak secondary extremum in the field. This is consistent with the relatively low upper limits to the field strengths at those phases, established by Landstreet and Bohlender's measurements. The most recent measurement should have sampled the strongest apparent field in the magnetic cycle of HD 60435. This is the only reading which differs from zero by more than the observational uncertainty; however, like the previous two measures, it is also consistent with a null field (at the 2σ level).

Despite the inconclusive results of direct observation in this case, there are still a few indirect methods we may use to infer some useful information about the magnetic field of HD 60435. For example, Cramer and Maeder (1980) have developed a photometric parameter, H_s, which appears to be influenced by the mean surface field in Ap stars:

$$H_s = -0.15 + (0.02Z - 0.0042)Z \times T_{eff}(X) \text{ Gauss} \qquad (6.4)$$

where $\log T_{eff}(X) = 4.496 - 0.453X + 0.086X^2$, and X and Z are linear combinations (defined by Cramer and Maeder (1979)) of the Geneva colours U, B_1, B_2, V_1, and G. Cramer and Maeder suggest that H_s is approximately equal to the surface field of the star, and that this dependence is an effect of the 5200 Å depletion found in the energy distributions of Ap and Bp stars.

The Geneva colours of HD 60435 (Hauck and North 1982), and the resulting values of X and Z, are provided in Table 6.2. Substituting these into equation (6.4) gives $H_s \approx 1.9$ kG. This implies - at first glance - that HD 60435 possesses a mean surface field near two kG. However, Thompson *et al.* (1986) have argued that H_s is influenced by

TABLE 6.2
GENEVA PHOTOMETRY OF HD 60435

U = 1.542	B_2 = 1.402
V = 0.670	V_1 = 1.381
B_1 = 0.985	G = 1.800

X = 1,4182

Z = -0.0394

$T_{eff}(X)$ = 10,630 K

H_s = 1.9 kG

both the magnetic field of a star *and* its abundance peculiarities. When they apply the H_s criterion to a homogeneous sample of stars (whose effective fields have been measured at least three times using a Balmer line Zeeman analyser), they find that there is no simple relationship between observed H_{eff} and photometrically-derived H_s. The few stars in the sample with an observed H_{eff} greater than ~2-3 kG do indeed also have large values of H_s. On the other hand, a smaller value of H_s does not seem to be so correlated; many stars predicted on the basis of their Geneva photometry to have fields as large as 2 kG are observed to have much weaker or undetected ones. Also, the calibration of the Geneva determinations appears to be incorrect. A predicted H_s of 2 kG corresponds to a measured value of the *effective* field $B_e \leq 2$ kG. Thus, the H_s parameter is useful for identifying candidates likely to be strongly magnetic Ap stars, but it is of limited effectiveness (if any) in picking out stars with fields of about 2-3 kG or less.

Consequently, the H_s value for HD 60435 probably represents a rough upper limit to that star's effective magnetic field; i.e. HD 60435 is unlikely to have a field above about 2-3 kG, but little more can be gleaned from the Geneva photometry. Of course, given an appropriate inclination i for the star, and obliquity β of the field axis, a *surface* field strength of 2 kG or more could result in a measured *effective* field of only 1300 G or less.

<u>Amplitude modulation and phase shifts</u> (ii, iii, iv)

All of the oscillations in HD 60435 appear to be modulated. Many are sufficiently transient (appearing on only one or a few nights) that no modulation period is apparent. Only the oscillations near 1.4 mHz

are persistent enough to exhibit a clear modulation cycle.

A 7-8 day cycle was recognized in the 1984 data and was seen again in the 1985 observations. This characteristic timescale is evident in Figure 4.3 and in the sample of amplitude spectra shown in Figure 4.10; those nights when the peaks near 1.4 mHz are highest are separated by 6-8 days, or some integer multiple thereof. In fact, if the amplitudes of oscillations near 1.4 mHz (estimated from spectra like those in that figure) are plotted in phase according to the 7.6662 d period derived from the photometry, there is a clear correlation (Figures 6.1*b* and 6.2*b*). Maximum oscillation amplitude occurs during or close to primary B minimum, which may also coincide with primary magnetic extremum. This is in accord with the prediction of the OPM. However, there is no hint of a second rise in amplitude at the phase of secondary B minimum (secondary magnetic extremum?), as is also predicted by the model. If such a rise is indeed present, it may be so small as to be masked by the noise.

The OPM also predicts that a 180° shift in oscillation phase should occur at phases of 0.25 and 0.75 cycles in the mean light curve (i.e. times of magnetic quadrature using the magnetic phasing adopted above). Figure 6.3 is a plot of oscillation phase for the 1.4-mHz oscillations vs. the phase of mean light. The oscillation phases were determined by measuring the times of maxima of the dominant oscillation in the nightly light curves, relative to an arbitrary epoch. Only those nights when the oscillation is easily distinguished above the noise in the light curve have been used to construct this figure.

Unfortunately, on any individual night, the oscillation phase covers a wide range, probably because of beating among the several fre-

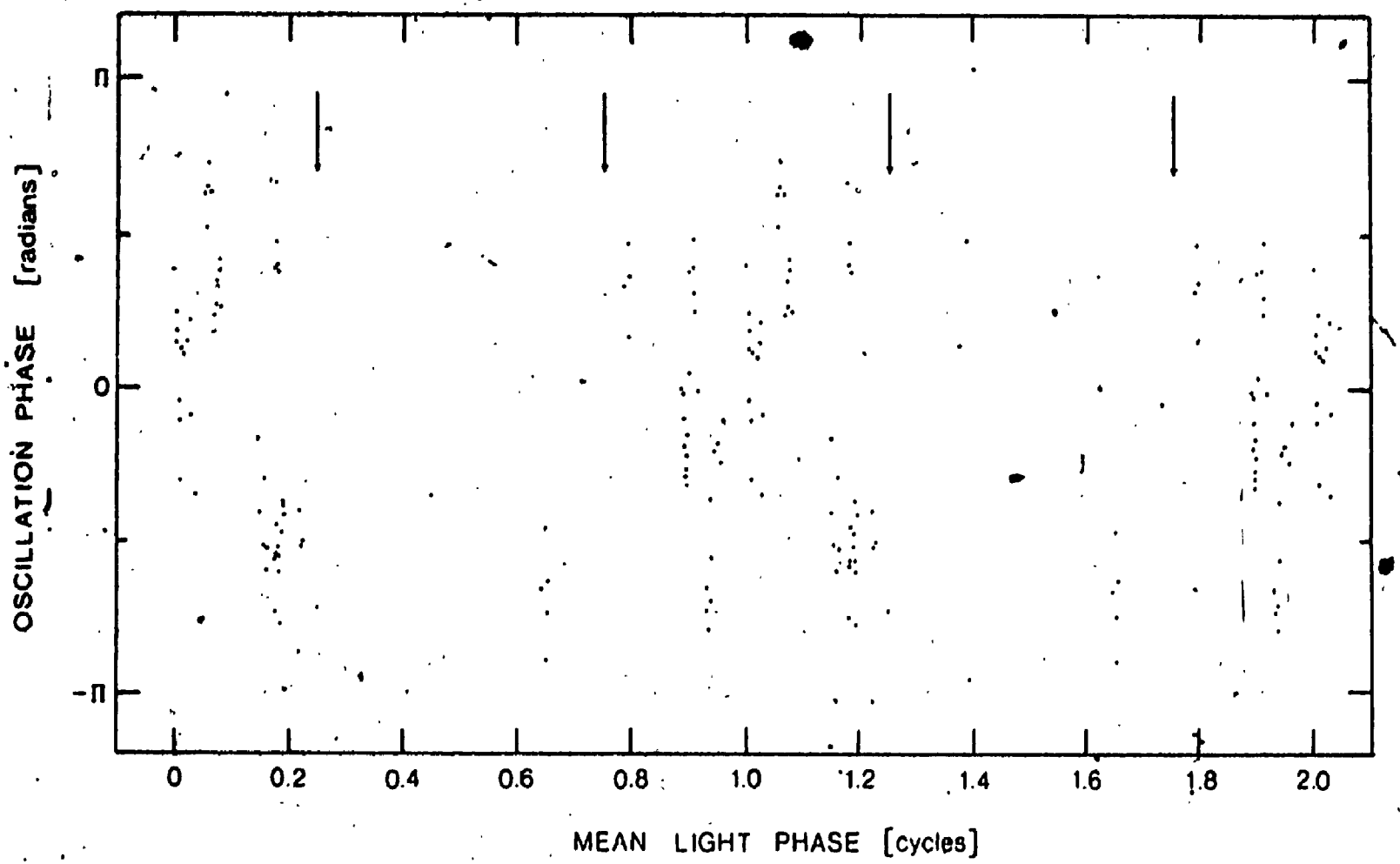

FIGURE 6.3 Phases of oscillations near 1.4 mHz measured from nightly light curves vs. the phase of the mean B light variation. The arrows indicate phases at which phase shifts of 180° (π radians) are expected.

quencies present in the star at one time (see below). The resultant scatter in Figure 6.4, and the paucity of oscillations of sufficiently large amplitude between mean light phases 0.25 and 0.75, obscures any phase shifts which may be taking place due to oblique pulsator effects.

Observe in Figure 6.2*b* that the amplitudes of oscillation at zero phase are not constant; the "maximum" amplitude ranges between almost 6 down to 1¼ mmag. This secular variation is not predicted by the OPM. It is symptomatic of still another modulation, yet one which preserves the 7.7-day modulation period. Beating between adjacent and/or nearby frequencies may be partly responsible for this effect.

There are many obvious signs of amplitude modulation which occurs over timescales less than a day. Since the separation of adjacent frequencies in the overall pattern of HD 60435 (-26 μHz) corresponds to a beat period of about 11 hours, this is not surprising. In fact, the nightly variations in phase shown in Figure 6.4 have a characteristic timescale near 11 hours.

One of the most dramatic examples of rapid modulation is found in the observations of JD 2446111 and 112 (the last two panels of Figure 4.10*b*). Figure 6.4 is a set of amplitude spectra of those two consecutive nights of rapid photometry, each divided into three equal segments. (The first third of JD 2446111 is omitted since it is little different from the two segments of that night shown.) The oscillation amplitude rises from a level below the noise on the first night to almost 6 mmag in less than a day. The modulation observed on the night of JD 2446112 alone can be explained by the beating of frequencies spaced by 26 μHz. However, the beat period should be approximately 11 hours or less. Therefore, another maximum in the beat cycle should

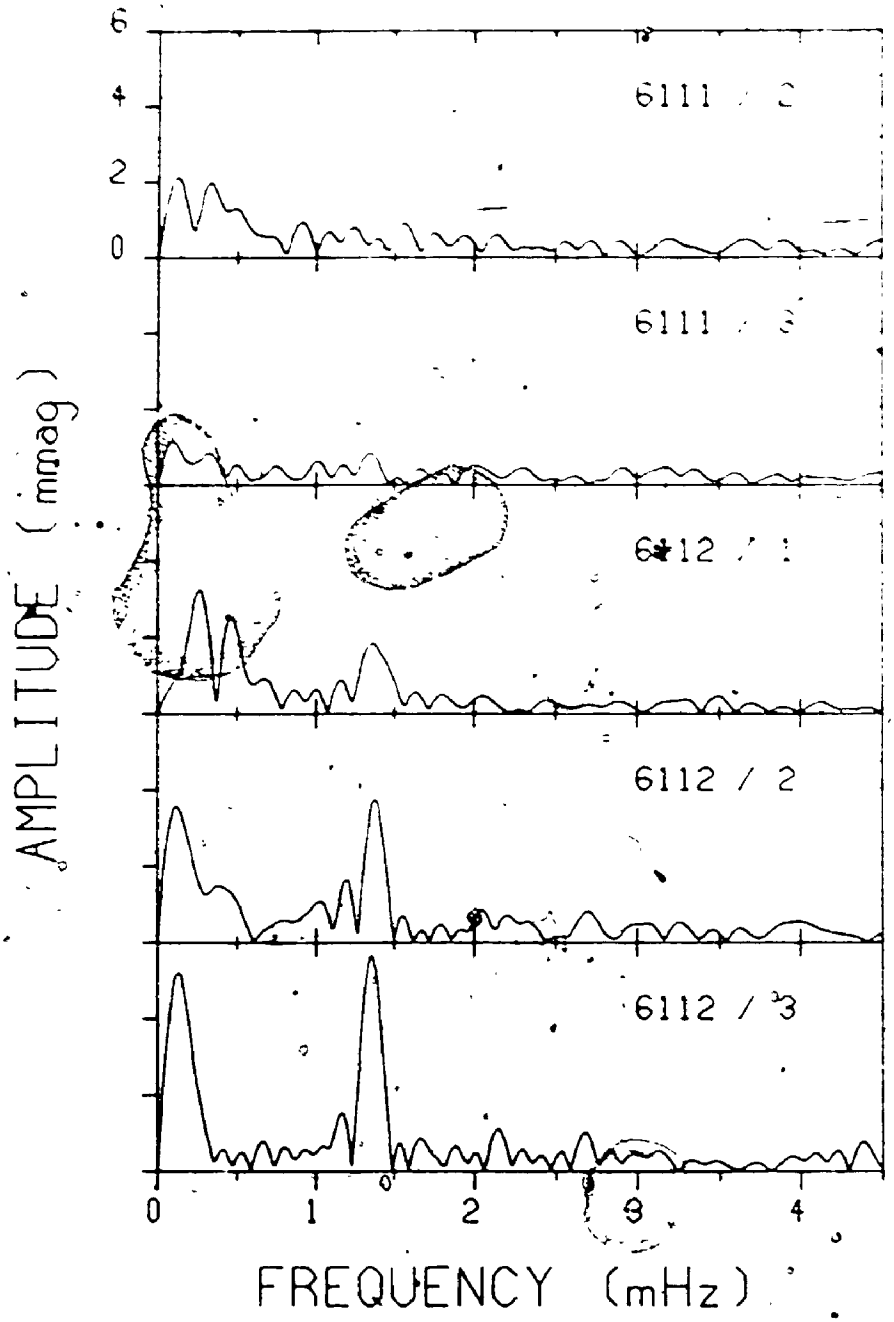

FIGURE 6.4 Amplitude spectra of the light curve of HD 60435 from the nights JD 2446111 and 2446112, in which the nightly data sets have been divided into thirds. The rapid apparent growth of oscillations near 1.4 mHz in less than 24 hours is evident.

occur during the observing interval on the previous night, but none is observed.

The presence of more than two frequencies does not alleviate the discrepency. A comb of equally-spaced frequencies separated by $\Delta\nu$ results in a modulation curve which repeats with period $\Delta\nu^{-1}$. As the number of components in the pattern is increased, the interval during which the net oscillation has a large amplitude becomes proportionally shorter. Beating of any combination of the identified frequencies, even coupled with the modulation of the OPM, does not seem to be able to account for the pronounced change in amplitude between the two nights. This may be the best evidence for actual growth and decay of pulsation modes in an *roAp* star. Dolez and Gough (1984) have shown that in a simple model of a magnetic star, pulsation modes with periods around 10 minutes may have growth and decay times of only a few hours.

Splitting of frequencies in the Fourier spectrum (v)

According to the OPM, each mode with $\ell = 1$ should be split into three equally spaced components, and each with $\ell = 2$ into five. Since tentative mode identifications were made in Chapter IV, these may be used to check whether frequencies linked with (n,1) and (n,2) modes have fine structure which is consistent with the model. Unfortunately, only the oscillations near 1.4 mHz recur often enough to clearly show rotational modulation and the associated frequency splitting; the others are too transient.

Also, the very richness of HD 60435's oscillation spectrum limits one's ability to unambiguously resolve any fine structure. Adjacent frequencies in the overall pattern are spaced by approximately 26 μHz.

One d^{-1} aliases of a real frequency in the spectrum occur on either side at frequency intervals of $n \times 11.57$ μHz, where $n = 1,2,3,\ldots$; the second alias sidelobes are therefore spaced by about 23 μHz from the true oscillation frequencies. As a result, one oscillation peak is only 3 μHz from the 2 d^{-1} aliases of its nearest neighbours. The frequency splitting predicted by the OPM, assuming $P_{rot} = 7.6662$ d, is about 1.5 μHz. Therefore, the outlying sidelobes of an $\ell = 2$ quintuplet would overlap with these alias peaks, altering the apparent amplitudes and perhaps the measured frequencies as well. Alternatively, an $\ell = 1$ triplet could be mistaken for an $\ell = 2$ quintuplet because of the coincidental spacing of the nearby alias peaks. The potential for confusion is dramatized by Figure 4.4, an amplitude spectrum of the 1984 rapid photometry showing only those frequencies near 1.4 mHz. The aliases of adjacent oscillation peaks and their actual sidelobes have combined to create an apparent frequency triplet at 1.42 mHz.

The fine structure of the peaks near 1.4 mHz in Figures 4.4 and 4.11a is seriously complicated by the aliasing. A periodogram (Figure 6.5) of a smaller sample, which covers only twelve sequential nights of CTIO and SAAO photometry (JD 2446101-112), should be less affected by the aliases, while still extending over more than 1½ modulation cycles. As a result, the frequency sidelobes may be resolved more clearly. The positions of frequencies identified from the earlier analysis (ν_n - ν_q) are labelled in Figure 6.5. One d^{-1} aliases of some of these frequencies (and associated sidelobes) are also indicated on the figure.

At frequencies less than about 1.40 mHz, the presence of so many

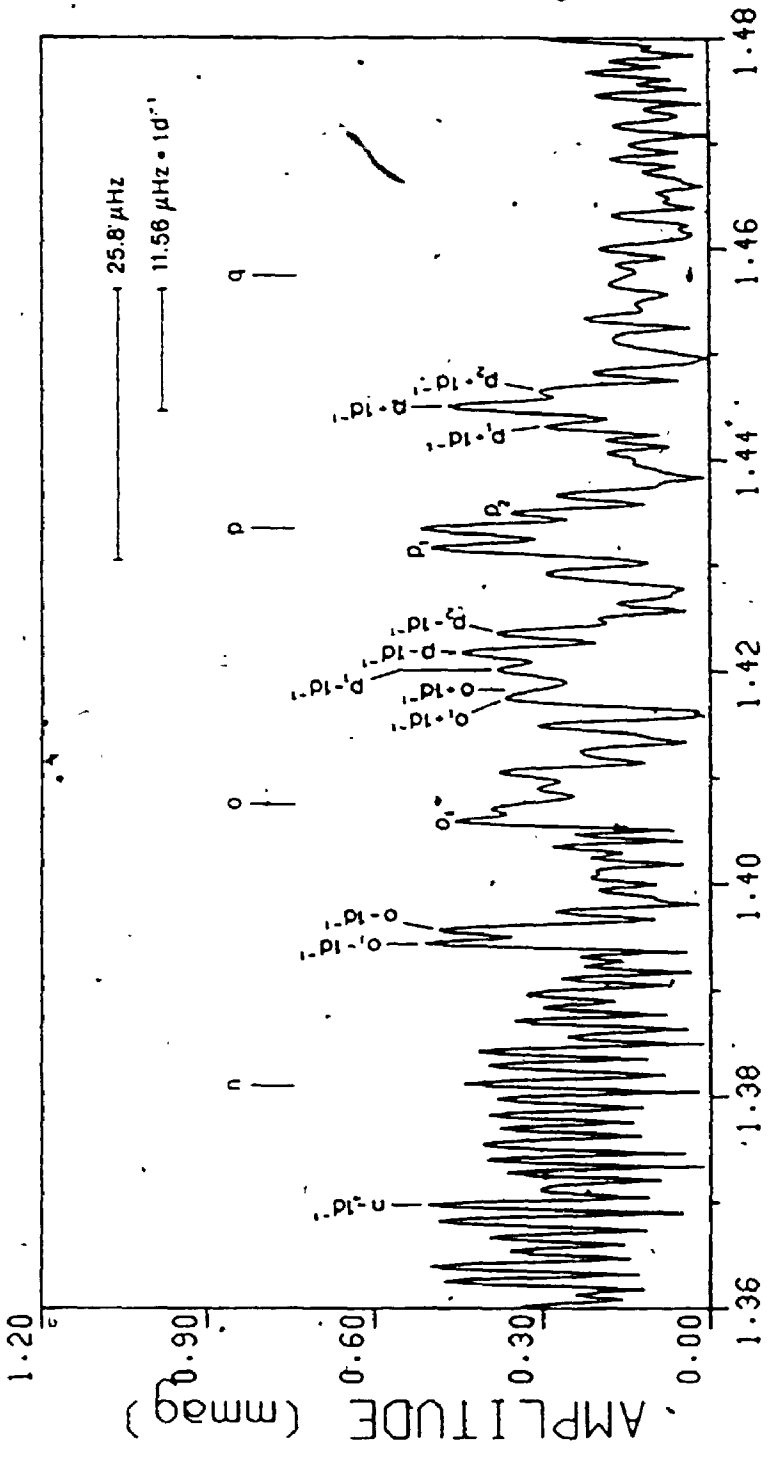

FIGURE 6.5 A high-resolution periodogram of the data set JD 2446101 - 2446112, containing twelve sequential nights. Only frequencies near 1.4 mHz are shown; values in this range from Table 4.1 (and presumed sidelobes) are labelled, as are the 1 c d^{-1} aliases. The noise level in this spectrum is approximately 0.12 mmag.

closely spaced peaks makes an identification of sidelobe structure unconvincing. However, since frequency ν_q is not present at any appreciable amplitude in this sample, the adjacent frequency ν_p does not appear to suffer from interference by overlapping aliases as severely. It is the most suitable candidate in which to study sidelobe structure. The peaks labelled p_1 and p_2 in Figure 6.5 are spaced from ν_p by 1.7 ± 0.2 and 1.6 ± 0.2 μHz respectively. (The peak just above p_2 in frequency is spaced from it by another 1.7 μHz; however, the peak before p_1 has a 2.4 μHz spacing. All five peaks cannot be part of a pattern of equal frequency splitting within the errors. The peak before p_1 is most likely a $+2\text{-d}^{-1}$ alias of ν_o.) The average spacing corresponds to a rotation period of 7 ± 1 days. The best interpretation is that ν_p is an $\ell = 1$ mode, having two sidelobes. This is also consistent with the prediction of equation (4.6*b*).

The sidelobe amplitudes of ν_p are distinctly asymmetric. The skewness is much greater than would be expected solely due to noise and coaddition of weak aliases from nearby frequencies. The amplitudes estimated from Figure 6.3 (and consistent with Figure 4.4) are:

$$A(p_1) = 0.50 \pm 0.03$$
$$A(p_0) = 0.52 \pm 0.03$$
$$A(p_2) = 0.35 \pm 0.03$$

These may be substituted into equations (6.1) and (6.2), where $A(p_1) = A_{-1}$, $A(p_0) = A_0$, and $A(p_2) = A_{+1}$.

The resulting values of $\tan i \tan\beta$ and $C\Omega/(\omega_1(\ell)\text{mag} - \omega_0(\ell)\text{mag})$ are given in Table 6.3. Also included are estimates of these parameters for three other *roAp* stars whose oscillation spectra show frequency triplets consistent with the OPM: HD 6532 (Kurtz and Cropper 1987), HR 1217 (Kurtz *et al.* 1985), and HR 3831 (Kurtz and Shibahashi 1986).

TABLE 6.3

PARAMETERS OF MAGNETIC FIELDS FOR FOUR *roAp* STARS FROM TRIPLET AMPLITUDES

Star	Triplet amplitudes (A_{+1}, A_0, A_{-1})	$\tan i \tan\beta$	$\frac{C\Omega}{\omega_{+}^{(2)mag} - \omega_{0}^{(2)mag}}$	$\Omega/2\pi$ (d^{-1})	K^{mag} (10^{-6})
HD 6532	0.55 ± 0.06 0.73 " 1.01 "	2.1 ± 0.3	-0.3 ± 0.1	0.559	-2
HR 1217	0.42 ± 0.06 1.22 " 0.47 "	0.7 ± 0.1 (0.63 ± 0.09)[1]	-0.06 ± 0.10	0.080	-2
HD 60435	0.35 ± 0.03 0.52 " 0.50 "	2.1 ± 0.2	-0.18 ± 0.09	0.130	-1
HR 3831	1.86 ± 0.04 0.39 " 2.20 "	10.4 ± 1.3 (19 ± 40)[2]	-0.08 ± 0.02	0.350	-4

[1] From magnetic measurements by Preston (1972)
[2] " " " " Thompson (1983)

For two of these stars (HR 1217 and HR 3831), periodic magnetic variations have been detected. The oblique rotator model (ORM) predicts that the ratio of magnetic field extrema, $r = H_e(min)/H_e(max)$, is related to the stellar geometry by

$$\frac{1 - r}{1 + r} = \tan i \tan\beta. \qquad (6.5)$$

Therefore, the magnetic observations can act as a test of the self-consistency of the ORM and OPM. In both cases, the two approaches produce values of $\tan i \tan\beta$ which agree within their respective uncertainties, although the precision of the HR 3831 magnetic curve (Thompson 1983) is inadequate to set a rigourous test.

Using equation (6.5) and the value of $\tan i \tan\beta$ for HD 60435 from Table 6.3, one finds: $r = -0.35 \pm 0.10$. Therefore, the OPM also predicts a polarity-reversing magnetic field, as was already inferred from the mean light curve. The maximum field consistent with the direct magnetic measurements described earlier is -1300 G at phase 0.99 (Figure 6.2). The derived value of r then leads to a maximum allowed secondary extremum of +455 ± 130 G near phase 0.50. The direct measurement at phase 0.49 permits a maximum field of +610 G (within 1 σ), which is certainly compatible with this result.

Inclination and obliquity of HD 60435

The value of $\tan i \tan\beta = 2.1 \pm 0.2$ for HD 60435 constrains the allowed values of inclination and obliquity of the star. These are plotted in Figure 6.6. An estimate of vsini, combined with the radius estimate in Chapter IV and the proposed rotation period derived from the mean photometry, would narrow the range of (i,β) values even

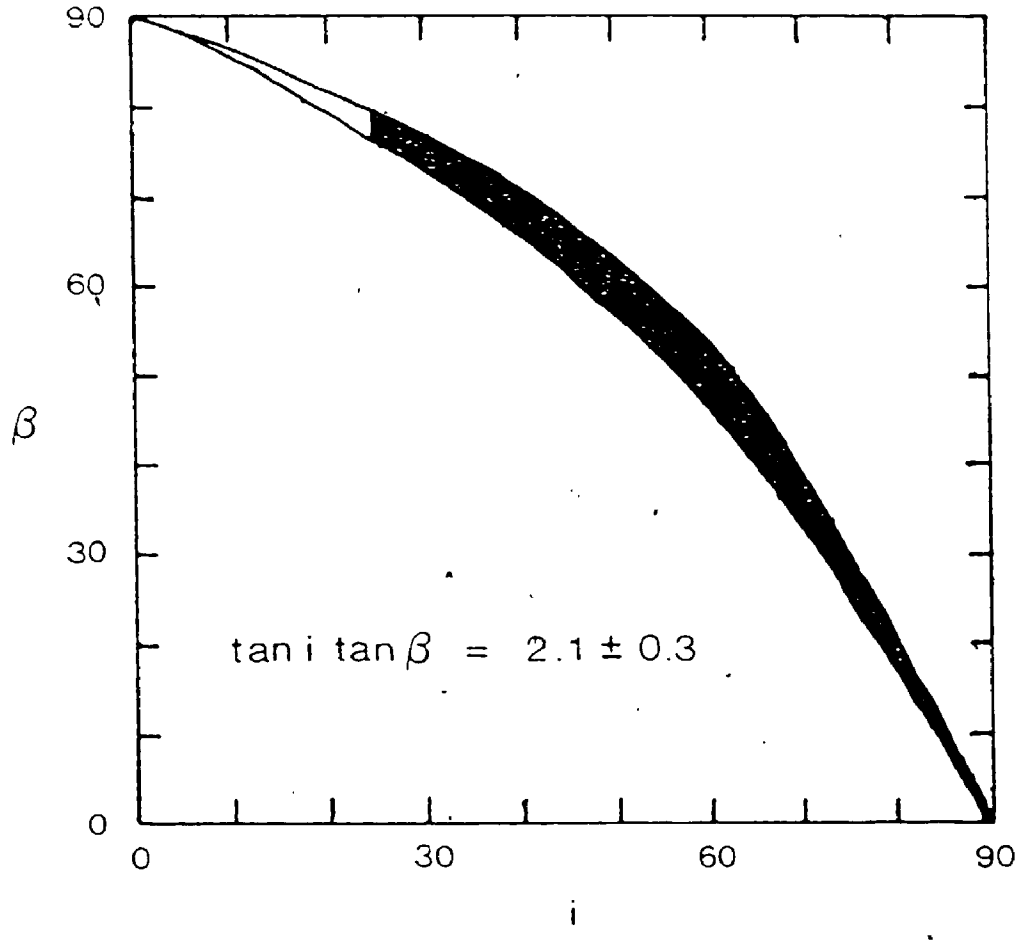

FIGURE 6.6 The values of inclination i and obliquity β for HD 60435 allowed by the oblique pulsator model, when applied to the triplet splitting observed in Figure 6.5.

further.

Ap stars are characteristically slow rotators. A sample of 24 SrEuCr stars examined by Abt *et al.* (1972) was found to have a mean vsini of 30 km s^{-1}; the later types within this class had preferentially smaller projected velocities. Unfortunately, the classification dispersion (67 A mm^{-1}) spectroscopy of HD 60435 described in Chapters II and V is not well suited to the measurement of such small velocities. The wavelength resolution of these spectra is 1.0 A (30 km s^{-1} at 5000 A). Still, these are the only spectra available at present for a vsini determination of this star.

Slettebak *et al.* (1975) have provided a system of standard stars (covering the main sequence range O9 - F8) for vsini determinations using direct measurements of the half-intensity widths of lines on photographic spectra. The resolution of their spectra is 0.25 A. They also provide a theoretical Mg II λ4481 line profile for their FOV model convolved with the 0.25 A instrumental profile. By adjusting for the extra width of the instrumental profile of the HD 60435 spectra, the observed half-widths of lines can be related to the Slettebak standards. The half-widths of the Mg II line profile were measured from microdensitometer tracings and corrected for the different resolution. The resulting values of vsini are in Table 6.4.

Blending and systematic measurement errors probably make the derived mean value, vsini = 10 ±.3 km s^{-1}, a slight overestimate. The quoted error is simply the standard deviation of the numbers in the last column of Table 6.4. Given the wavelength resolution of the spectra, the actual uncertainty in vsini is probably more like 0 - 30 km s^{-1}. Since each spectral exposure extended through 8 - 11 oscillation

TABLE 6 4
ROTATION VELOCITY ESTIMATES FROM Mg II λ4481 LINE

Line width (Å)	Corrected width (Å)	vsini (km s^{-1})
1.39	0.64	18
1.13	0.38	10
1.26	0.51	12
1.13	0.38	10
1.19	0.44	11
1.19	0.44	11
1.13	0.38	8
1.09	0.34	7
1.09	0.34	7
1.26	0.51	12
1.19	0.44	11
1.13	0.38	8

<vsini> = 10 ± 3

cycles, the star's pulsation would also contribute to the line width. The detection of RV oscillations in HR 1217 by Matthews *et al.* (1987*a*) yields a velocity-to-light amplitude ratio of $2K/\Delta m_B = 59 \pm 12$ km s^{-1} mag^{-1}. For HD 60435, this implies pulsation-induced broadening of only ~0.5 km s^{-1}, which is unlikely to be a significant factor in the vsin*i* determination.

Given the equatorial rotation velocity v of a star, its radius is

$$R = \frac{P \cdot v}{50.6} \qquad (6.6)$$

where R is in solar radii, and P is the rotation period in days. The arguments in Chapter IV led to a radius for HD 60435 of $R = 2.2 \pm 0.3$ $R_\odot$. Substituting this value of R, and $P = 7.6662 \pm 0.0001$ d, gives an equatorial velocity of 14.5 ± 2.0 km s^{-1}. If vsin*i* $= 10 \pm 3$ km s^{-1}, then the combined uncertainties permit a range in inclination:

$$25° \leq i < 90°.$$

This in indicated by the shaded portion of Figure 6.6. Coude spectra of HD 60435 with better resolution would improve the accuracy of these results. For example, a precision in vsin*i* of ±1 km s^{-1} translates into a range in *i* of only ~15°.

The restrictions on *i* and β illustrated by Figure 6.6 also result in a limited range of α_p and α_s, the line-of-sight angles of the magnetic (= pulsation) axis at primary and secondary magnetic extrema, respectively. These are plotted in Figure 6.7. However, the OPM also relates the angle α to the observed amplitude of pulsation through equation (1.1). Assuming $l = 1$ (consistent with the frequency triplet used for the determination of tan*i* tanβ in Table 6.3), then that equation states that the ratio of primary to secondary maximum amplitude of

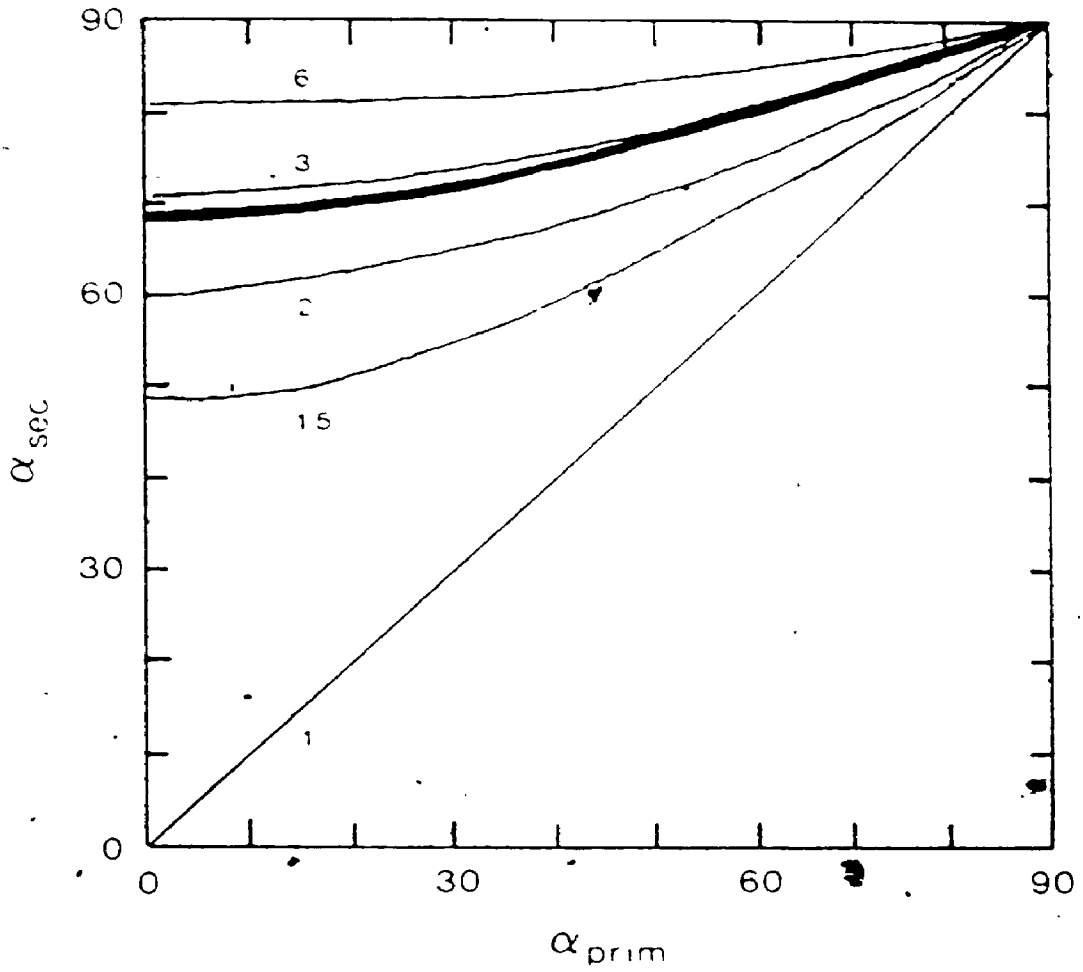

FIGURE 6.7 A plot of the line-of-sight angles of the pulsation (magnetic) axis at primary (α_{prim}) and secondary (α_{sec}) extrema of the observed field strength and maxima of the oscillation amplitude. The thin lines are the curves predicted by the oblique pulsator model based on the ratio (ranging from 1 to 6) of the primary-to-secondary maximum in oscillation amplitude (equation (6.7)). The thick line is the curve predicted by the dynamical OPM based on the triplet splitting in the frequency spectrum.

the oscillations is

$$\frac{A_p}{A_s} \approx \frac{\cos \alpha_p}{\cos \alpha_s} \qquad (6.7)$$

The curves corresponding to amplitude ratios of 1, 1.5, 2, 3, and 6 are shown in Figure 6.7. Since no secondary maximum in oscillation amplitude has been actually detected in the light curves of HD 60435, only upper limits to A_s - and hence, a lower limit to A_p/A_s - can be set. In addition, this observed ratio reflects the *net* amplitude modulation of the many pulsational modes present near 1.4 mHz in HD 60435, whereas the curves of Figure 6.7 assume only a single mode of $\ell = 1$. Therefore, any comparison must be made with caution. The lower limit to the observed ratio A_p/A_s derived from nightly amplitude spectra of the oscillations is approximately 3. The α_s vs. α_p curve for that ratio falls just above the curve obtained indirectly from the amplitudes of the ν_p triplet in Figure 6.5. Any argument claiming significance for such a correspondence may seem circular. After all, both curves are based on predictions of the OPM, and use aspects of the observed oscillations which are not independent from one another (i.e. amplitude modulation, and frequency splitting related to that modulation). However, this does serve as a rough check on the internal consistency of the model.

The global magnetic field of HD 60435

Dziembowski and Goode (1984) have shown that, if the star has a dipole-like field, the frequency perturbation should be of the form

$$\omega_{\ell,m}^{mag} = \frac{\ell(\ell+1) - 3m^2}{4\ell(\ell+1) - 3} K^{mag} \qquad (6.6)$$

where K^{mag} is a coefficient based on a $|Y^m_\ell|^2$-weighted integration over the perturbation of the gas by the magnetic field. K^{mag} is an indicator of the magnetic field strength throughout the oscillating region of the star, not merely at the surface. For *p*-modes of high overtone (Dziembowski and Goode 1984),

$$\frac{K^{mag}}{\omega_0} \sim < \frac{p^{mag}}{P_{gas}} > \qquad (6.7)$$

where p^{mag} and P^{gas} are the magnetic and gas pressures, ω_0 is the unperturbed frequency, and < > denotes an average through the oscillating portion of the star.

For the stars in Table 6.3, rotation frequencies Ω are inferred from available magnetic and/or photometric variation periods. If one assumes both the presence of a dipole field, a pulsation geometry with $(\ell,m) = (1,0)$, and a Ledoux constant $C = 0.01$ (an upper limit based on the long-term synchronism of magnetic and oscillation amplitude maxima in HR 1217 (Kurtz *et al.* 1985)), then values of K^{mag} can be calculated by substituting equation (6.6) into (6.2). The results are included in the last column of the table.

The values should reflect the relative strengths of the global magnetic fields. The results suggest that *HD 60435 has the weakest internal field of the four stars*. The direct field measurements do not contradict this finding (although a weak surface field does not necessarily imply a weak one in the interior). However, it is interesting to observe that - according to Table 6.3 - the field strength of HR 3831 should be twice that of HR 1217, whereas direct magnetic measurements of the longitudinal fields (Table 1.1) show that the ratio of

extrema is $H_{max}(3831) / H_{max}(1217) = 0.6$. But note that the value of $\tan i \tan \beta$ is much larger for the former star. This means that, if the inclination of HR 3831 is small, then the obliquity is large, and vice versa. In either case, the measured longitudinal field would be considerably smaller than the true strength. This geometric projection effect alone is sufficient to reconcile the measured field strengths and the predictions of the OPM.

VII. SUMMARY

Before this study was undertaken, the list of properties known for HD 60435 was a rather short one...

apparent brightness	V = 9.0
photometric indices:	measurements in the Johnson, Stromgren and Geneva systems
spectral type	Ap (SrEu) ?

Analysis of the star's rapid oscillations, and of its slow light and spectrum variations, has refined and extended the list to include...

spectral type	A7-9p (SrCrEu)
luminosity class:	IV?, slightly evolved off of main sequence
radius:	$2.2 \pm 0.3\ R_\odot$
vsini:	≤ 13 km s^{-1}
magnetic field:	≤ 1.3 kG, probably weaker than the global fields of HR 1217, HR 3831; evidence of polarity reversal
rotation period:	~7.67 days

The rapid variability of HD 60435 is certainly one of the most complicated of the class of *roAp* stars, and now, one of the best studied to date. This star has been observed to oscillate in a number of frequencies, extending across at least 0.8 mHz, which belong to a pattern of roughly equal spacing $\Delta\nu \approx 26\ \mu$Hz. The best interpretation is that these frequencies correspond to a series of p-modes of alternating degree ($\ell = 1$ and 2) with high radial overtones ($13 \leq n \leq 28$), such that consecutive overtones of a given degree are in fact spaced by $\nu_o = 2 \times \Delta\nu \approx 52\ \mu$Hz. This spacing is consistent with HD 60435 being a slightly evolved A star with a radius of $R = 2.2 \pm 0.3\ R_\odot$.

Of the many oscillation frequencies detected in the star, those close to 1.4 mHz (P ≈ 12 min) are by far the most persistent. The net amplitude of these oscillations undergo long-term modulation with a period which closely coincides with the mean photometric period (7.6662 ± 0.0001 d). According to the oblique rotator model for Ap stars, this is the rotation period of HD 60435.

There is also short-term amplitude modulation over timescales of hours which is consistent with the expected beating among the many frequencies spaced by 26 μHz (beat period ≈ 11 hr). However, at least one instance of a rapid amplitude increase from one night to the next is difficult to explain by beating of the identified frequencies alone. This may be the best evidence for actual growth (and, by inference, decay) of some modes in HD 60435 with timescales of only a few hours. It agrees with the predictions of Dolez and Gough (1982), who calculated growth and decay times of the order of hours for certain rapid nonradial pulsations in a magnetic A star.

HD 60435 as a test of the Oblique Pulsator Model

The long-term amplitude modulation can be used to test the validity of the oblique pulsator model for the *roAp* stars (Kurtz 1982). The OPM predicts that the amplitude of the rapid oscillations will be modulated with the magnetic period of the star, and that the phases of maximum amplitude and maximum effective magnetic field are identical. Unfortunately, there are no field measurements of sufficient accuracy and quantity to test this directly in the case of HD 60435.

However, the first prediction is satisfied by the equality of the periods of modulation and mean light, since in Ap stars for which there

are magnetic and photometric data, the mean light period is equivalent to the magnetic period. Also, in this star, maximum oscillation amplitude occurs roughly at the same phase as B light minimum; there are indications that this is also the phase of Sr II line strength maximum in the spectrum of the star. Literature surveys of photometry, spectroscopy and magnetic measurements of Ap stars suggest that B light minimum and Sr II maximum are usually associated with magnetic maximum. Hence, the available data on HD 60435 are also consistent with the second prediction above.

The OPM further predicts that a mode of degree ℓ in an *roAp* star should be split into a set of $(2\ell + 1)$ components spaced by the rotation frequency of the star, as given by the observed frequency of the mean light or magnetic curves. Thus, for HD 60435, this spacing is $(7.6662)^{-1}\ d^{-1} = 1.509\ \mu Hz$. The recognition of this type of frequency splitting in this star is complicated by the aliases of the many individual modes present. However, a high-resolution amplitude spectrum of the oscillations does reveal one frequency identified with a mode of $\ell = 1$ which does appear to have been split into a triplet with a spacing of $1.6 \pm 0.2\ \mu Hz$. (The spacing is characteristic of the fine structure seen in other high-resolution periodograms of the HD 60435 oscillations.) Again, this is in agreement with the prediction of the OPM, within the uncertainties of the frequency resolution of the data.

Application of the dynamical OPM (Dziembowski and Goode 1985) to the frequency triplet described above predicts that the ratio of the magnetic field extrema of HD 60435 to be $r = -0.35 \pm 0.10$. The negative sign signifies polarity reversal. Once more, the lack of suitable magnetic data prevents confirmation of this assertion, but as before,

the mean light curve provides some indirect observational support. That curve has a primary and a secondary minimum; in other Ap stars, this has been associated with a polarity-reversing field.

Another test of the polarity-reversal hypothesis would be the search for a secondary maximum in the oscillation amplitude, and determinations of the phases of the oscillation throughout the rotation cycle of the star. An oblique pulsator with a polarity-reversing field is expected to exhibit such a secondary maximum and 180° phase shifts in the dominant oscillation, as depicted in Figure 1.5. This test is inconclusive for HD 60435, since (i) the amplitudes are so low that a secondary maximum may easily be hidden in the noise, and (ii) the beating of the multiple frequencies present introduces apparent phase shifts which obscure any genuine oblique pulsator effects.

Essentially, the case for HD 60435 as an oblique pulsator is one of consistency among the different types of observations of the star currently available and the various approaches to the analysis of those data.

Recommendations for future observations

Clearly, most of the predictions of the OPM can be tested most simply by the determination of an accurate magnetic curve for HD 60435. However, due to this star's relative faintness, measurements with a 1 σ precision as poor as 600 gauss still require exposure times of about two hours on a telescope of 2.5 m aperture. An eight-hour exposure would only reduce the standard deviation to about 300 G. Even if the maximum field of HD 60435 were -1300 G, and the ratio of the extrema matched that predicted by the OPM at r = -0.35, magnetic readings

of such precision would only narrow the value of r to between roughly -0.1 and -0.76. Hardly an "acid test" for the model.

Observations of even 300 G precision would be of value in perhaps establishing the presence of a magnetic field in HD 60435, or at least setting a more stringent upper limit. However, if future magnetic observations of HD 60435 are to be attempted using photoelectric polarimetry, a telescope of at least 4 m aperture seems to be the only practical option.

Tests of the OPM also hinge on reliable determinations of the rotation period from methods independent of the oscillation data. The mean photometry of HD 60435 has provided one estimate, but a more accurate mean light curve for the star would both refine and lend further weight to that estimate. The Johnson B bandpass used for the differential photometry in this programme was not selected to optimize the detection of long-term light variability; it was prescribed by factors related to the rapid oscillations of *roAp* stars (see Chapter II). Jones and Wolff (1973) have shown that the Stromgren v filter is much more sensitive to changes in the mean brightness of many Ap stars. Future studies of the mean light curve of HD 60435 should incorporate Stromgren photometry. Also, it will be important to monitor one or two check stars in addition to the comparison HD 59994 to ensure that no low-level light variations are present in that star which could contaminate the HD 60435 curve.

Spectroscopic observations are another means of estimating the period. Clearly, spectra of much higher signal-to-noise and in greater quantity than those obtained in this study are required. Although moderate wavelength resolution should prove adequate for the purpose of

period determination, a few high-resolution spectra would be desireable to accurately measure vsini.

Better spectroscopy of HD 60435 and its fellow *roAp* stars may also be of value in finding an empirical parameter which could be used in photometric or low-resolution spectroscopic searches for new members of the class. For the most part, the spectra of individual *roAp* stars are not well studied, and the spectroscopic properties of the entire group have not been investigated at all.

One region of the spectrum that may deserve particular attention is the λ5200 depression which is characteristic of peculiar A stars. This feature appears to change with effective temperature. Pyper and Adelman (1986) have observed that - for the cooler Ap(SrCrEu) stars of interest here - the shape of the red side of this broad feature is fairly uniform from star to star, but there are absorption minima near 5000 Å which occur for only some of the same group. The Stromgren (b-y) index would not be sensitive to such changes in the blueward profile of the λ5200 feature. This is an example of the type of discriminant of the *roAp* phenomenon which may be present in the spectrum but might not manifest itself in photometric surveys.

The author, in collaboration with Drs. T.J. Kreidl (Lowell Observatory) and W.H. Wehlau, has already started planning a spectroscopic and Stromgren photometric survey of the *roAp* stars which would include observations of HD 60435 as described above.

The oscillation behaviour of HD 60435 is so complicated that additional rapid photometry is essential if that behaviour is to be specified. If practical, multi-colour measurements would be a useful extension of the observing programme. The phase lags between the brightness

variations in different colours may help to independently identify the modes of pulsation present in HD 60435, although this approach has met with limited success in other *roAp* stars (Kurtz 1982, Weiss 1986).

One of the most important aspects of the oscillation spectrum in both testing and applying the OPM is the fine-scale splitting of frequencies. Identification of the number of components for a given mode and accurate measurement of their amplitudes are easiest using amplitude spectra which have low noise levels and high frequency resolution, and are not confused by strong cycle/day aliases. These in turn can only be produced by long runs of accurate rapid photometry of which major portions are not interrupted by large daily gaps. A more ambitious multi-site observing campaign is called for, involving at least four or five observatories. Such a campaign, organized by Dr. D.W. Kurtz to monitor the *roAp* star HR 1217, was recently completed. The success of this programme, in which data were collected from seven sites during October-December 1986, proves that coordinated observations of this type are also feasible for HD 60435.

The importance of HD 60435 to stellar astrophysics

The recommendations above entail a considerable expenditure of observing time on many telescopes. Do the anticipated returns justify the investment?

The *roAp* variables represent the only main sequence stars other than the Sun in which rapid oscillations have been convincingly detected to date. As such, they are the only candidates on the main sequence to which the techniques of "asteroseismology" may be applied. Comparison of the observed oscillation frequencies and their spacings

to the eigenfrequency spectra of detailed stellar models which include such features as a differentiated atmosphere and magnetic field can be a powerful probe of the physical properties of these stars. This type of *forward analysis* is only practical when several frequencies are present in the star.

HR 1217 is a candidate for such modelling, but it has only six identified frequencies. On the other hand, 19 frequencies have been recognized in the *p*-mode oscillation spectrum of HD 60435. The many frequencies present in this star make it more likely that a unique model solution (or at least a restricted range of solutions) may be found for this star.

Therein lies the primary importance of HD 60435. The data on its rapid oscillations are already of sufficient quantity and accuracy for forward analysis. At present, however, the theoretical foundation is lacking. As new and more realistic models of peculiar A stars are developed, HD 60435 will be the best proving ground available to advance theoretical understanding of this interesting region of the HR diagram.

APPENDIX A

NONRADIAL PULSATIONS IN STARS

Nonradial pulsations in a star may be treated as waves propagating and reflected within one or more natural resonant cavities in the interior. A pulsation mode is observed when a standing wave is established between the two boundaries of such a cavity. The normal modes are in general characterized by eigenfunctions of the form:

$$\xi_{n\ell m}(r,\theta,\phi,t) = A_n(r)\ Y^m_\ell(\theta,\phi)\ e^{-2\pi i\nu t} \qquad (A.1)$$

where Y^m_ℓ is a spherical harmonic for which $\ell = 0,1,2,\cdots$ and $m = 0,\pm1,\pm2,\cdots,\ell$; and $2\pi\nu$ is the eigenfrequency (ω). The eigenfrequencies for these modes depend on ℓ but in the absence of rotation or perturbations by the magnetic field are $(2\ell + 1)$-fold degenerate in m. Each mode also has a series of harmonics expressed by the radial amplitude term $A_n(r)$. All three "quantum numbers" ℓ,m,n represent numbers of nodes in the pulsation pattern: the *degree* ℓ is the total number of nodes on the surface of the star; the *azimuthal number* m, the number of those nodes which pass through latitude $\theta = 0°$ on the star (relative to some physical axis of symmetry, such as the rotation axis); and the *radial order* or *overtone* n, the number of nodes in radial displacement counted from the stellar centre. A few representative examples of (ℓ,m) surface pulsation patterns are depicted in Figure A.1.

The aforementioned degeneracy in m may be resolved by rotation of the pulsating star. Ledoux (1951) demonstrated that a frequency $\nu_{\ell,m}$ in a star rotating with angular frequency Ω[+] would be perturbed by

[+] The star should be rotating sufficiently slowly that centrifugal effects may be safely neglected.

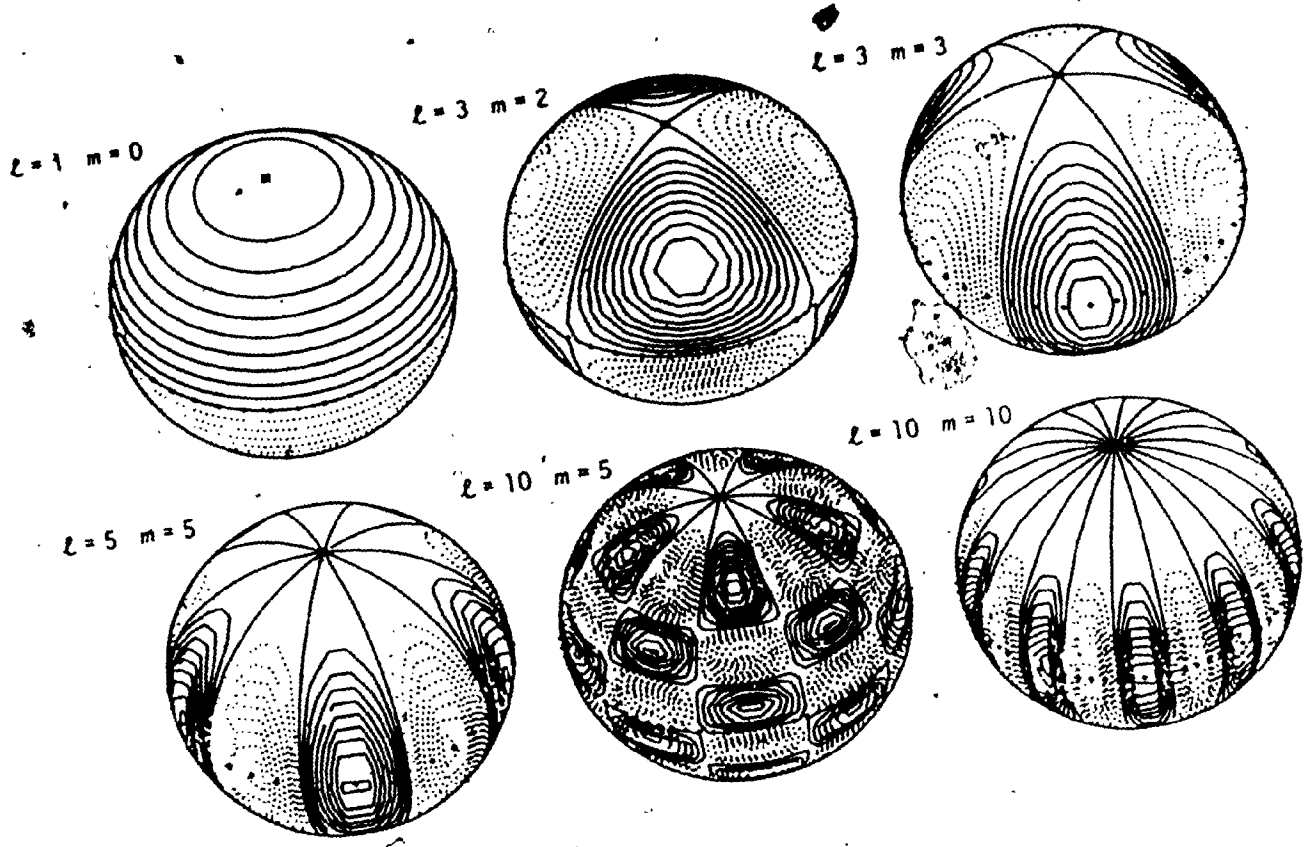

FIGURE A.1 Examples of several nonradial pulsation patterns with different (ℓ,m). The solid and dotted closed contours represent surface motions (and luminosity variations) which are opposite in phase. *[Taken from Toomre (1984)]*

Coriolis effects and transformation from its rotating frame to an observer's inertial frame such that

$$\nu_{\ell,m} = \nu_{\ell,0} + m(1 - C_{n,\ell})\frac{\Omega}{2\pi} \qquad (A\ 2)$$

where $\nu_{\ell,0}$ is the frequency of a mode with $m = 0$ (which is identical to the frequencies of all modes (ℓ,m) in the non-rotating star), m is defined to be positive for a wave travelling in the same sense as the rotation (i.e. prograde). $C_{n,\ell}$ is the "Ledoux constant" which depends on the structure of the star as well as the degree and overtone of the pulsation, and (θ,ϕ) in equation (A.1) are referred to the rotation axis of the star. Aizenman *et al.* (1984) have further shown that, if the axis of pulsation is inclined to the rotation axis by an angle β, then the above equation becomes

$$\nu_{\ell,m} = \nu_{\ell,0} + m(1 - C_{n,\ell})\frac{\Omega}{2\pi}\cdot\cos\beta. \qquad (A.2a)$$

$C_{n,\ell}$ is typically less than 1. In fact, as ℓ and/or n grow large, $C_{n,\ell}$ approaches zero. For the Sun's five-minute pulsations of high overtone and low degree, $C_{n,\ell} \approx 0.01$ (Dolez and Gough 1982).

Pulsation modes

Two types of waves are thought to be responsible for the global pulsations observed in a variety of stars. They are distinguished by the restoring forces which maintain the respective oscillations. Sound waves are a side-effect of the compressibility of a gas; hence, these vibrations are known as *pressure* or *p*-modes. Waves driven by buoyancy set up pulsations which have been dubbed *gravity* or *g*-modes.

Pressure (p-) modes

A *p*-mode is produced by a standing wave in an acoustic cavity in the star. The cavity's upper boundary occurs where the gas density drops off so rapidly that the wave can no longer propagate and is totally reflected. This point is equivalent to the surface of the star. A wave penetrating deeper into the star encounters gas of increasing temperature. Since the local sound speed c increases with temperature such that

$$c = \left[\frac{kT}{m} \right]^{\frac{1}{2}} \qquad (A.3)$$

(where k = Boltzmann's constant and m = the average mass of a particle in the gas), then the vertical wavelength of the wave also increases. The wave is eventually refracted such that it is heading back towards the surface. The "reflection" point corresponds to the depth where the sound speed equals the horizontal phase speed of the wave. That speed depends on the frequency ν and horizontal wavenumber k_x,

$$v_x = \frac{2\pi\nu}{k_x} = \frac{[l(l+1)]^{\frac{1}{2}}}{r} \qquad (A.4)$$

(Because ν and k_x can be determined from disc-resolved observations of the solar *p*-mode oscillations, equation (A.4) is the key to helioseismological estimates of the run of sound speed - and, through equation (A.3), temperature - with depth in the Sun.)

The vertical wavenumber k_z of the oscillation is also constrained by the requirement for a standing wave that an integral number of half-wavelengths must fit exactly between the upper and lower boundaries of the cavity (at radii r_u and r_l):

$$\int_{r_l}^{r_u} k_z \, dz = (n + \tfrac{1}{2})\,\pi \qquad (A\ 5)$$

where n is again the number of nodes of zero radial displacement in the standing wave (i.e., the radial overtone)

Equations (A 3), (A.4) and (A.5) lead to an approximate dispersion relation for modes where $\ell \gg n$. In this limit, waves do not penetrate very deeply into the star; the acoustic cavity is relatively shallow. Therefore, one can safely approximate the temperature at a given depth within this narrow range as

$$T(r) \simeq \left.\frac{dT}{dz}\right|_a (R-r) - \frac{g(r)}{C_p}\,(R-r) \qquad (A\ 6)$$

where $\left.\frac{dT}{dz}\right|_a$ is the adiabatic temperature gradient, g(r) is the local gravity at radius r, C_p is the heat capacity at constant pressure, and R is the radius of the star. Substituting equation (A 6) into (A.3) eventually yields

$$c(r) = [(\gamma-1)g(R-r)]^{\frac{1}{2}} \qquad (A.7)$$

where $\gamma = C_p/C_v$.

Thus, at the depth of the lower boundary of the acoustic cavity,

$$\omega = 2\pi\nu = k_x[(\gamma-1)g(R-r_l)]^{\frac{1}{2}}. \qquad (A.8)$$

Introducing equations (A.7) and (A.8) into the solution of (A.5), where the thinness of the cavity permits the approximation $\int k_z dz = k_z(R-r_l)$, finally gives the approximate dispersion relation:

$$\nu^2 \propto (n + \tfrac{1}{2})gk_x. \qquad (A.9)$$

The derivation for $\ell << n$ is similar but more involved since several of the above simplifications are no longer valid given the greater extent of the acoustic cavity in this case. The result is a dispersion relation of the same form as that derived by Tassoul, (1980):

$$\nu_{n\ell} \approx \nu_o(n + \frac{\ell}{2} + \epsilon) \qquad \text{(A.10) [4.1]}$$

where $\nu_o = \left[2\int^R \frac{dr}{c}\right]^{-1}$. Therefore, modes of low degree and high overtone are characterized by consecutive overtones which are uniformly spaced in frequency.

Gravity (g-) modes

The resonant cavity for gravity waves is defined by the region in the star where the oscillation frequency is less than the Brunt-Vaisala (or buoyancy) frequency

$$f_{BV} = \left[\frac{g}{T}\left(\frac{dT}{dz}\Big|_a - \frac{dT}{dz}\right)\right]^{\frac{1}{2}} \qquad \text{(A.11)}$$

For these modes, the dispersion relation is of the form (Toomre 1984):

$$\frac{1}{\nu_{n\ell}} \approx \frac{1}{\nu_o'} \frac{n + \frac{1}{2}\ell + \epsilon'}{[\ell(\ell+1)]^{\frac{1}{2}}} \qquad \text{(A.12)}$$

where $\nu_o' = \frac{1}{2\pi^2}\left[\int_0^{r_u} \frac{f_{BV}}{r}\, dr\right]$, such that r_u is just below the convective zone of the star (within which gravity waves are evanescent) and ϵ' is another small constant which depends on the stellar structure.

Note that consecutive overtones of a *g*-mode of given degree are equally spaced in *period*, not frequency. These modes also have longer periods than the *p*-modes that would be found in the same star. Both

the longer periods and the equal period spacing are incompatible with the observations of *roAp* stars, so the rapid oscillations of those stars have been attributed to *p*-mode pulsation.

Pulsational driving

Most stars are stable to pulsation. If a star is, say, compressed from its equilibrium configuration (perhaps by some turbulent process in the atmosphere), the resulting overall decrease in opacity and increase in density gradient both allow the excess luminosity to escape more easily. When the star then slightly overshoots its equilibrium state, the opposite occurs. In this way, any oscillation is effectively damped after only a few cycles.

However, at certain levels in the atmosphere, this situation does not necessarily hold. Consider the He II ionization zone, which is located at a temperature near 4×10^4 K. When the star is most highly compressed, much of the excess luminosity is absorbed in the ionization of He II to He III. The large opacity of He II dams the outflow of radiation and increases the local temperature gradient. The excess pressure drives the outer layers of the star to expand more than its normal relaxation response. Conversely, at maximum expansion, recombination takes place in the He III region. Not only is He III almost transparent to the UV flux that was blocked before by He II, but the recombination also cools the gas more efficiently. Both the temperature and pressure fall, as do the outer layers of the star, and the pulsation cycle repeats. This is an oversimplified picture, but it does describe the fundamental mechanism at work.

All stars have He II ionization zones, but not all pulsate. If

the He II zone is too deep in the atmosphere (as in a smaller, cooler star), there is insufficient driving to move the weight of the overlying gas. If the zone is too high (larger, hotter star), there is insufficient mass in the upper layers to recompress the star effectively. Also, the region which contains the ionization zone will be nonadiabatic, so the density and temperature adjust themselves to keep the luminosity gradient from becoming steep enough to drive pulsation.

The narrow range of effective temperature over which this envelope ionization mechanism will drive pulsation in stellar models corresponds closely to that observed for the Cepheid instability strip. Where the lower portion of this strip crosses the main sequence are found the δ Scuti pulsators. This is also the vicinity of the *roAp* stars, so the He II ionization mechanism may be relevant to these stars, even with their anomalous atmospheric compositions.

APPENDIX B

FORTRAN V Listings of:

1. Fourier Periodogram Routines PRGRM1 and PRGRM2.
2. "Lafler and Kinman" Periodogram Routine FAZCURV

```
/JOB
PRGRM1.
/USER
CHARGE,2005.
/NOSEQ
SETTL,3CO.
GET,INFILE.
ATTACH,SUMTEMP/M=W.
REWIND,INFILE,SUMTEMP.
FTN5,L=C,PL=250CO.
REWIND,LGC.
LGO.
STORE,SUMTEMP.
/EOR
C
C   THIS PROGRAMME ACCEPTS AS INPUT A FILE "INFILE"
C   CONTAINING A TIME SERIES - JDTMP = TIME IN ARBITRARY
C   UNITS (USUALLY DAYS); BTMP = MEASURED QUANTITY
C   (USUALLY PHOTOMETRIC MAGNITUDE) - WITH AN ARBITRARY
C   NUMBER NUMPTS OF DATA.  "INFILE" MUST HAVE ONE DATUM
C   PER LINE, BUT MAY BE FORMAT-FREE.
C
C   IT ALSO READS PARAMETERS FROM A DATA FILE APPENDED TO
C   THE BATCH VERSION OF THE PROGRAMME.  THE PARAMETERS
C   AND THEIR FORMATS ARE GIVEN IN THE LISTING BELOW.
C
C   THE OUTPUT IS A FILE "SUMTEMP" CONTAINING NMDENU
C   LINES. EACH LINE HAS A FREQUENCY, SUM OF (B(I)*
C   SIN(2*PI*FREQ*JD(I)), AND SUM OF (B(I)*COS(2*PI*
C   FREQ*JD(I); THE LATTER TWO SUMMED OVER I=1,NUMPTS.
C
      PROGRAM PRGRM1 (INPUT,OUTPUT,TAPE5=INPUT)
      INTEGER I, NUMPTS, NMDENU
      REAL JD(7000),B(7000),LONU,DELTNU,TWOPI
      REAL SIDEL(25000),CODEL(25000),SI(25000),CO(25000)
      REAL SISUM,COSUM,SN,SIGB,NU
      DOUBLE PRECISION JDTMP,LOJD,HIJD,BTMP


C     DEFINES DATA USED
C       LOJD = TIME OF FIRST DATUM
C       HIJD = TIME OF LAST DATUM
C      JDZRO = ARBITRARY EPOCH
      READ (5,*) LOJD,HIJD,JDZRO

C     DEFINES FREQUENCIES
C        LONU = LOWEST FREQUENCY TO BE SAMPLED IN
C               PERIODOGRAM
C      DELTNU = FREQUENCY INTERVAL
C      NMDENU = NUMBER OF FREQUENCIES IN PERIODOGRAM
C     NOTE: FREQUENCY UNITS = 1/(UNITS OF TIME USED)
      READ (5,*) LONU,DELTNU,NMDENU

C     READS DATA FROM INFILE
      OPEN (UNIT = 61, FILE = 'INFILE')
      I =0
    3 READ (61,*,END = 13) JDTMP,BTMP
      IF ((LOJD.GT.JDTMP).OR.(JDTMP.GT.HIJD)) GO TO 3
      I = I + 1
      JD(I) = JDTMP - JDZRO
      B(I) = BTMP
      GO TO 3
   13 NUMPTS = I
      CLOSE(61)

C     NORMALIZES B(I) VALUES TO A MEAN OF ZERO
```

```
      CALL AVG(NUMPTS,B)

      OPEN (50,FILE='SUMTEMP')
      TWOPI = 6.2831853
      NU = LONU

      DO 61 I = 1,NUMPTS
        SI(I) = SIN(TWOPI*LONU*JD(I))
        CO(I) = COS(TWOPI*LONU*JD(I))
        SIDEL(I) = SIN(TWOPI*DELTNU*JD(I))
        CODEL(I) = COS(TWOPI*DELTNU*JD(I))
   61 CONTINUE

      DO 51 J = 1, NMDENU
        SISUM = 0
        COSUM = 0

        DO 41 I = 1, NUMPTS
          SISUM = SISUM + B(I)*SI(I)
          COSUM = COSUM + B(I)*CO(I)
   41   CONTINUE

      WRITE (50,*) NU,SISUM,COSUM

        DO 31 I = 1, NUMPTS
          SN = SI(I)
          SI(I) = SN*CODEL(I) + CO(I)*SIDEL(I)
          CO(I) = CO(I)*CODEL(I) - SN*SIDEL(I)
   31   CONTINUE

        NU = NU + DELTNU

   51 CONTINUE


      END


      SUBROUTINE AVG (NUMPTS,B)
      INTEGER NUMPTS
      REAL B(7000),SIGB

      DO 81 I = 1, NUMPTS
        SIGB = SIGB + B(I)
   81 CONTINUE
      SIGB = SIGB/NUMPTS

      DO 91 I = 1, NUMPTS
        B(I) = B(I) - SIGB
   91 CONTINUE
      END
/EOR
0.07104 4.17272 0.0
0.0 0.005 400
/EOR
/EOF
```

```
      PROGRAM PRGRM2 (INPUT,OUTPUT,TAPE6=INPUT)
C
C   THIS PROGRAMME ACCEPTS THE "SUMFILE" PRODUCED BY
C   BPRGRM1.  ITS OUTPUT IS A FILE "SPECT" CONTAINING
C   THE PERIODOGRAM WHOSE AMPLITUDE HAS BEEN NORMALIZED
C   BY THE NUMBER OF POINTS, NUMPTS, IN THE ORIGINAL
C   TIME SERIES.
C
      CHARACTER *7 SUMFILE,SPECT
      PI = 3.141593

      PRINT *,'NUMBER OF DATA POINTS?'
      READ (6,*) NUMPTS
      PRINT *,'NUMBER OF FREQUENCIES?'
      READ (6,*) NUMFRQ
      PRINT *,'SUM FILE?'
      READ (6,1) SUMFILE
    1 FORMAT (A7)
      PRINT *,'SPECTRUM FILE?'
      READ (6,1) SPECT

      OPEN (UNIT=55,FILE=SUMFILE,STATUS='OLD')
      OPEN (UNIT=66,FILE=SPECT,STATUS='NEW')

      DO 10 I=1,NUMFRQ
      READ (55,*) FREQ,SI,CO
      AMP = (2./NUMPTS)*SQRT(SI**2. + CO**2.)
      PHI = ATAN(-SI/CO)
      IF (CO.LT.0) PHI = PHI + PI
      IF ((SI.GT.0).AND.(CO.GE.0)) PHI = PHI + 2*PI
      WRITE (66,*) FREQ,AMP,PHI
   10 CONTINUE

      CLOSE (55)
      CLOSE (66)
      STOP
      END
```

```
      PROGRAM FAZCURV(INPUT,OUTPUT,TAPE5=INPUT)
C
C     THIS PROGRAMME CALCULATES A PERIODOGRAM BASED ON THE
C     METHOD OF LAFLER AND KINMAN (1965, AP. J. SUPPL. 11, 216),
C     IN WHICH THE BEST FIT TO A PERIOD IS ASSUMED TO OCCUR
C     WHEN THE SUM OF THE 'STRING LENGTHS' BETWEEN THE DATA
C     ORDERED IN PHASE ACCORDING TO THAT PERIOD IS A MINIMUM.
C
C     IT DOES THIS FOR A SET OF NUMP TRIAL PERIODS SPACED BY
C     DELTAP AND STARTING AT P0.  (THE TIME UNITS MUST BE
C     CONSISTENT WITH THE DATA IN THE INPUT FILE, "INFILE",
C     USUALLY DAYS.  AN ARBITRARY EPOCH MAY BE SPECIFIED
C     FOR THE INPUT TIMES.)
C
C     THE PERIODOGRAM IS STORED IN A FILE "OUTFILE".
C
      CHARACTER *7 INFILE,OUTFILE
      REAL JD0,JD(200),B(200),LOW,NUFAZ(200),NUB(200),FAZ(200)
      REAL BTEMP(200)

      PRINT *,'PHOTOMETRY FILE?'
      READ (6,1) INFILE
    1 FORMAT (A7)
      PRINT *,'OUTPUT FILE?'
      READ (6,1) OUTFILE
      PRINT *,'EPOCH?'
      READ (6,*) JD0
      PRINT *,'STARTING PERIOD, INTERVAL, & NO. OF PERIODS?'
      READ (6,*) P0,DELTAP,NUMP

C     READS DATA FROM INFILE
      OPEN (UNIT=55,FILE=INFILE,STATUS='OLD')
      I = 1
  200 READ (55,*,END=100) JD(I),B(I)
      I = I + 1
      GO TO 200
  100 N = I - 1
      CLOSE (55)

      OPEN (UNIT=66,FILE=OUTFILE,STATUS='NEW')
      DO 10 II=1,NUMP

C     CALCULATES PHASES RELATIVE TO SPECIFIED PERIOD P0
        DO 20 I=1,N
          BTEMP(I) = B(I)
          TERM = (JD(I) - JD0)/P0
          FAZ(I) = TERM - INT(TERM)
          IF (FAZ(I).LT.0) FAZ(I) = FAZ(I) + 1
   20     CONTINUE

        N1 = N

C     RESORTS DATA IN ORDER OF INCREASING PHASE
        DO 30 J=1,N
          LOW = FAZ(1)
          NUM = 1

          DO 40 I=2,N1
            IF (FAZ(I).GT.LOW) GO TO 40
            LOW = FAZ(I)
            NUM = I
   40       CONTINUE

          NUFAZ(J) = LOW
          NUB(J) = BTEMP(NUM)
          K = 1
```

```
            DO 50 I=1,N
              IF (FAZ(I).EQ.LOW) GO TO 50
              FAZ(K) = FAZ(I)
              BTEMP(K) = BTEMP(I)
              K = K + 1
   50         CONTINUE

            N1 = N1 - 1
   30       CONTINUE

         SUM = 0.

C        CALCULATES 'STRING LENGTH' BETWEEN EACH PAIR OF
C        ADJACENT POINTS (IN PHASE) AND KEEPS A RUNNING TOTAL
           DO 60 I=1,N-1
              TERM1 = NUB(I+1) - NUB(I)
              TERM2 = FAZ(I+1) - FAZ(I)
   60         SUM = SUM + SQRT(TERM1**2. + TERM2**2.)
C        ADDS 'STRING LENGTH' BETWEEN LAST AND FIRST PHASE
C        POINTS ACROSS PHASE 0.0 = 1.0
         TERM1 = NUB(N) - NUB(1)
         TERM2 = (FAZ(1) + 1) - FAZ(N)
         SUM = SUM + SQRT(TERM1**2. + TERM2**2.)

           WRITE (66,*) PO,SUM
    2      FORMAT (1X,F8.5,1X,F7.4)
           PO = PO + DELTAP
   10      CONTINUE

         CLOSE (66)
         STOP
         END
```

APPENDIX C

FORTRAN V Listing of Cubic Spline Filter Programme SPLINE

```
      PROGRAM SPLINE (INPUT,OUTPUT,TAPE5=INPUT)
C
C     THIS PROGRAMME FITS A NATURAL CUBIC SPLINE TO A SET OF
C     POINTS (JD(I),MAG(I)), USING AN ALGORITHM FROM BURDEN,
C     FAIRES AND REYNOLDS' (1981, "NUMERICAL ANALYSIS", 2ND ED.
C     (BOSTON: PRINDLE, WEBER AND SCHMIDT); P. 112).  IT SELECTS
C     TIMES IN THE ORIGINAL DATA 120 POINTS APART (40 MIN. IF
C     THE POINTS ARE SAMPLED EVERY 20 SEC, AS IN THE HD 80439
C     DATA) AND TAKES 60 POINT AVERAGES CENTRED ON THOSE TIMES.
C     THESE ARE THE VALUES TO WHICH THE SPLINE IS MATCHED.
C     IT THEN SUBTRACTS THAT SPLINE FUNCTION FROM THE ORIGINAL
C     DATA TO PRODUCE A "FLATTENED" CURVE.
C
C     THE INPUT FILE IS "RAWFILE", THE FILE CONTAINING THE
C     SPLINE IS "SPLNFN", AND THE FLATTENED DATA FILE IS
C     "FLTFIL".
C
      DOUBLE PRECISION JD(2000),MAG(2000),X(10),A(10),H(10),
     1L(10),MU(10),Z(10),B(10),C(10),D(10),S(2000),ALPHA(10)
      CHARACTER *14 RAWFIL,SPLNFN,FLTFIL

      PRINT *,'RAW DATA FILE?'
      READ (6,1) RAWFIL
    1 FORMAT (A7)
      PRINT *,'SPLINE FUNCTION TO BE STORED IN?'
      READ (6,1) SPLNFN
      PRINT *,'FLATTENED FILE?'
      READ (6,1) FLTFIL

      OPEN (UNIT=55,FILE=RAWFIL,STATUS='OLD')
      OPEN (UNIT=66,FILE=SPLNFN,STATUS='NEW')
      OPEN (UNIT=67,FILE=FLTFIL,STATUS='NEW')

      I = 1
      J = 2
      II = 1
C     READS DATA FROM RAWFIL
  200 READ (55,*,END=100) JD(I),MAG(I)
      I = I + 1
      GO TO 200
  100 CLOSE (55)

C     DETERMINES AVERAGED POINTS TO BE FIT BY SPLINE
      N = I - 1
      NMAX = N - 120
      X(1) = JD(1)
      A(1) = MAG(1)
  300 IF (II.GT.NMAX) GO TO 400
      SUM = 0.

      DO 10 I=II,II+120
   10   SUM = SUM + MAG(I)

      A(J) = SUM/120.
      X(J) = JD(II+60)
      II = II + 240
      J = J + 1
      GO TO 300

C     CALCULATES SPLINE CURVE
  400 X(J) = JD(N)
      A(J) = MAG(N)
      H(1) = X(2) - X(1)

      DO 20 I=2,J-1
        H(I) = X(I+1) - X(I)
```

```
      20    ALPHA(I) = 3.*(A(I+1)*H(I-1) - A(I)*(X(I+1)
     1    - X(I-1)) + A(I-1)*H(I))/(H(I-1)*H(I))

            L(1) = 1.
            MU(1) = 0.
            Z(1) = 0.

            DO 30 I=2,J-1
              L(I) = 2.*(X(I+1) - X(I-1)) - H(I-1)*MU(I-1)
              MU(I) = H(I)/L(I)
      30      Z(I) = (ALPHA(I) - H(I-1)*Z(I-1))/L(I)

            L(J) = 1.
            Z(J) = 0.
            C(J) = 0.

            DO 40 I=J-1,1,-1
              C(I) = Z(I) - MU(I)*C(I+1)
              B(I) = (A(I+1) - A(I))/H(I)
     1      - H(I)*(C(I+1) + 2.*C(I))/3.
      40      D(I) = (C(I+1) - C(I))/(3.*H(I))

            I = 1
            K = 1
            SUM = 0.
      600   IF (I.GT.N-1) GO TO 700
            IF (JD(I).GE.X(K).AND.JD(I).LT.X(K+1)) GO TO 500
            K = K + 1
            GO TO 600
      500   DIFF = JD(I) - X(K)
            S(I) = A(K) + B(K)*DIFF + C(K)*DIFF**2. + D(K)*DIFF**3.
            MAG(I) = MAG(I) - S(I)
            WRITE (66,7) JD(I),S(I)
        7   FORMAT (1X,F10.5,1X,F7.4)
            SUM = SUM + MAG(I)
            I = I + 1.
            GO TO 600
      700   AVER = (SUM + MAG(N))/N

      C     WRITE SPLINE FILTER TO SPLNFN
            WRITE (66,7) JD(N),MAG(N)
            MAG(N) = 0. - AVER

      C     WRITE FLATTENED DATA FILE TO FLTFIL
            DO 50 I=1,N
              MAG(I) = MAG(I) - AVER
       50   WRITE (67,7) JD(I),MAG(I)

            CLOSE (66)
            CLOSE (67)
            STOP
            END
```

REFERENCES

Abt, H.A., Chaffee, F.H., and Suffolk, G. 1972. *Ap. J.* 175, 779.

Adelman, S.J. 1985. *Publ. A. S. P.* 97, 970.

Aizenman, M.L., Hansen, C.J., Cox, J.P. and Pesnell, W.D. 1984. *Astrophys. J. (Letters)* 286, L43.

Babcock, H.W. 1958. *Astrophys. J. Suppl.* 3, 141.

Baschek, B. and Oke, J.B. 1965. *Astrophys. J.* 141, 1404.

Beutler, F.J. 1966. *S.I.A.M. Rev.* 8, 328.

Bevington, P.R. 1969. *Data Reduction and Error Analysis for the Physical Sciences* (New York: McGraw-Hill).

Bidelman, W.P. and MacConnell, D.J. 1973. *Astron. J.* 78, 687.

Blackman, R.B. and Tukey, J.W. 1958. *The Measurement of Power Spectra from the Point of Communications Engineering* (New York: Dover).

Blanco, V.M., Demers, S., Douglass, G.G., and Fitzgerald, M.P. 1970 *Publ. U.S. Naval Obs.* 11, 1.

Bonsack, W.K. 1979. *Publ. A. S. P.* 91, 648.

Bonsack, W.K. and Pilachowski, C.A. 1974. *Astrophys. J.* 190, 327.

Borra, E.F. and Landstreet, J.D. 1975. *Publ. A. S. P.* 87, 961.

Borra, E.F. and Landstreet, J.D. 1980. *Astrophys. J. Suppl.* 42, 421.

Breger, M. 1979. *Publ. A. S. P.* 91, 5.

Burg, J.P. 1965. Ph.D. thesis, Stanford University

Clarke D. 1980. *M.N.R.A.S.* 190, 641.

Cox, J.P. 1984*a*. *Astrophys. J.* 280, 220.

Cox, J.P. 1984*b*. *Publ. A. S. P.* 96, 577.

Cramer, N. and Maeder, A. 1979. *Astron. Astrophys.* 78, 305.

Cramer, N. and Maeder, A. 1980. *Astron. Astrophys.* 88, 135.

Crawford, D.L. 1958. *Astrophys. J.* 128, 190.

Crawford, D.L. 1979. *Astron. J.* 84, 1858.

Deeming, T.J. 1975. *Astrophys. Space Sci.* **36**, 137

Dolez, N. and Gough, D.O. 1982. in *Pulsations in Classical and Cataclysmic Variables*, eds. J.P. Cox and C.J. Hansen (Boulder: JILA), p. 248.

Dziembowski, W. 1977. *Acta. Astr.* **27**, 203.

Dziembowski, W. and Goode, P.R. 1984. *Mem. Soc. Astr. Italiana* **55**, 185

Dziembowski, W. and Goode, P.R. 1985. *Astrophys. J (Letters)* **296**, L27.

Fahlman, G.G. and Ulrych, T.J. 1982. *M.N.R.A.S.* **199**, 53.

Fernie, J.D. 1976. *Publ. A. S. P.* **88**, 969.

Floquet, M. 1979. *Astron Astrophys.* **74**, 250.

Floquet, M. 1981. *Astron. Astrophys.* **101**, 176.

Gabriel, M., Noels, A., Scuflaire, R., and Mathys, G. 1985. *Astron. Astrophys.* **143**, 206.

Global Oscillation Network Group 1985. *A Proposal to Study the Solar Interior by Measuring Global Oscillations with a World-wide Network of Instruments* (Sunspot: National Solar Observatory).

Golay, M. 1974*a*. *Introduction to Astronomical Photometry* (Dordrecht: Reidel), p. 199.

Golay, M. 1974*b*. *ibid*, p. 26-27.

Gray, D.F. and Desikachary, K. 1973. *Astrophys. J.* **181**, 523.

Hardie, R.H. and Schroeder, N.H. 1963. *Astrophys. J.* **138**, 350.

Harris, D.L., Strand, K.A. and Worley, C.E. 1963. in *Basic Astronomical Data - Stars & Stellar Systems III*, ed. K.A. Strand (Chicago: University of Chicago Press), p. 273.

Harris, W.E., Fitzgerald, M.P., and Reed, B.C. 1981. *Publ. A. S. P.* **93**, 507.

Hauck, B. and Mermilliod, M. 1975. *Astron. Astrophys. Suppl.* **22**, 235.

Hauck, B. and Mermilliod, M. 1980. *Astron. Astrophys. Suppl.* **40**, 1.

Hauck, B. and North, P. 1982. *Astron. Astrophys.* **114**, 23.

Hill, R.J. 1986. M.Sc. thesis, University of Western Ontario.

Hoffleit, D. 1982. *Bright Star Catalogue*, 4th Ed., Yale University Observatory.

Horne, J.H. and Baliunas, S.L. 1986. *Astrophys. J.* **302**, 757.

Houk, N. 1982. *Michigan Spectral Catalogue, Vol. 3* (Ann Arbor: University of Michigan).

Houk, N. and Cowley, A.P. 1975. *Michigan Spectral Catalogue, Vol. 1* (Ann Arbor: University of Michigan).

Jarzebowski, T. 1960. *Acta. Astr.* **10**, 31.

Jenkins, G.M. and Watts, D.G. 1968. *Spectral Analysis and its Implications*, (San Francisco: Holden-Day).

Joncas, G. and Borra, E.F. 1981. *Astron Astrophys.* **94**, 134.

Jones, T.J. and Wolff, S.C. 1973. *Publ. A. S. P.* **85**, 760.

Kreidl, T.J. 1985*a*. *Inform. Bull. Var. Stars* #2739.

Kreidl, T.J. 1985*b*. *M.N.R.A.S.* **216**, 1013.

Kreidl, T.J. 1987. *Lecture Notes in Physics* **274**, "Stellar Pulsation", eds. A.N. Cox *et al.* (Berlin: Springer-Verlag), p. 134.

Kurtz, D.W. 1978. *Infor. Bull. Var. Stars* #1436.

Kurtz, D.W. 1982. *M.N.R.A.S.* **200**, 807.

Kurtz, D.W. 1983*a*. *M.N.R.A.S.* **202**, 1.

Kurtz, D.W. 1983*b*. *M.N.R.A.S.* **205**, 3.

Kurtz, D.W. 1984. *M.N.R.A.S.* **209**, 841.

Kurtz, D.W. 1985. preprint.

Kurtz, D.W. 1986. in the proceedings of the NATO Workshop on *Seismology of the Sun and Distant Stars*, ed. D.O. Gough (Cambridge: CUP).

Kurtz, D.W. and Cropper, M. 1987. preprint.

Kurtz, D.W. and Marang, F. 1987. preprint.

Kurtz, D.W. and Seeman, J. 1983. *M.N.R.A.S.* **205**, 11.

Kurtz, D.W. and Shibahashi, H. 1986. *M.N.R.A.S.* **223**, 557.

Kurtz, D.W. and Wegner, G. 1979. *Astrophys. J.* **232**, 510.

Kurtz, D.W., Schneider, H., and Weiss, W.W. 1985. *M.N.R.A.S.* **215**, 77.

Kurucz, R.L. 1979. *Astrophys. J. Suppl.* **40**, 1.

Lafler, J. and Kinman, T.D. 1965. *Astrophys. J. Suppl.* **11**, 216.

Ledoux, P. 1951. *Astrophys. J.* **114**, 373.

Matthews, J.M., Kurtz, D.W. and Wehlau, W.H. 1986. *Astrophys. J.* **300**, 348.

Matthews, J.M., Kurtz, D.W. and Wehlau, W.H. 1987. *Astrophys. J.* **313**, 782.

Matthews, J.M., Slawson, R.W. and Wehlau, W.H. 1986. in *Hydrogen Deficient Stars and Related Objects*, ed. K. Hunger *et al.* (Dordrecht: Reidel), p. 313.

Matthews, J.M. and Wehlau, W.H. 1985. *Publ. A. S. P.* **97**, 841.

Matthews, J.M., Wehlau, W.H., Walker, G.A.H., and Yang, S. 1987*a*. *Astrophys. J.*, submitted.

Olsen, E.H. 1983. *Astron. Astrophys. Suppl.* **54**, 55.

Olsen, E.H. and Perry, C.L. 1984. *Astron. Astrophys. Suppl.* **56**, 229.

Papoulis, A. 1977. *Signal Analysis* (New York: McGraw-Hill).

Preston, G.W. 1969. *Astrophys. J.* **158**, 243.

Preston, G.W. 1972. *Astrophys. J.* **175**, 465.

Preston, G.W. and Pyper, D. 1965. *Astrophys. J.* **142**, 983.

Preston, G.W. and Stepien, K. 1968*a*. *Astrophys. J.* **151**, 577.

Preston, G.W. and Stepien, K. 1968*b*. *Astrophys. J.* **151**, 583.

Preston, G.W. and Stepien, K. 1968*c*. *Astrophys. J.* **154**, 971.

Preston, G.W. and Wolff, S.C. 1970. *Astrophys. J.* **160**, 1071.

Preston, G.W., Stepien, K. and Wolff, S.C. 1969. *Astrophys. J.* **156**, 653.

Pyper, D. and Adelman, S. 1986. in *Upper Main Sequence Stars With Anomalous Abundances*, eds. C.R. Cowley *et al.* (Dordrecht: Reidel).

Rakos, K.D. 1962. *Zs. f. Astrophys.* **56**, 153.

Scargle, J.D. 1982. *Astrophys. J.* **263**, 835.

Scholz, G. 1979. *Astr. Nachr.* **300**, 213.

Shibahashi, H. 1983. *Astrophys. J. (Letters)* **275**, L5.

Shibahashi, H. 1987. *Lecture Notes in Physics* **274**, "Stellar Pulsation", eds. A.N. Cox *et al.* (Berlin: Springer-Verlag).

Shibahashi, H. and Saio, H. 1985. *Publ. A. S. Japan* 37, 245.

Shibahashi, H., Noels, A., and Gabriel, M. 1983. *Astron. Astrophys.* 123, 283.

Sinnerstad, U. 1961. *Stockholm Obs. Ann.* 21, 6.

Slettebak, A., Collins, G.W., Boyce, P.B., White, N.M., and Parkinson, 1975. *Astrophys. J. Suppl.* 29, 137.

Stellingwerf, R.F. 1978. *Astrophys. J.* 224, 953.

Stepién, K. 1968. *Astrophys. J.* 154, 945.

Stepién, K. and Muthsam, H. 1980. *Astron. Astrophys.* 92, 171.

Tassoul, M. 1980. *Astrophys. J. Suppl.* 43, 469.

Thompson, I.B. 1983. *M.N.R.A.S.* 205, 43D.

Thompson, I.B., Landstreet, J.D. and Brown, D. 1986. preprint.

Toomre, J. 1984. in *Solar Seismology from Space*, JPL Publication 84-84, eds. R.K. Ulrich *et al.* (Pasadena: NASA), p. 7.

Trasco, J.D. 1972. *Astrophys. J.* 171, 569.

Vogt, N. and Faundez, M. 1979. *Astron. Astrophys. Suppl.* 36, 477.

Wehlau, W.H. and Leung, K.C. 1964. *Astrophys. J.* 139, 843.

Weiss, W.W. 1986. in IAU Colloquium #90, *Upper Main Sequence Stars with Anomalous Abundances*, (Dordrecht: Reidel).

Weiss, W.W. and Kurtz, D.W. 1987. in preparation.

Winzer, J.E. 1974. Ph.D. thesis, University of Toronto.

Wolff, S.C. 1967. *Astrophys. J. Suppl.* 15, 21.

Wolff, S.C. 1975. *Astrophys. J.* 202, 127.

Wolff, S.C. 1983. *The A-stars: Problems and Perspectives*, NASA Monograph SP-463.

Wolff, S.C. and Hagen, W. 1976. *Publ. A. S. P.* 88, 119.

Wolff, S.C. and Wolff, R.J. 1970. *Astrophys. J.* 160, 1049.

Wolff, S.C. and Wolff, R.J. 1971. *Astron. J.* 76, 422.

Wolff, S.C. and Wolff, R.J. 1972. *Astrophys. J.* 176, 433.

Wood, H.J. and Campusano, L.B. 1975. *Astron. Astrophys.* 45, 303.